Electronic Supplementary Material (ESI) for Dalton Transactions.
This journal is © The Royal Society of Chemistry 2022

Supporting Information

Novel 1,2,3-Triazole appended monophosphines with pyridine functionalities: synthesis of coinage metal complexes, photophysical studies and Cu(I) catalyzed C-O coupling of phenols with aryl bromide †

Sonu Sheokand, Dipanjan Mondal, Basvaraj S. Kote, Latchupatula Radhakrishna and Maravanji S. Balakrishna*

Phosphorus Laboratory, Department of Chemistry, Indian Institute of Technology Bombay, Powai, Mumbai 400076, India.

*Author to whom correspondence should be addressed. E-mail: krishna@chem.iitb.ac.in, msb_krishna@iitb.ac.in (M. S. Balakrishna); Fax: +91-22-5172-3480/2576-7152.

Table of content

Crystal structure determination of complexes **2-5** and **7-9**	S1
Crystallographic information for complexes **2-5** and **7-9**	S2
Molecular orbitals, TD-DFT and NBO calculations	S3-S10
NMR and HRMS spectra of complexes **1-9**	S11-S37
PXRD profiles for **2-4**	S37-S38
Solid state UV- absorption spectra for **1-5**	S39-S40
NMR spectra of catalytic products	S41-S58
References	S58-S59

Crystal structure determination of complexes 2-5 and 7-9.

Single crystals of all complexes were mounted on a Cryoloop with a drop of paratone oil and positioned in the cold nitrogen stream on a Bruker D8 Venture diffractometer. The data collections were performed at 100 K to 150 K using Bruker D8 Venture diffractometer with a graphite monochromated Mo Kα radiation source (λ = 0.71073 Å) with the ω-scan technique. The data were reduced using CrysalisPro Red 171.41_64.93a software.[1] The structures were solved using Olex2 1.5[2] with the ShelXT[3] structure solution program using intrinsic phasing and refined with SHELXL[4] refinement package using least-squares minimization. All non-hydrogen atoms were refined anisotropically. Hydrogen atoms were placed in calculated positions and included as riding contributions with isotropic displacement parameters tied to those of the attached non-hydrogen atoms. The given chemical formula and other crystal data do not take into account the unknown solvent molecule(s). The reflections with error/esd more than 10 were excluded in order to avoid problems related to better refinement of the data. The data completeness is more than 99.8% in most of the cases, which is enough to guarantee a very good refinement of data. The details of X-ray structural determinations are given in Tables S1. Crystallographic data for the structures reported in this paper have been deposited with the Cambridge Crystallographic Data Centre as supplementary publication no. CCDC: 2221869–2221872 (for **2-5**) and 2221873–2221875 (for **7-9**).

Table S1 Crystallographic information of compounds **2-5** and **7-9**

code	**2**	**3**	**4**	**5**	**7**	**8**	**9**
Formula	$C_{50}H_{38}Cl_2Cu_2N_8P_2$	$C_{50}H_{38}Br_2Cu_2N_8P_2$	$C_{50}H_{38}Cu_2I_2N_8P_2$	$C_{37}CuIN_6P$	$C_{50}H_{38}Ag_2Br_2N_8P_2$	$C_{54}H_{44}Ag_2I_2N_{10}P_2$	$C_{25}H_{19}AuClN_4P$
Formula weight	1010.80	1099.72	1193.70	749.84	1188.38	1364.47	638.83
Temperature/K	150.15	150.15	150.15	100.15	150.15	150.15	150.00(10)
Crystal system	monoclinic	monoclinic	triclinic	monoclinic	monoclinic	triclinic	monoclinic
Space group	$P2_1/n$	$P2_1/n$	P-1	$P2_1/c$	$P2_1/n$	P-1	$P2_1/c$
a/Å	9.6601(3)	9.6861(2)	10.1156(2)	12.6389(2)	9.4370(2)	10.22310(10)	10.1388(5)
b/Å	13.6102(5)	13.5067(3)	10.2713(2)	16.3194(2)	13.3374(2)	10.86800(10)	9.0469(5)
c/Å	17.3381(6)	17.6907(4)	13.6838(3)	15.3635(2)	18.7527(4)	13.3111(2)	25.0966(15)
α/°	90	90	106.577(2)	90	90	99.4390(10)	90
β/°	96.065(3)	95.2177(19)	91.571(2)	91.7510(10)	93.552(2)	112.0120(10)	101.230(6)
γ/°	90	90	118.819(2)	90	90	101.4420(10)	90
Volume/$Å^3$	2266.78(13)	2304.86(8)	1170.63(5)	3167.39(8)	2355.78(8)	1296.81(3)	2257.9(2)
Z	2	2	1	4	2	1	4
$\rho_{calc}g/cm^3$	1.481	1.585	1.693	1.572	1.675	1.747	1.879
μ/mm^{-1}	1.173	2.771	2.340	1.751	2.640	2.055	6.726
F(000)	1032.0	1104.0	588.0	1444.0	1176.0	668.0	1232.0
Crystal size/mm^3	0.092 × 0.069 × 0.066	0.098 × 0.079 × 0.075	0.095 × 0.075 × 0.071	0.085 × 0.068 × 0.065	0.077 × 0.075 × 0.01	0.095 × 0.067 × 0.065	0.098 × 0.069 × 0.066
2θ range, deg	4.726 to 67.196	4.624 to 73.902	3.168 to 71.638	3.642 to 50	4.72 to 68.142	4.344 to 60	3.31 to 49.996
Total no of reflection	66979	69933	64162	59365	68618	89799	19634
Independent reflections	8226 [R_{int} = 0.0862]	9069 [R_{int} = 0.0584]	8690 [R_{int} = 0.0429]	5574 [R_{int} = 0.0801]	8512[R_{int} = 0.1526]	10573 [R_{int} = 0.0406]	3966 [R_{int} = 0.0478]
Goodness-of-fit on F^2	1.039	1.037	1.035	1.066	0.894	1.052	1.081
R_1 (all data)	0.0491	0.0388	0.0345	0.0505	0.0347	0.0297	0.0317
wR_2 (I > 2σ(I))	0.1097	0.0869	0.0766	0.1618	0.0943	0.0629	0.0615

Molecular orbitals, TD-DFT and NBO calculations

All DFT calculations were performed with the Gaussian09 (Rev. D.01) suite of programs.[5] Initially we optimized all of the structures (**2-4**) with different basic sets (using the hybrid density functional B3LYP with TZVP basic sets for C, H, N, P, Cl, Br, and SDD basic sets for Cu and I atoms with the relativistic electron core potential) and the results obtained are given below in Table S2. We found that the optimization calculation revealed the optimized structures of **2** and **3** having almost identical bonding parameters and Cu···Cu′ distances with respect to X-ray structures, whereas it is not fit with its X-ray data in case of **4**, especially Cu···Cu′ distance (Table S2). Henceforth, we performed all of this calculation by considering crystal coordinates only keeping all the basic sets remain unchanged. Frequency calculations were performed subsequently to confirm the presence of local minima (only positive frequencies). Vertical excitations (100 singlet excited states) were calculated by TD-DFT method. To find out the nature of Cu···Cu′ interaction, natural bond order (NBO) analysis is carried out using Gaussian 09. Molecular orbitals were visualised using Chemcraft software with countor value: 0.030.

Table S2 Selected bond length and bond angles of **2-4** obtained from X-ray diffraction analysis and *DFT* calculation

	2 (X = Cl)		**3** (X = Br)		**4** (X = I)	
Bond lengths (Å)						
	X-ray	***DFT***	***X-ray***	***DFT***	***X-ray***	***DFT***
Cu1–P1	2.1786(6)	2.23528	2.1861(5)	2.25420	2.2168(5)	2.27138
Cu1′–X1	2.4513(6)	2.42155	2.5535(3)	2.53044	2.6628(3)	2.73623
Cu1–X1	2.2993(6)	2.38861	2.4026(3)	2.50772	2.5789(3)	2.74395
Cu1-Cu1′	3.1039(6)	3.08569	3.0387(4)	3.02069	2.6924(5)	3.18213
Cu1–N1	2.1046(8)	2.16105	2.0974(15)	2.18626	2.0934(16)	2.17568

Bond angles (°)						
Cu1–X1–Cu1’	81.525(18)	79.803	75.562(10)	73.676	61.792(9)	70.994
X1–Cu1–X1’	98.474(18)	100.197	104.439(10)	106.324	118.208(9)	107.526
P1–Cu1–N1	100.64(5)	98.028	100.43(4)	96.648	98.48(5)	96.935
X1-Cu1-N1	105.99(5)	106.104	108.47(4)	106.489	110.32(5)	109.302

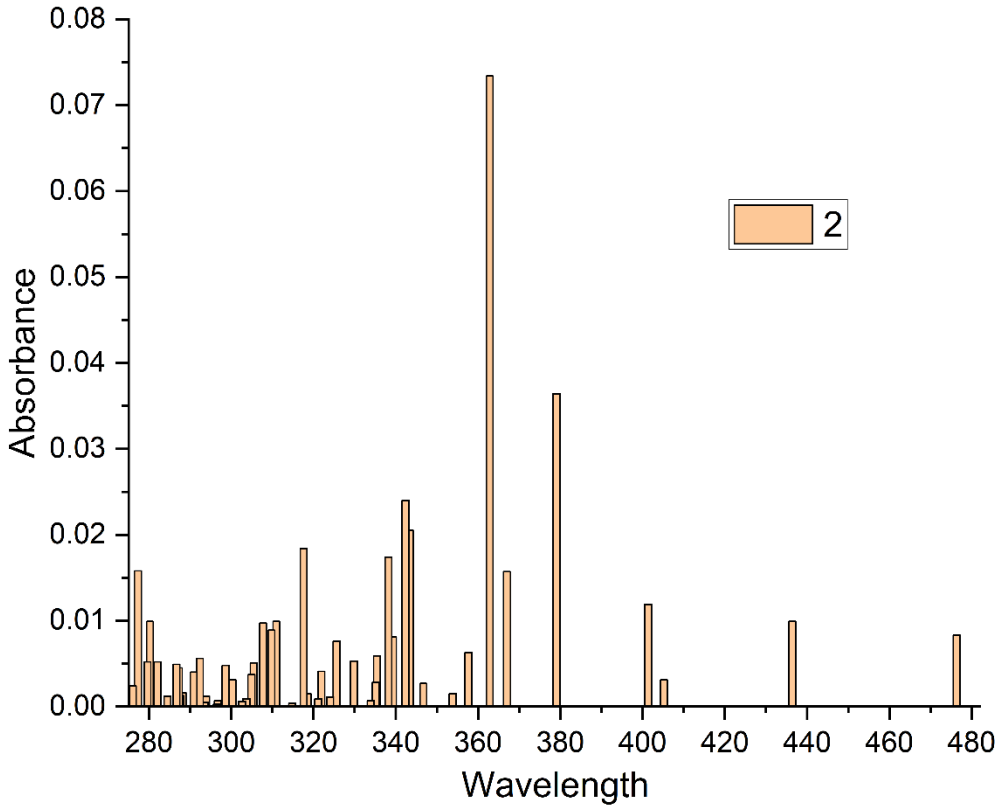

Fig. S1. Calculated absorption spectrum of **2** based on the TDDFT method.

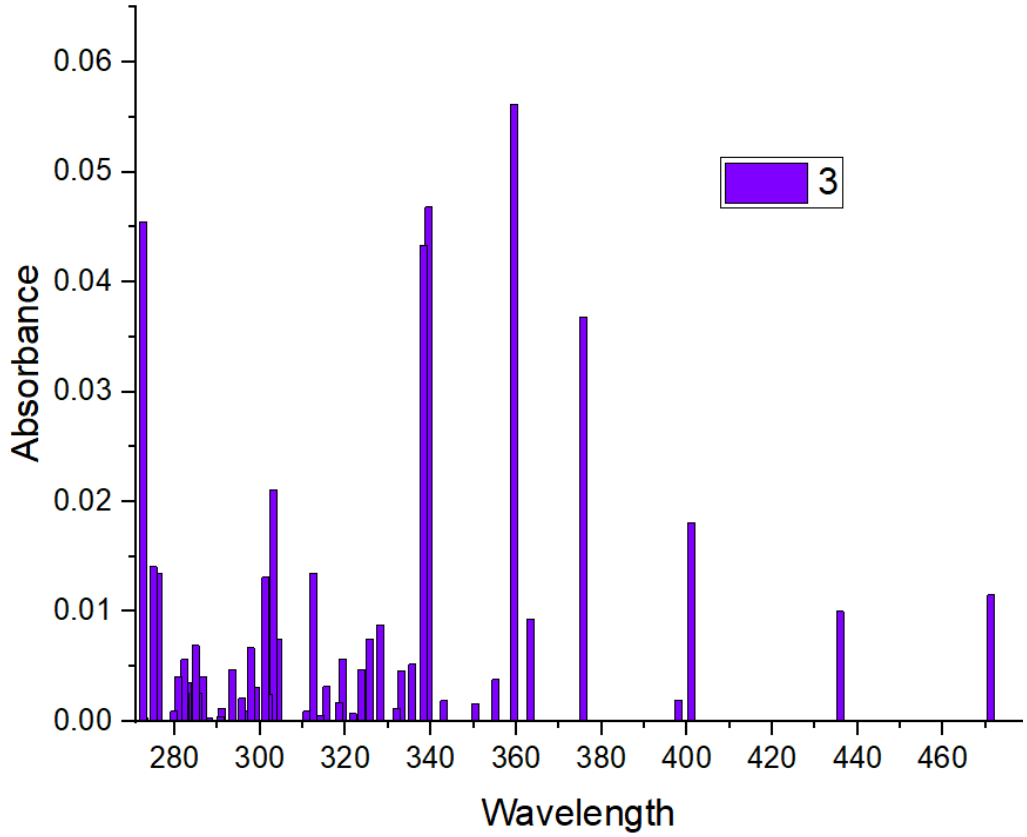

Fig. S2. Calculated absorption spectrum of **3** based on the TDDFT method.

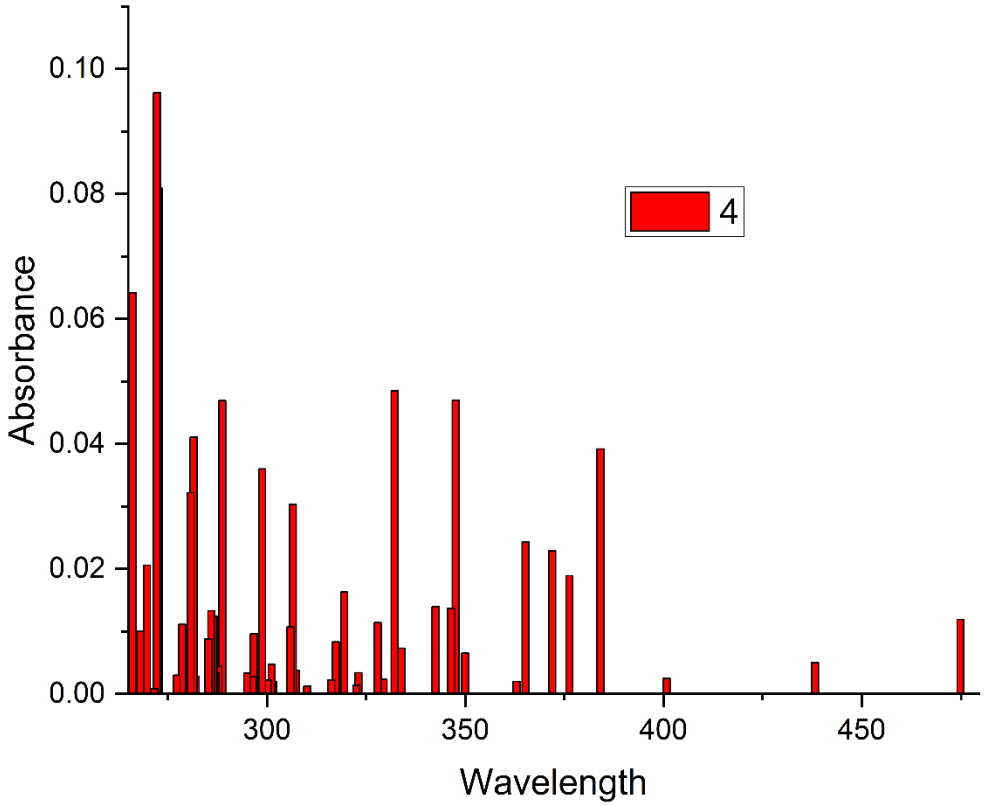

Fig. S3. Calculated absorption spectrum of **4** based on the TDDFT method.

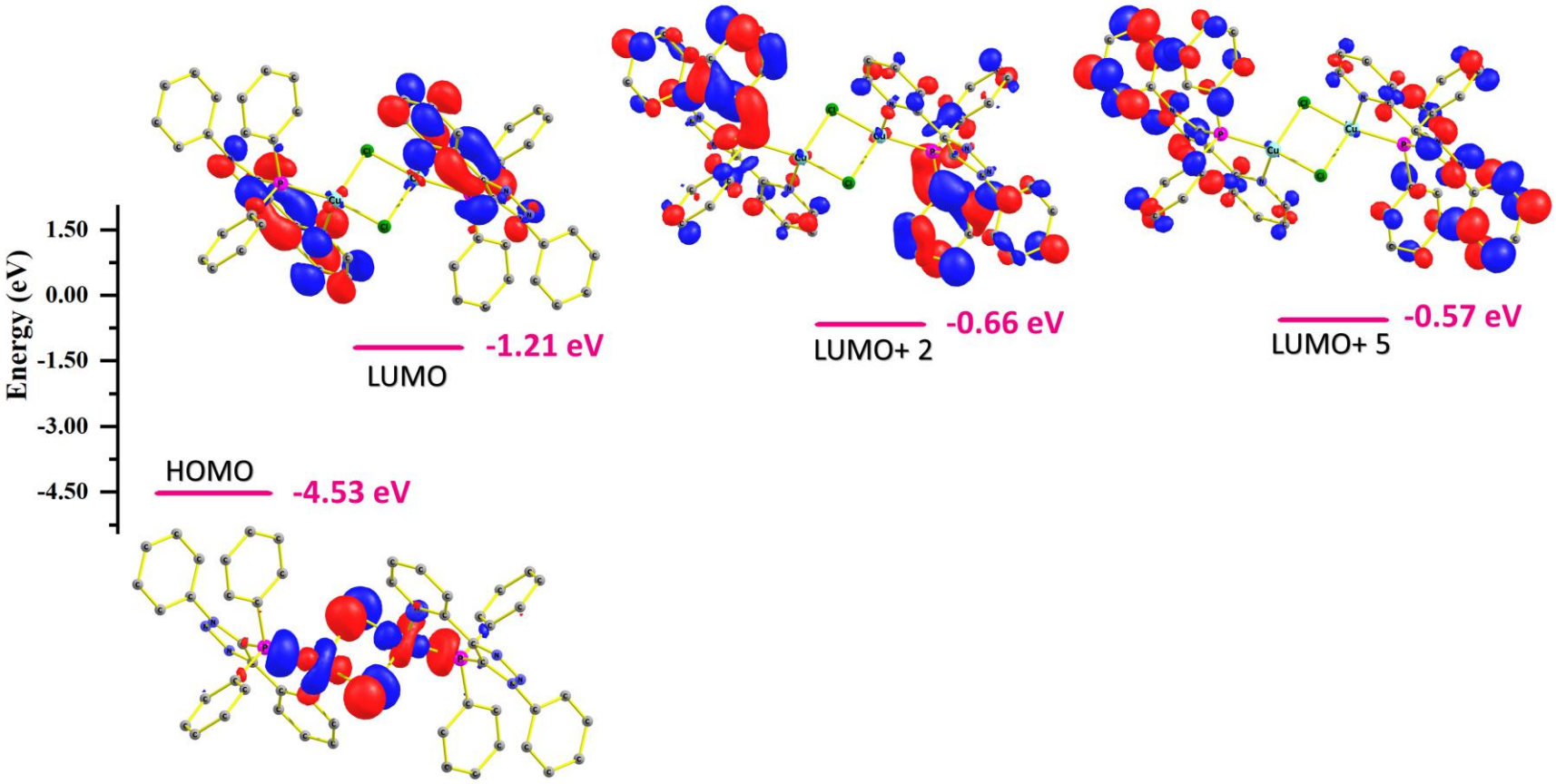

Fig. S4. Extended energy level plots for complex **2**.

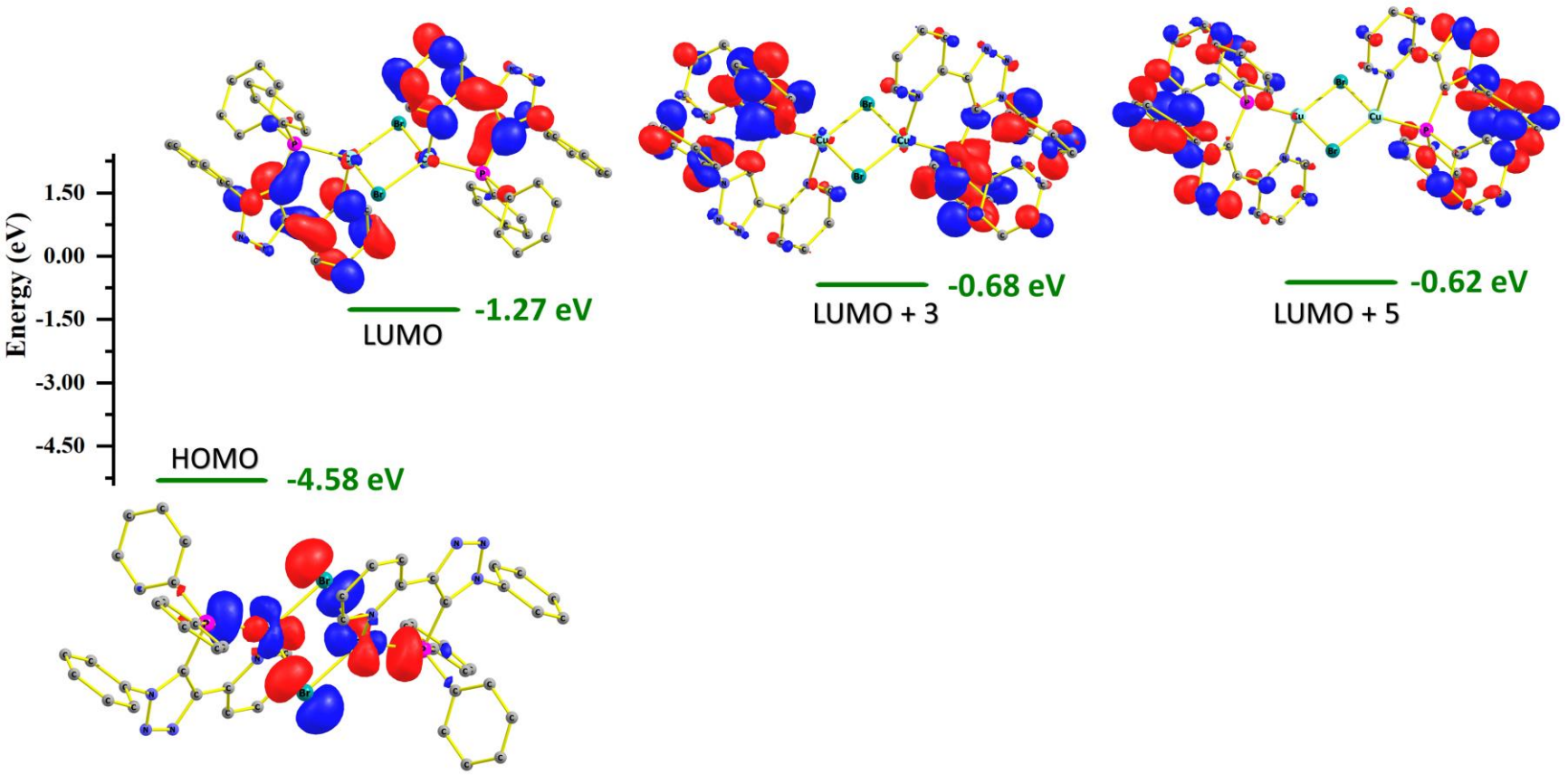

Fig. S5. Extended energy level plots for complex **3**.

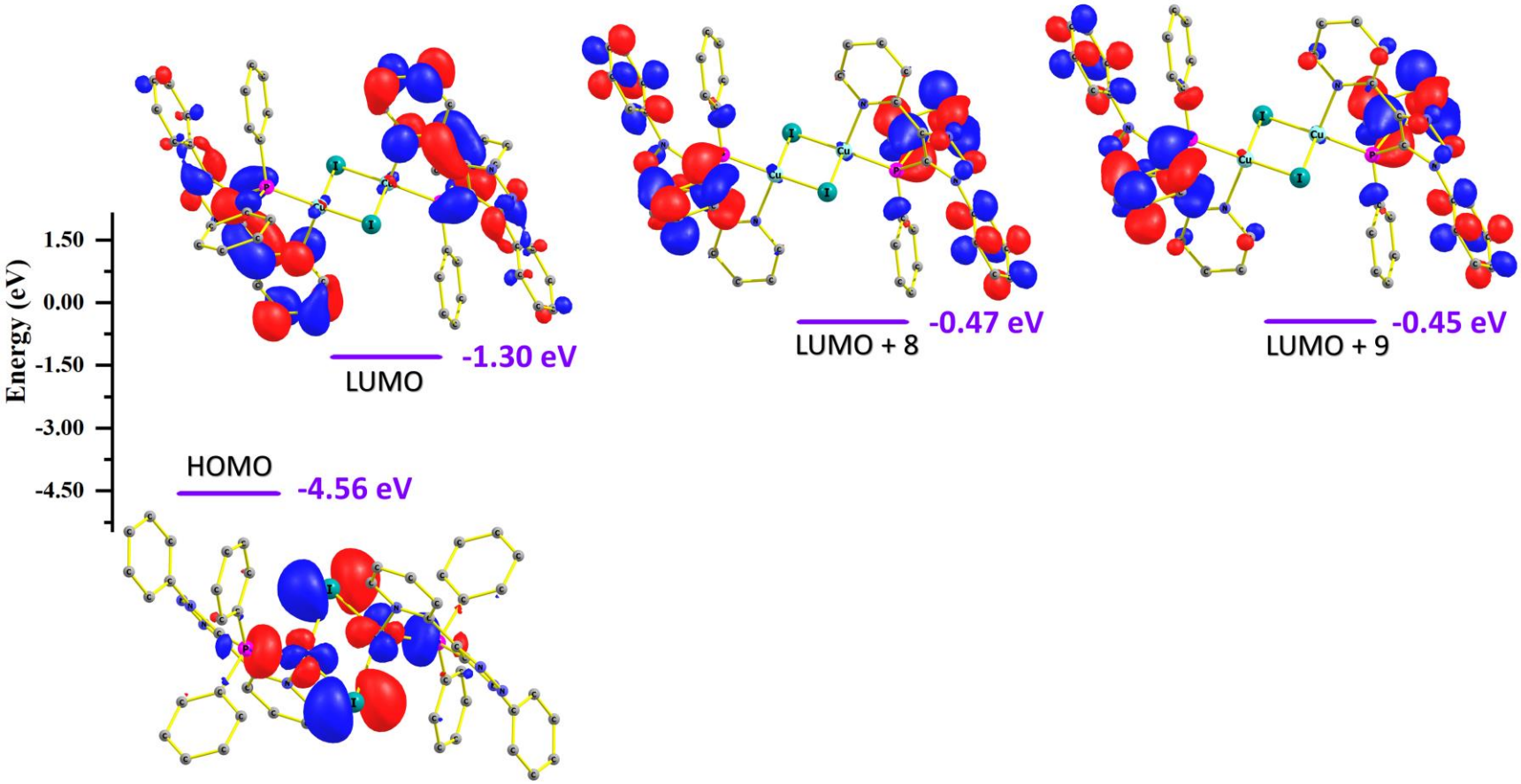

Fig. S6. Extended energy level plots for complex **4**.

Table S3 TD-DFT data for complexes **5-7**

Comp	λ (nm)	E_{ex} (eV)	Oscillator strength f	Orbitals involved	
2	401	3.0890	0.0119	H-3 → L+1	(0.59)
				H-3 → L	(0.23)
	362	3.4171	0.0734	H-2 → L+3	(0.13)
				H-2 → L+4	(0.12)
				H → L+5	(0.53)
	379	3.2704	0.0364	H→ L+2	(0.62)
				H→ L+6	(0.24)
3	400	3.0919	0.0181	H-6→ L	(0.10)
				H-3→ L+1	(0.68)
	375	3.2994	0.0368	H→ L+2	(0.64)
				H→ L+6	(0.22)
	359	3.4502	0.0562	H→ L+5	(0.55)
				H→ L+6	(0.32)
				H→ L+7	(0.17)
4	384	3.2277	0.0392	H-3→ L	(0.69)
	347	3.5668	0.0470	H→ L+9	(0.56)
				H-1→ L+10	(0.13)
	272	4.5539	0.0962	H-12→ L+1	(0.25)
				H-9→ L+1	(0.34)
				H-4→ L+10	(0.42)

NMR and HRMS spectra of complexes 1-9

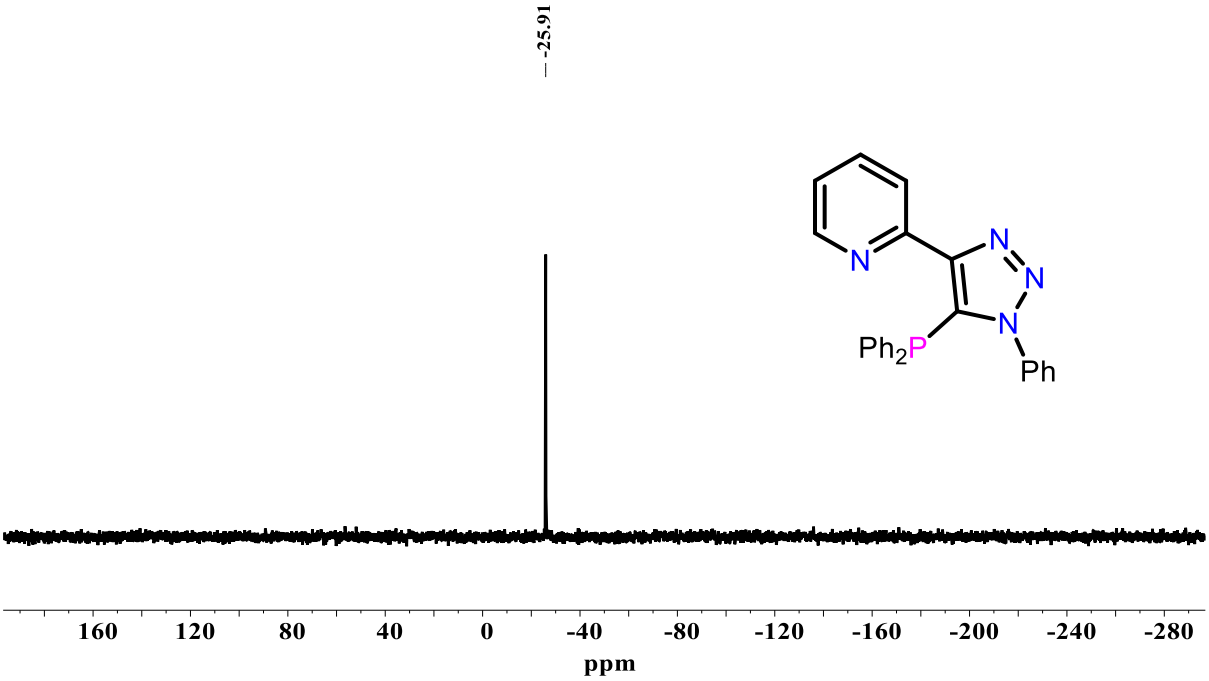

Fig. S7. $^{31}P\{^{1}H\}$ NMR spectrum of **1** in $CDCl_3$ (202 MHz).

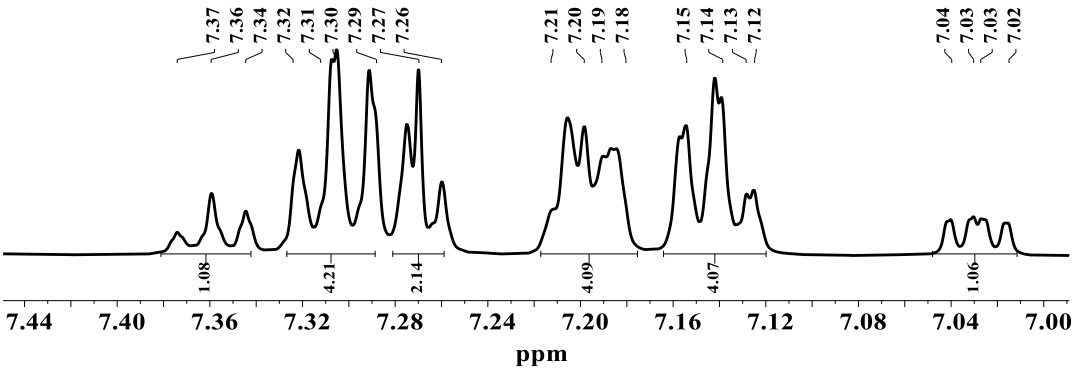

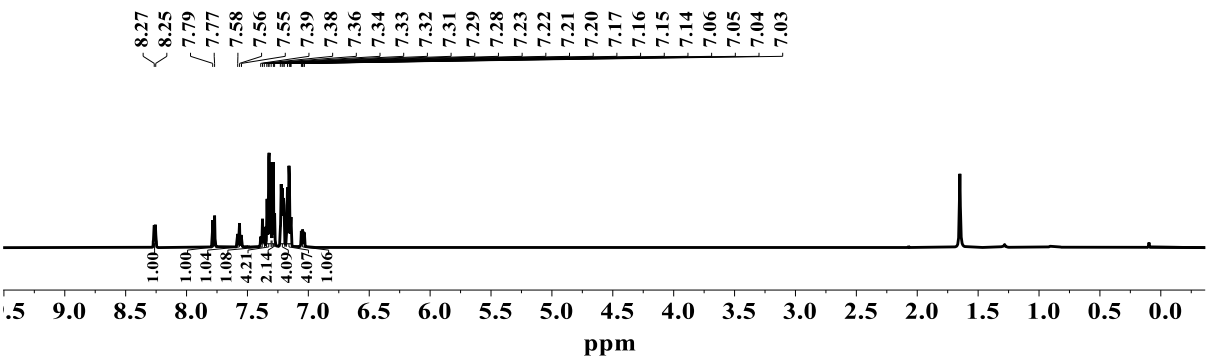

Fig. S8. ^{1}H NMR spectrum of **1** in $CDCl_3$ (500 MHz).

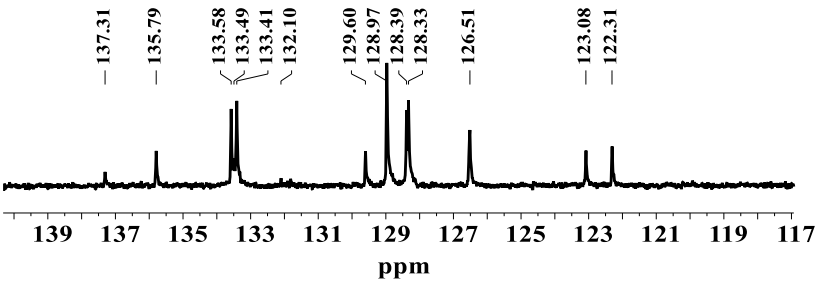

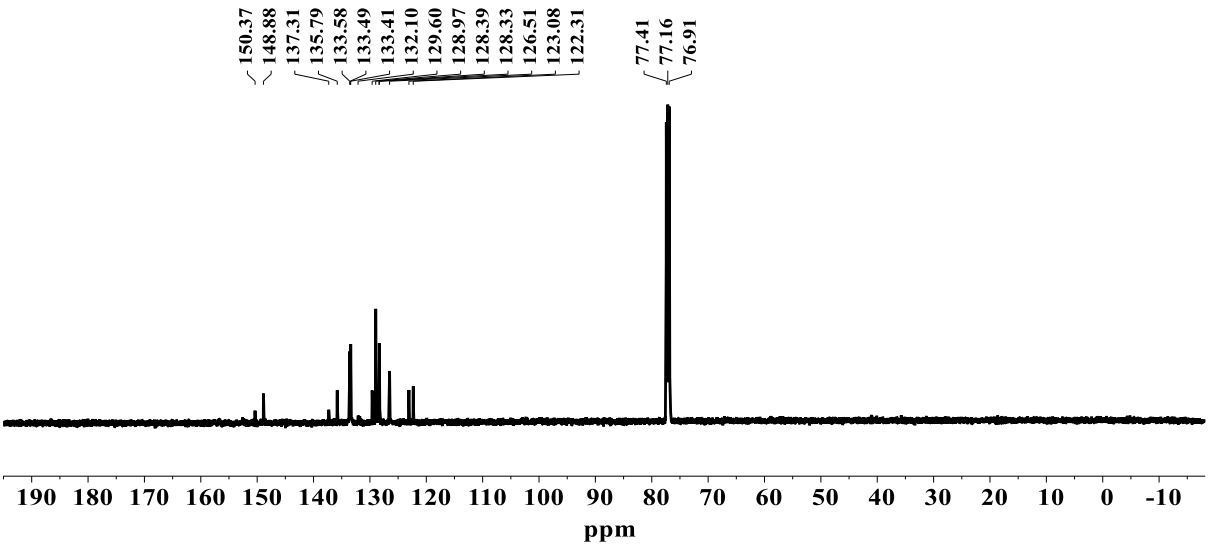

Fig. S9. $^{13}C\{^{1}H\}$ NMR spectrum of **1** in $CDCl_3$ (126 MHz).

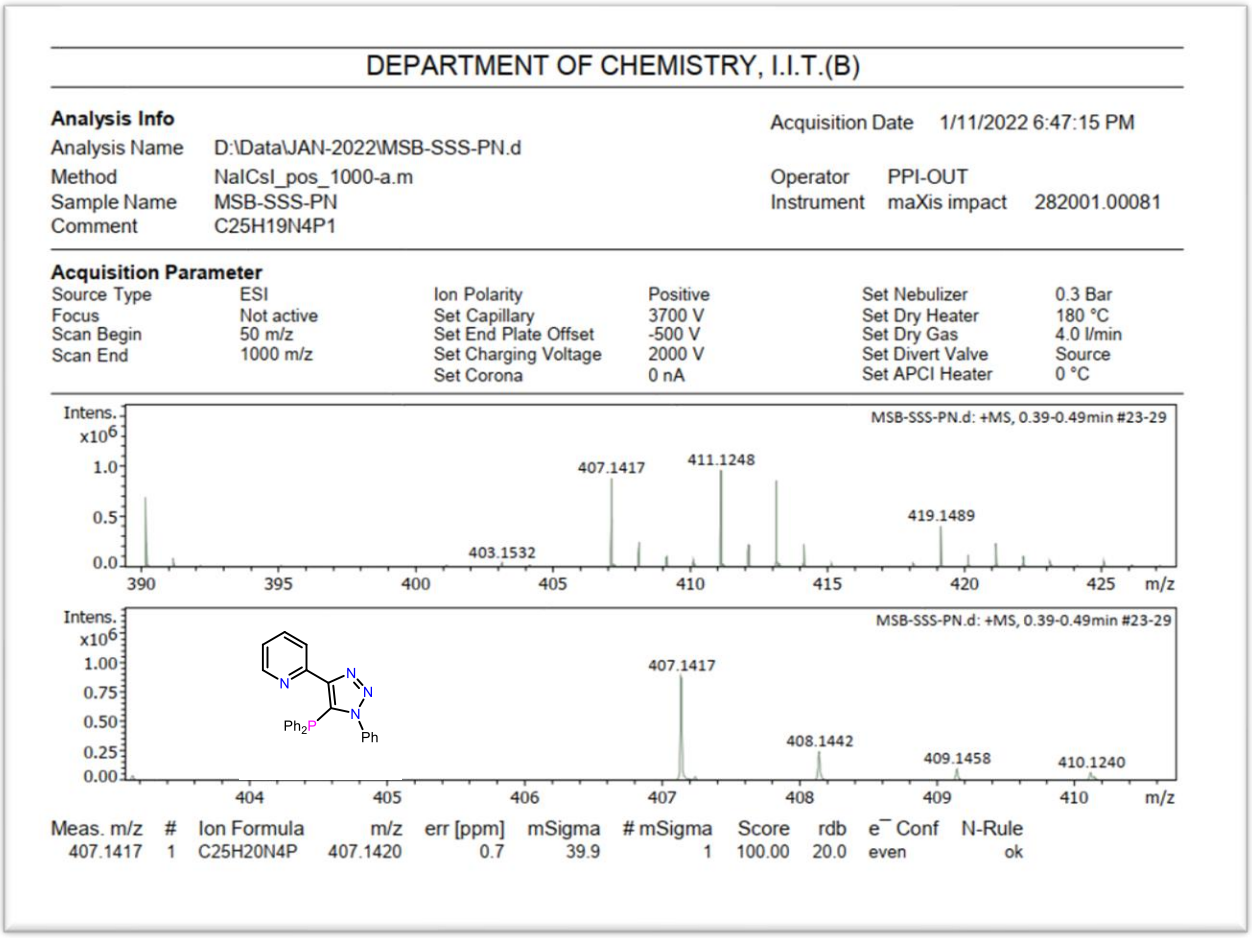

Fig. S10. HRMS spectrum of **1**.

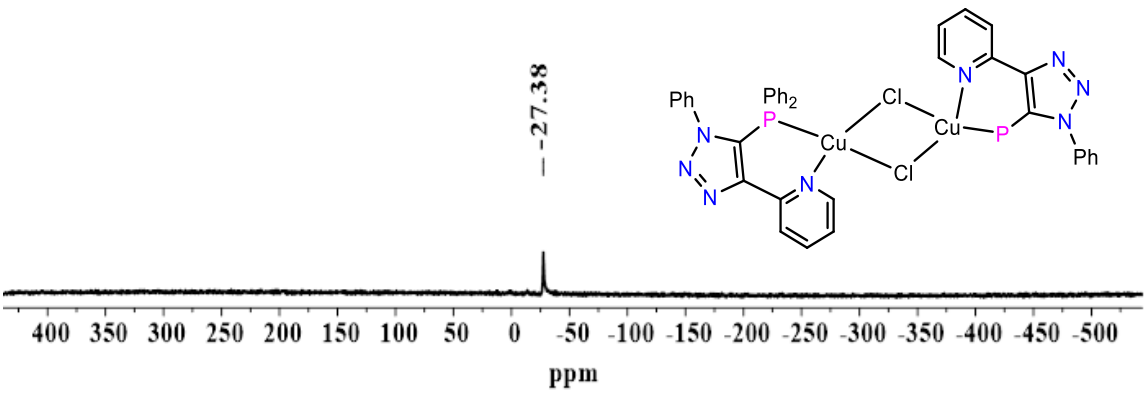

Fig. S11. $^{31}P\{^{1}H\}$ NMR spectrum of **2** in DMSO-d_6 (162 MHz).

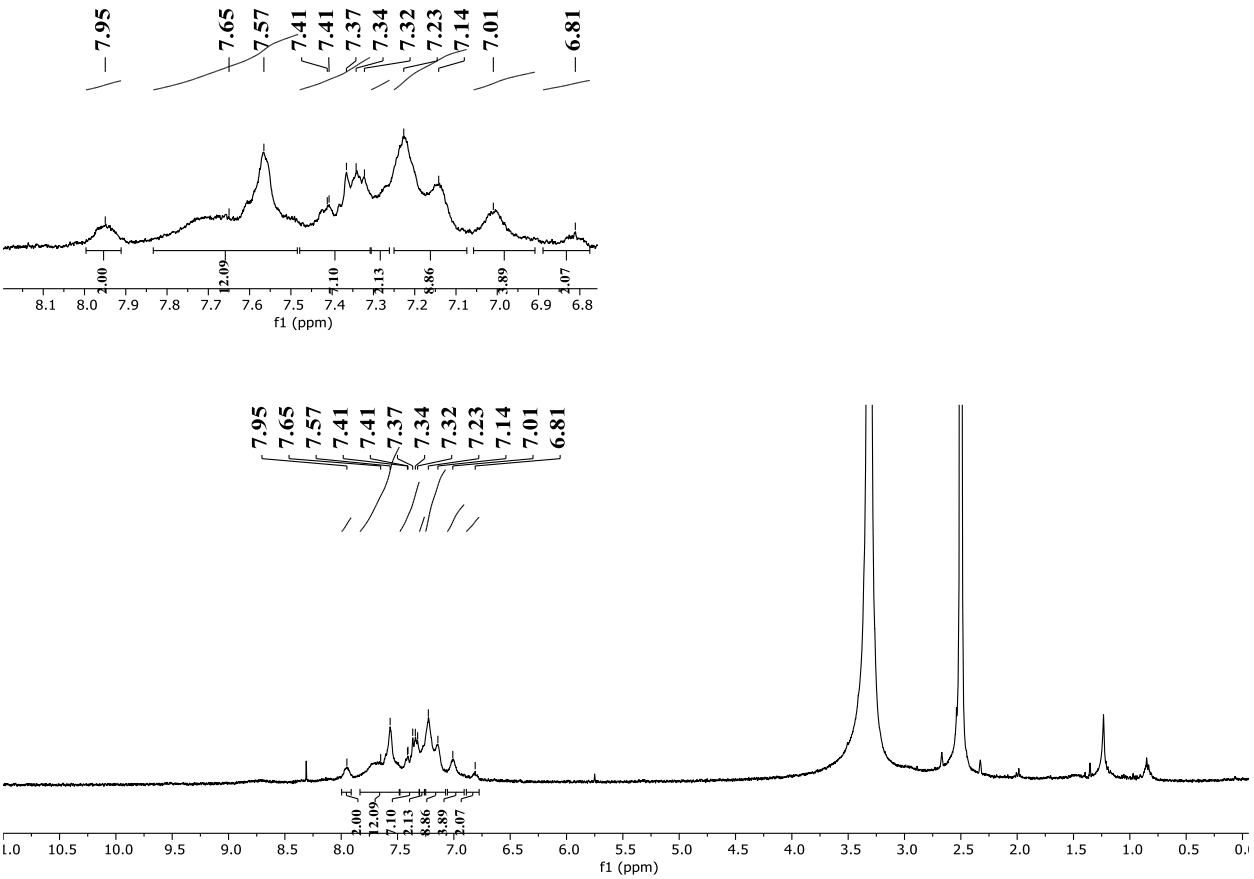

Fig. S12. ^{1}H NMR spectrum of **2** in DMSO-d_6 (400 MHz).

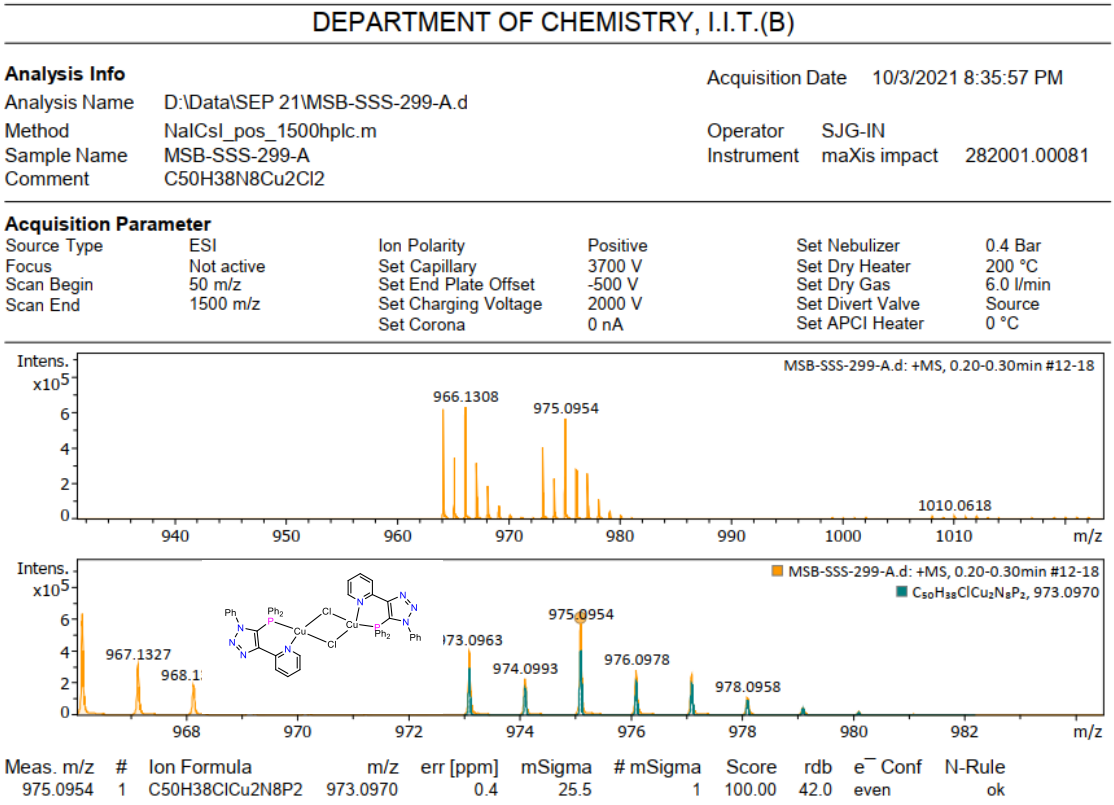

Fig. S13. HRMS spectrum of **2**.

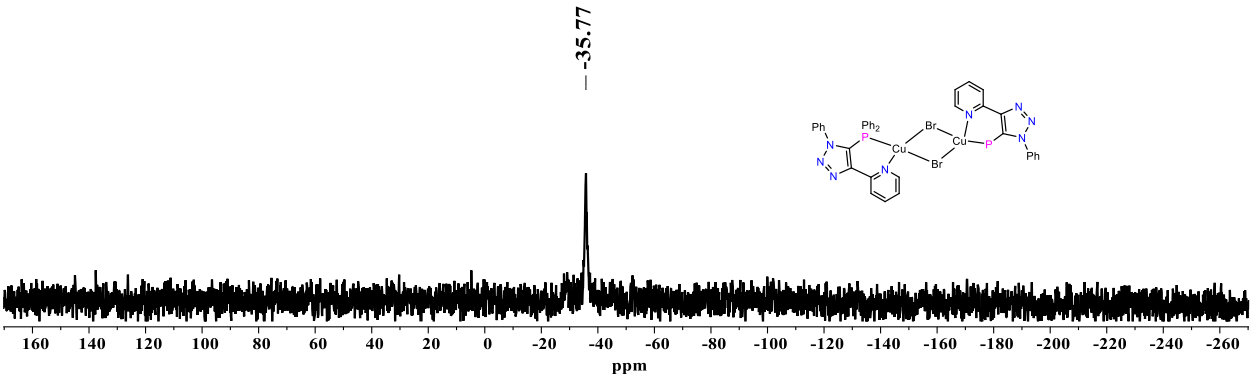

Fig. S14. $^{31}P\{^{1}H\}$ NMR spectrum of **3** in DMSO-d_6 (162 MHz).

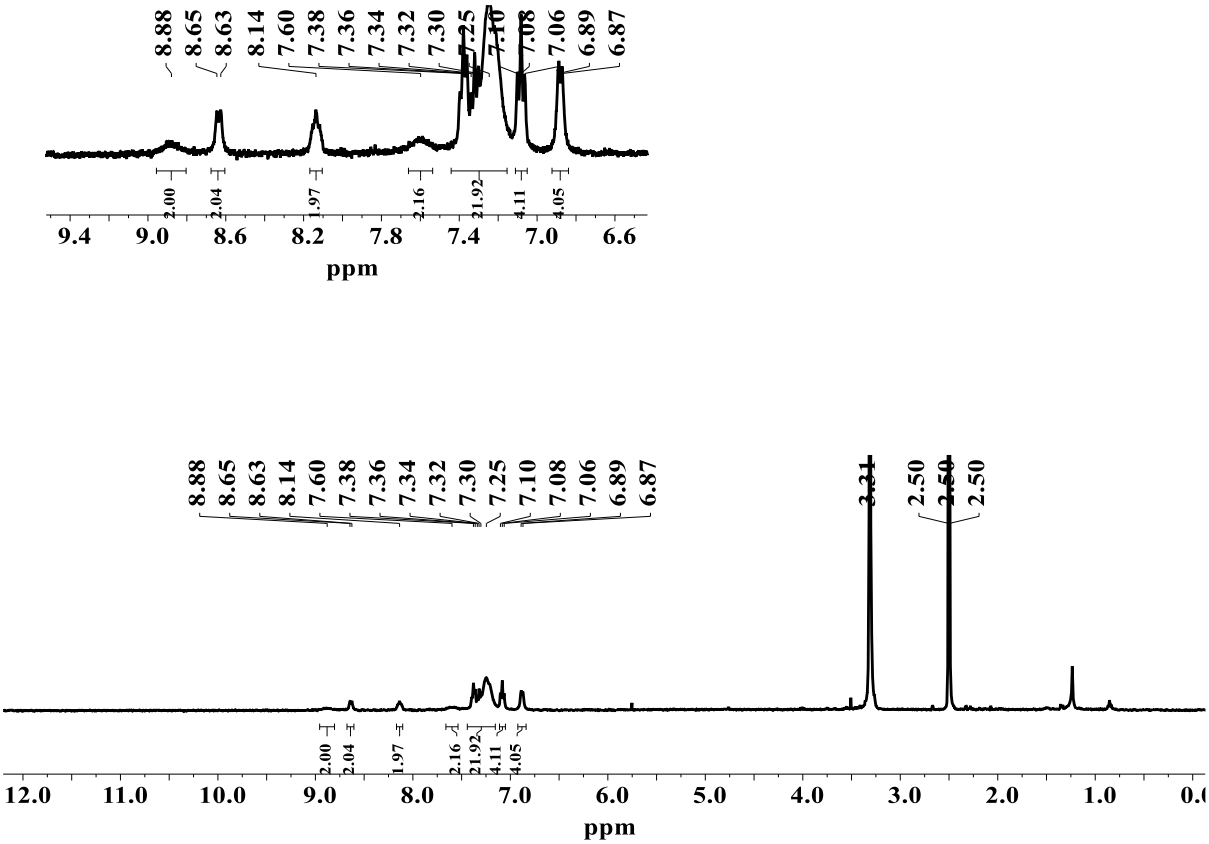

Fig. S15. ^{1}H NMR spectrum of **3** in DMSO-d_6 (400 MHz).

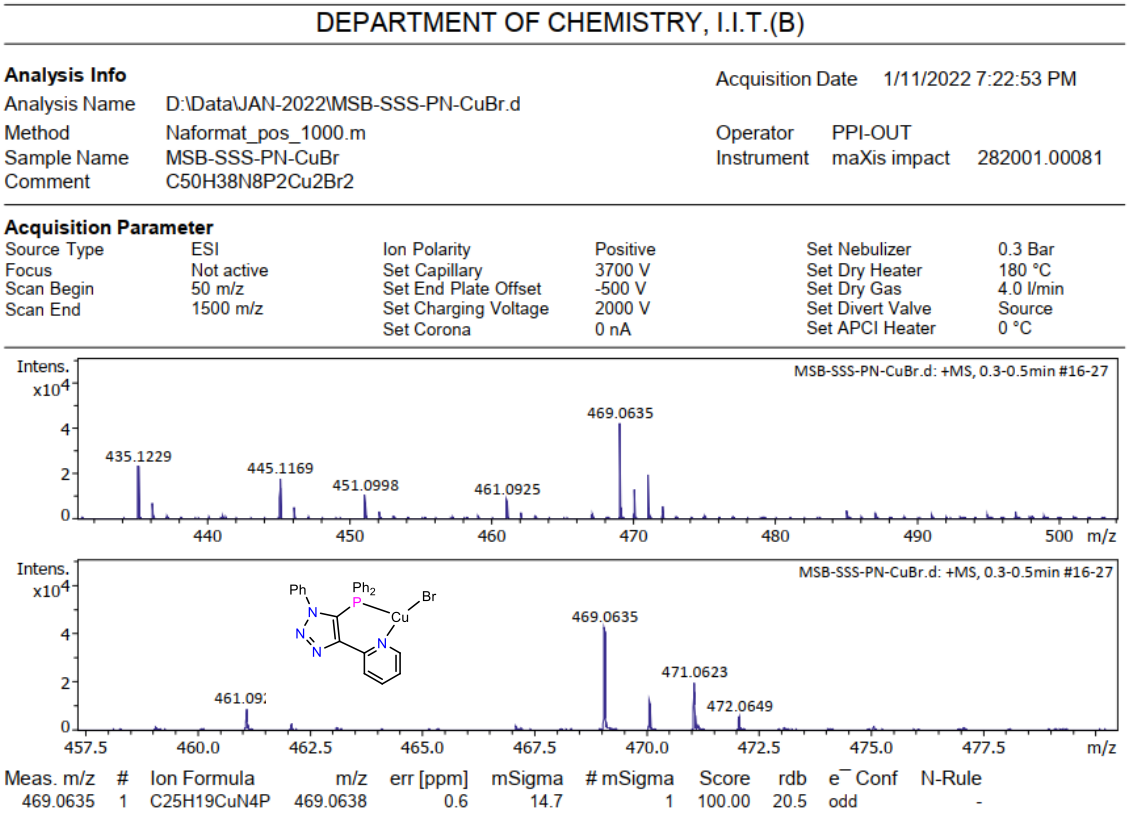

Fig. S16a. HRMS spectrum of **3**.

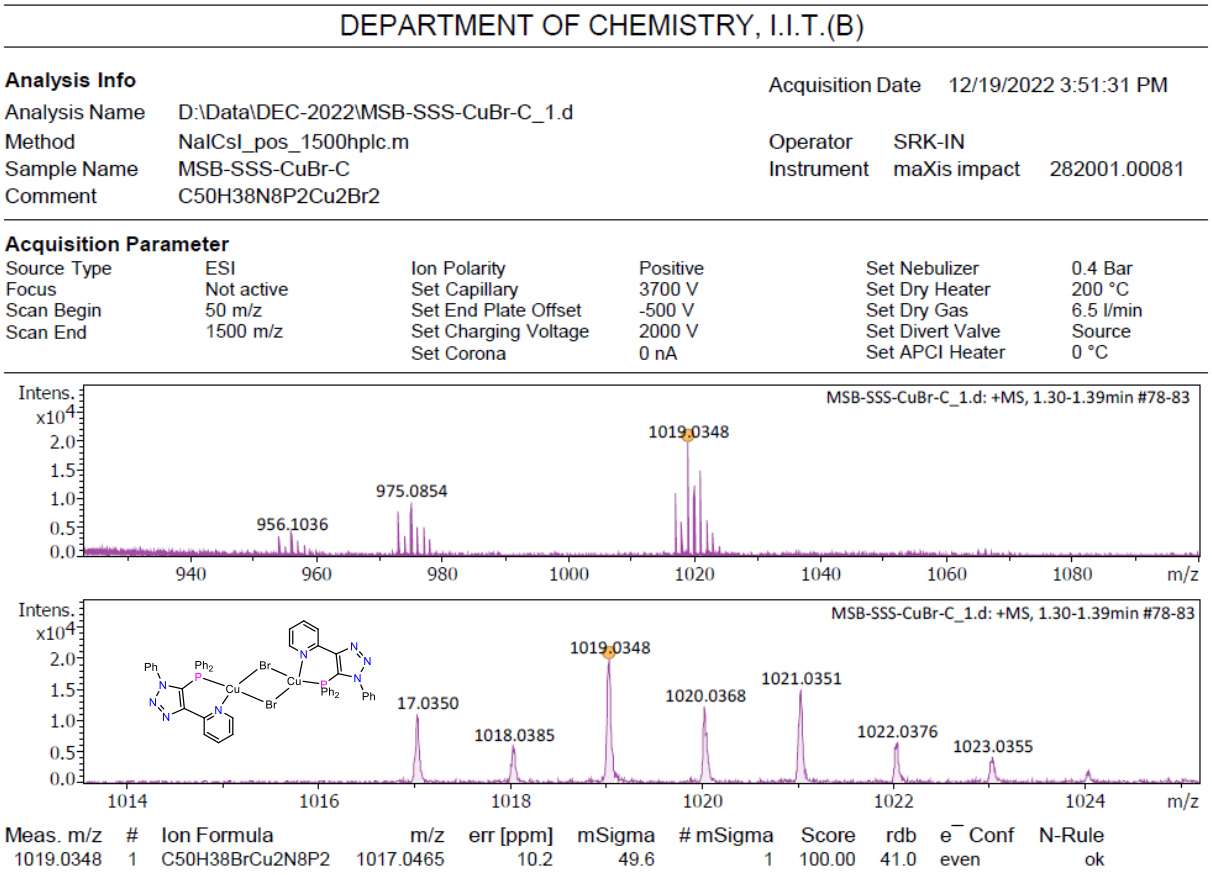

Fig. S16b. HRMS spectrum of **3**.

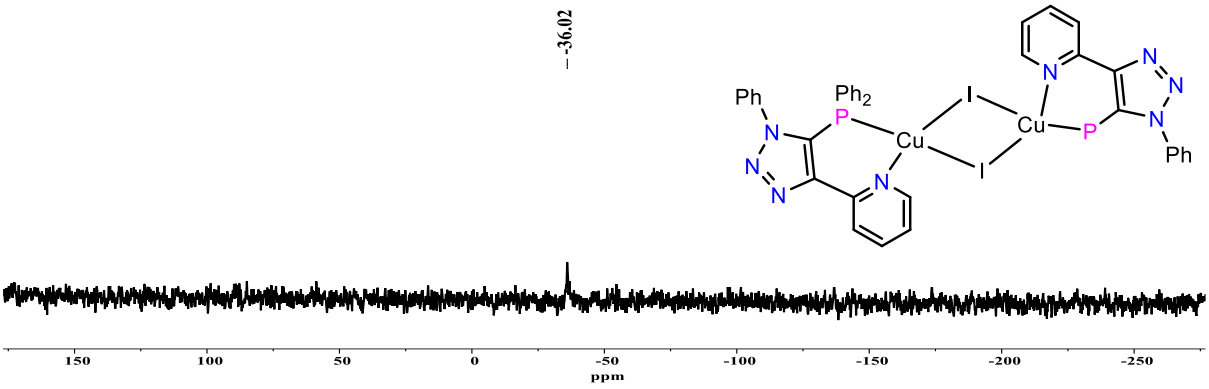

Fig. S17. $^{31}P\{^{1}H\}$ NMR spectrum of **4** in DMSO-d_6 (162 MHz).

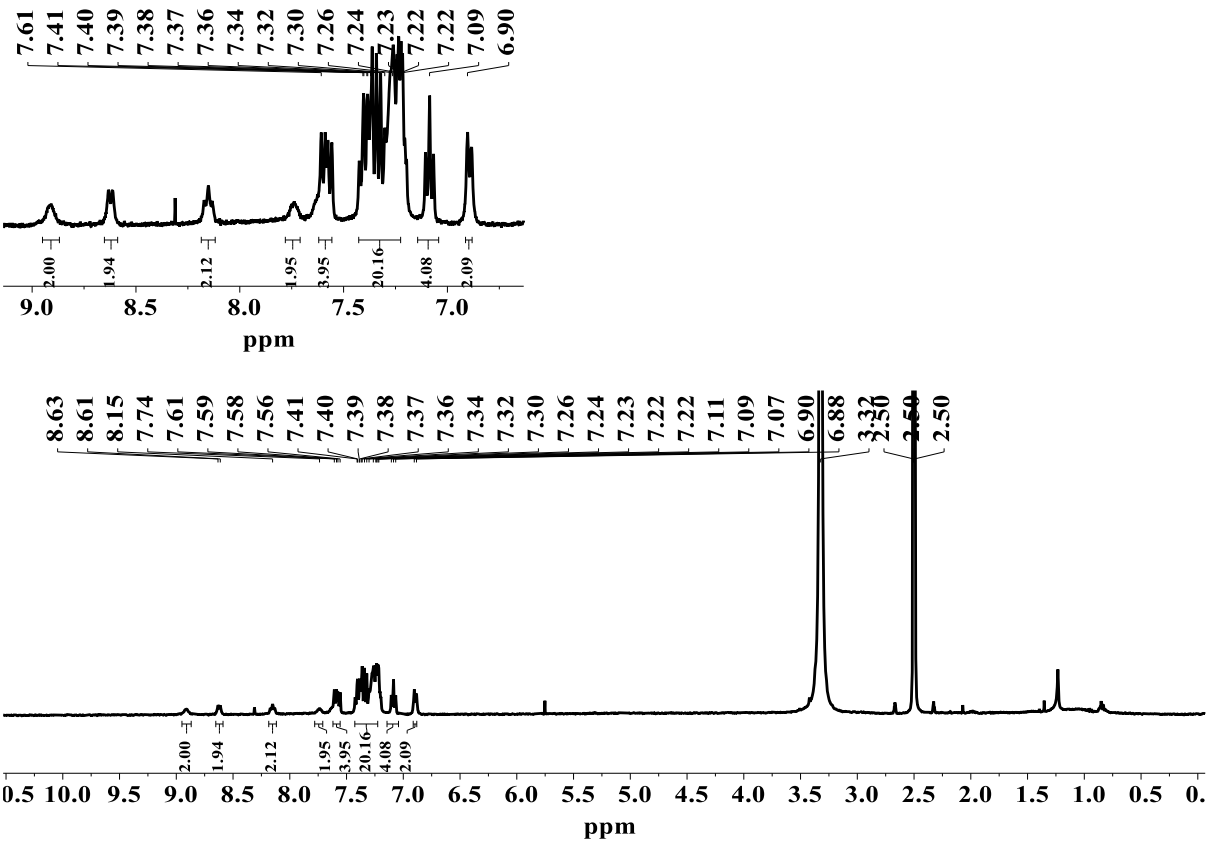

Fig. S18. ^{1}H NMR spectrum of **4** in DMSO-d_6 (400 MHz).

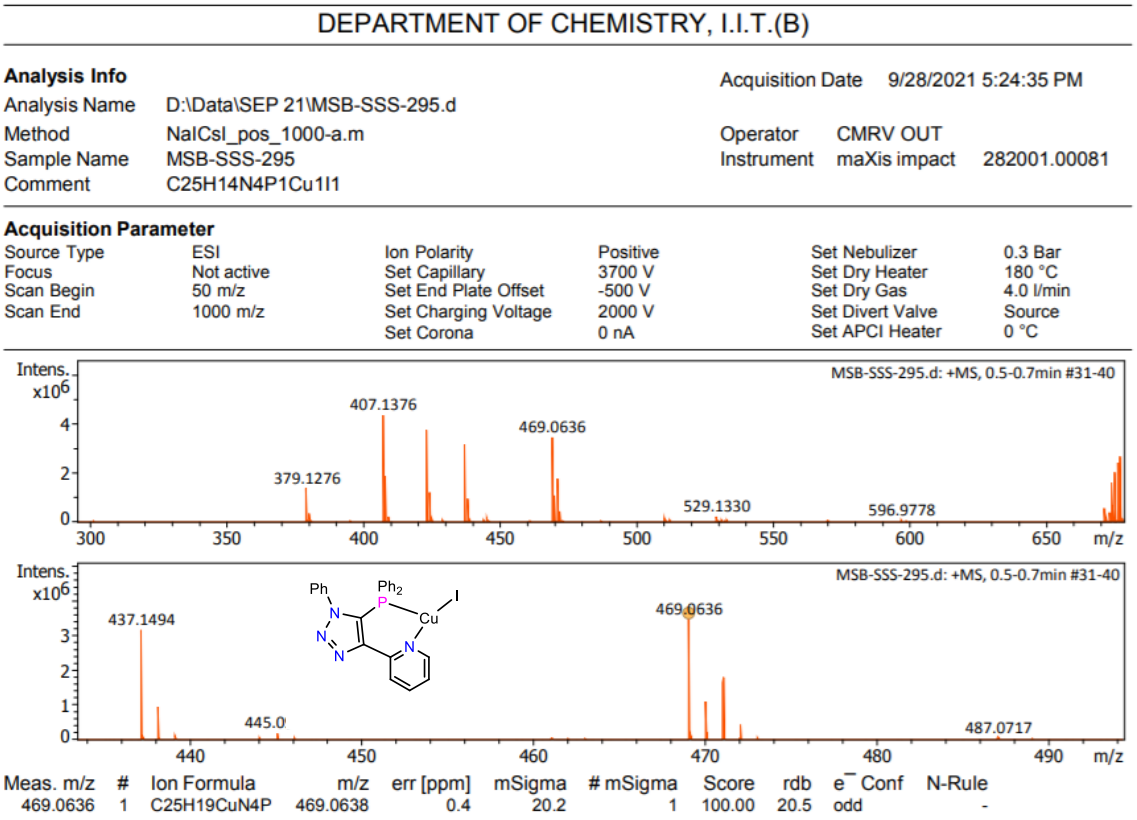

Fig. S19a. HRMS spectrum of **4**.

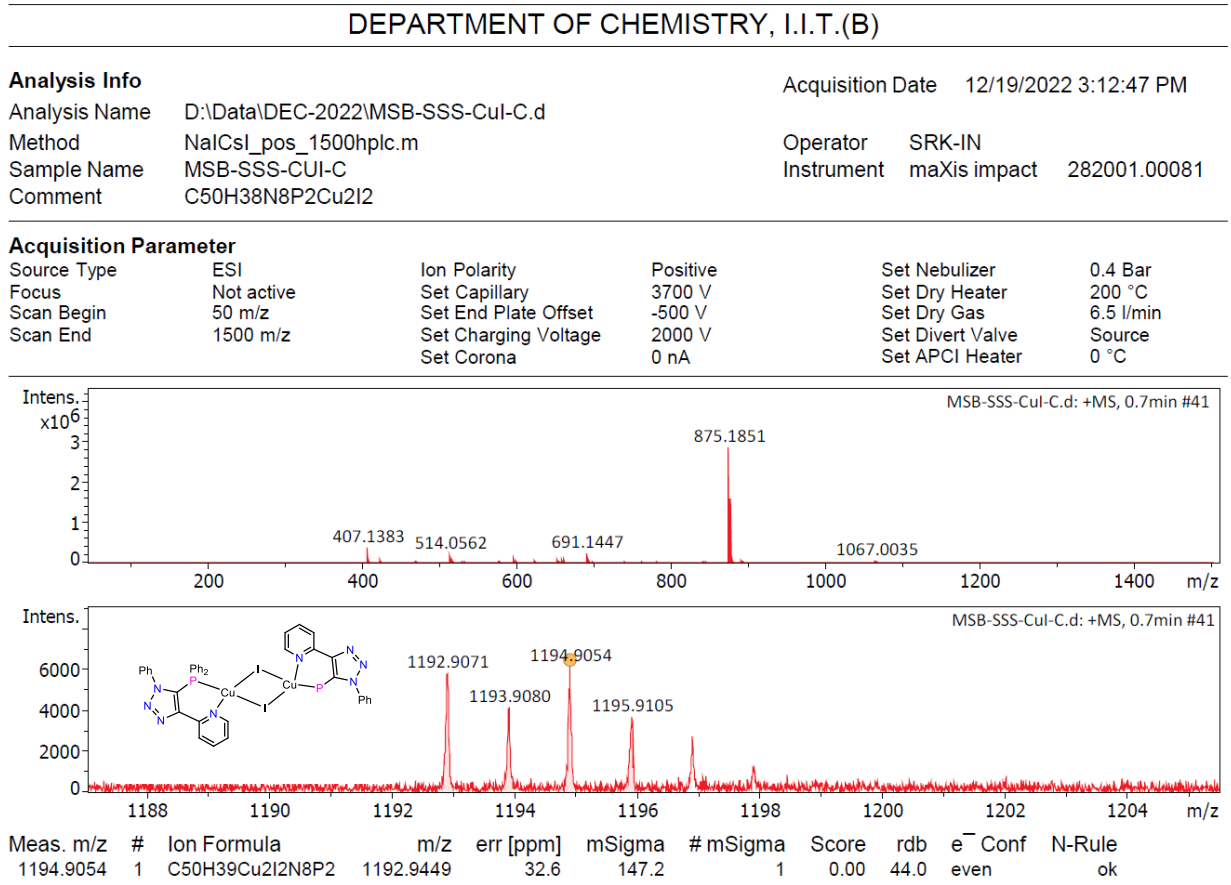

Fig. S19b. LRMS spectrum of **4**

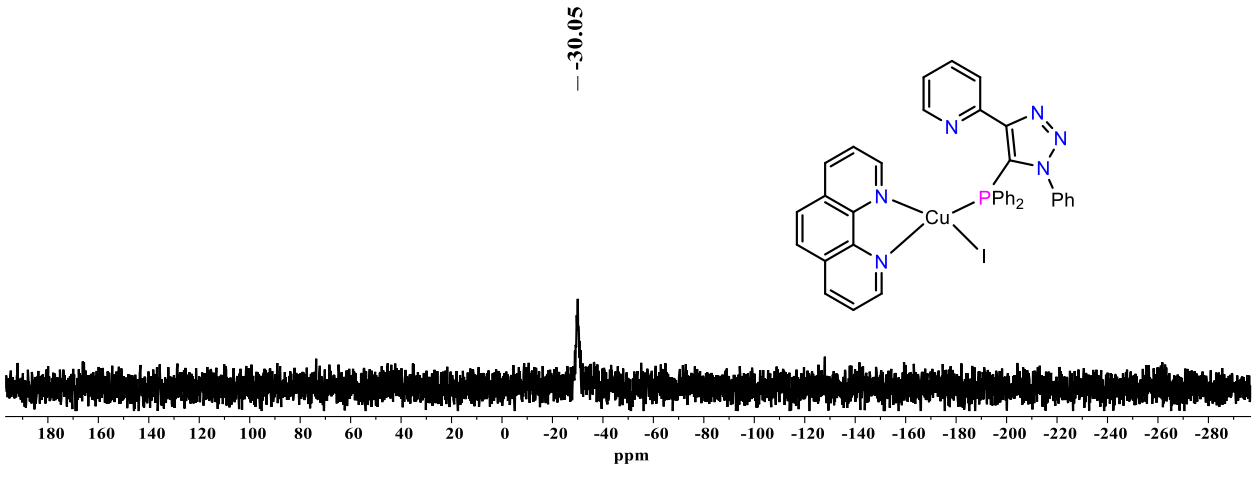

Fig. S20. $^{31}P\{^{1}H\}$ NMR spectrum of **5** in DMSO-d_6 (202 MHz).

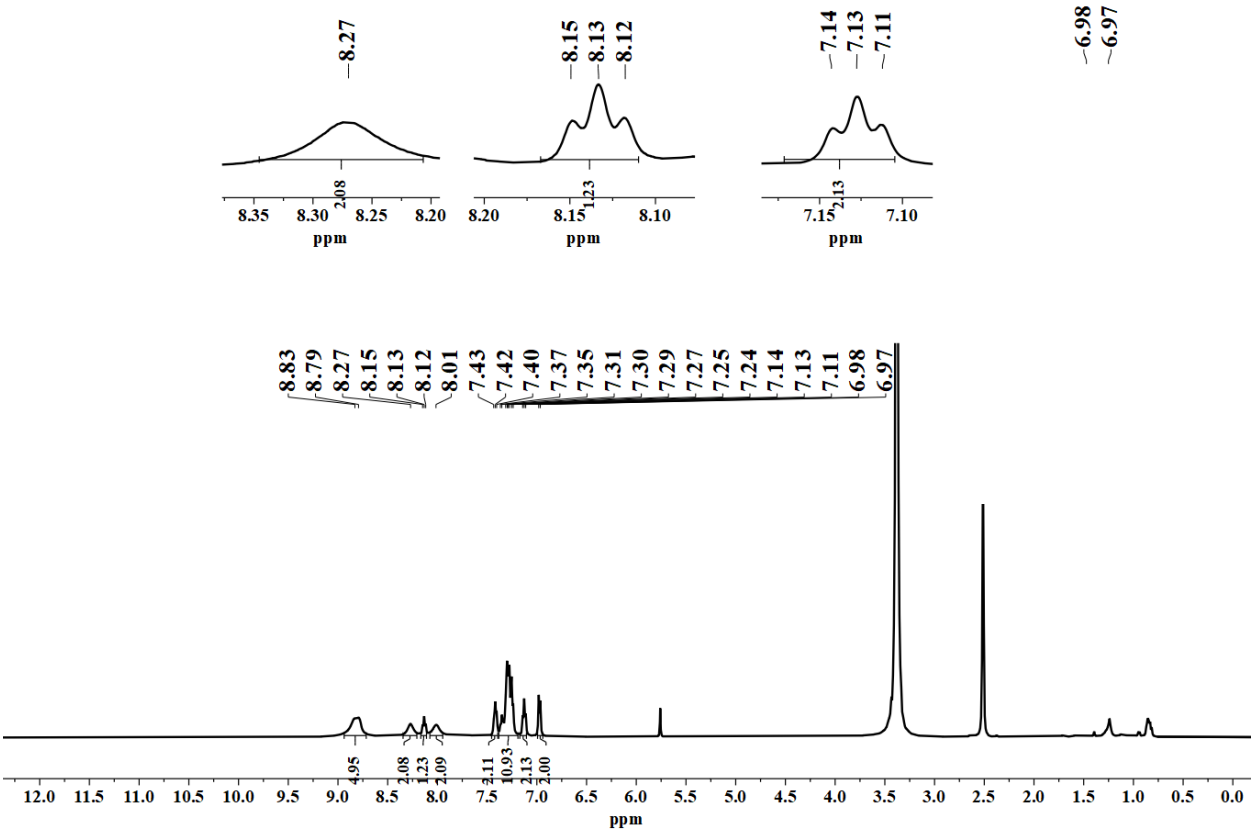

Fig. S21. ^{1}H NMR spectrum of **5** in DMSO-d_6 (500 MHz).

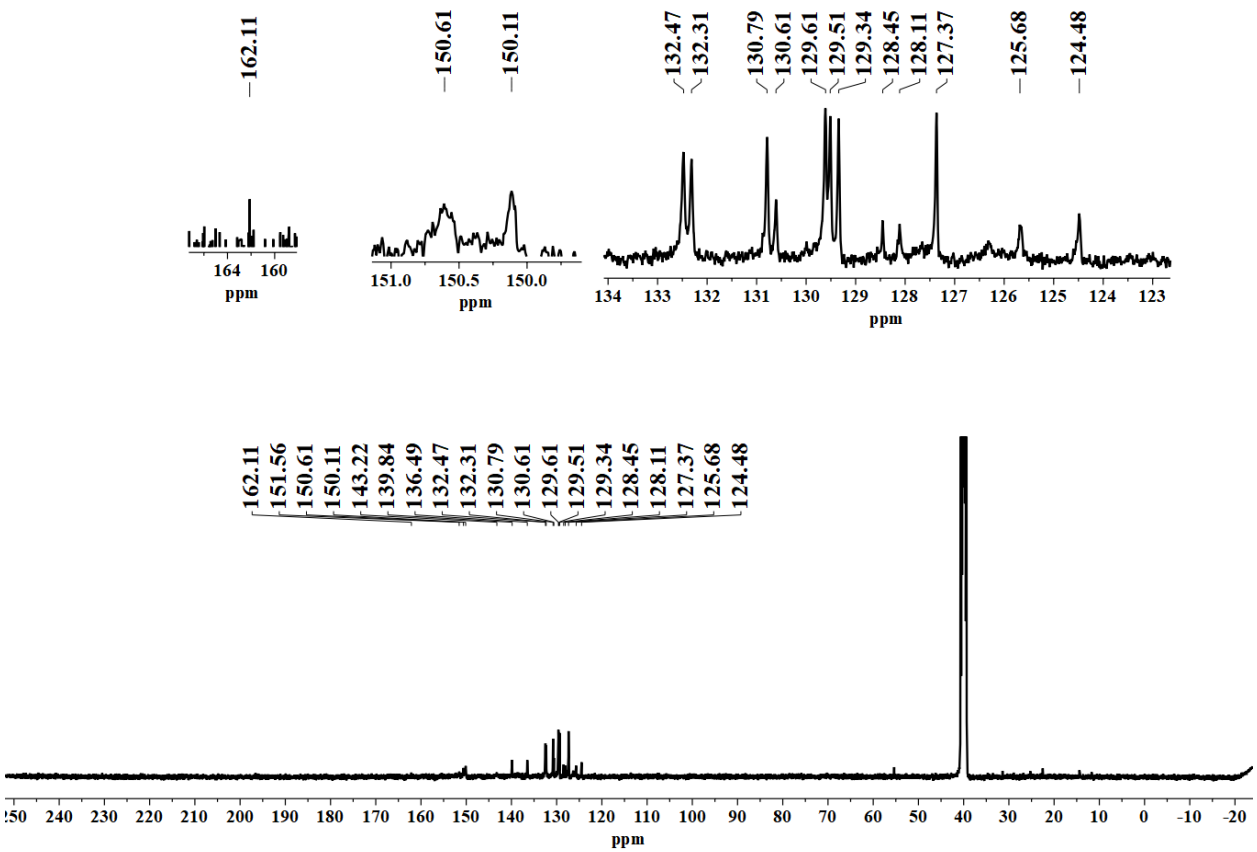

Fig. S22. $^{13}C\{^{1}H\}$ NMR spectrum of **5** in DMSO-d_6 (101 MHz).

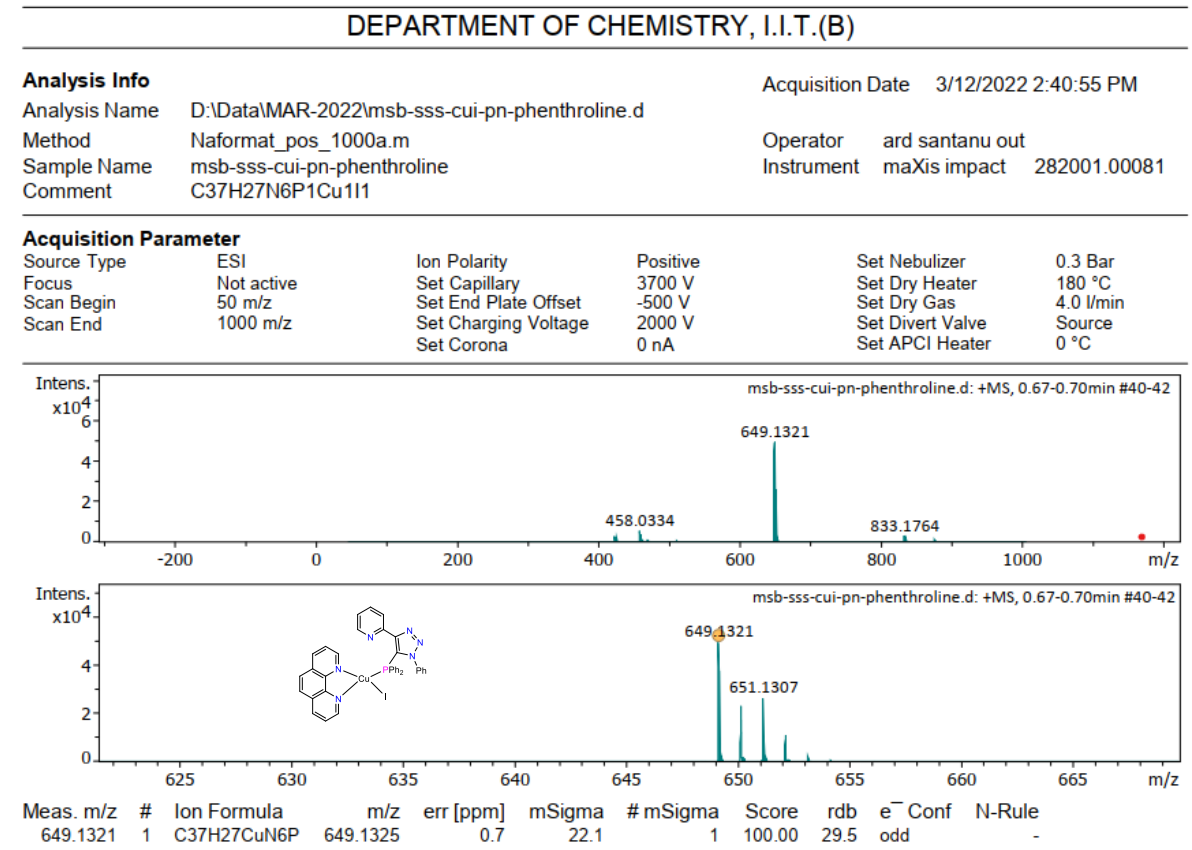

Fig. S23. HRMS spectrum of **5**.

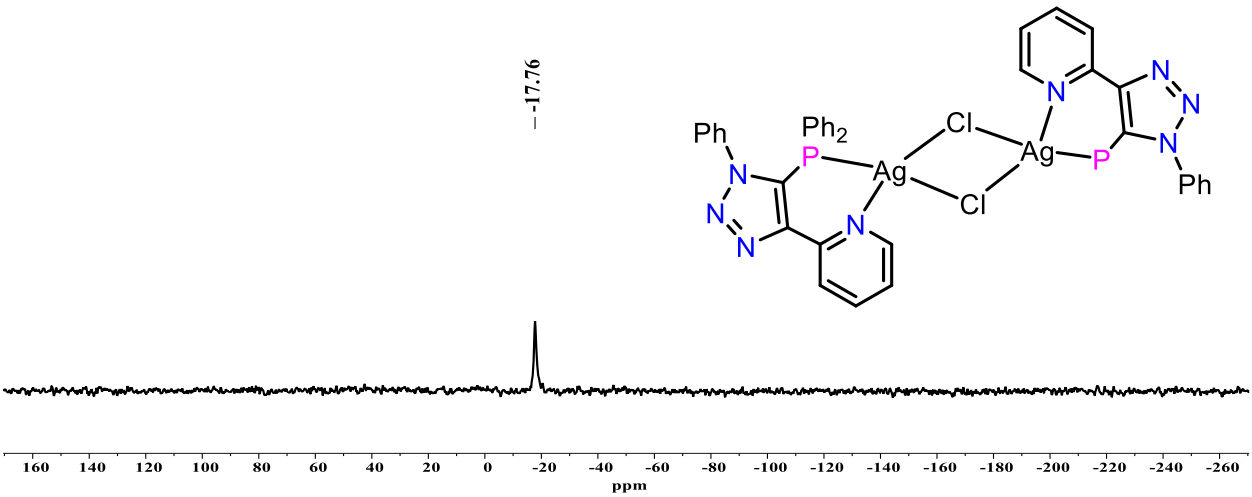

Fig. S24. $^{31}P\{^{1}H\}$ NMR spectrum of **6** in $CDCl_3$ (162 MHz).

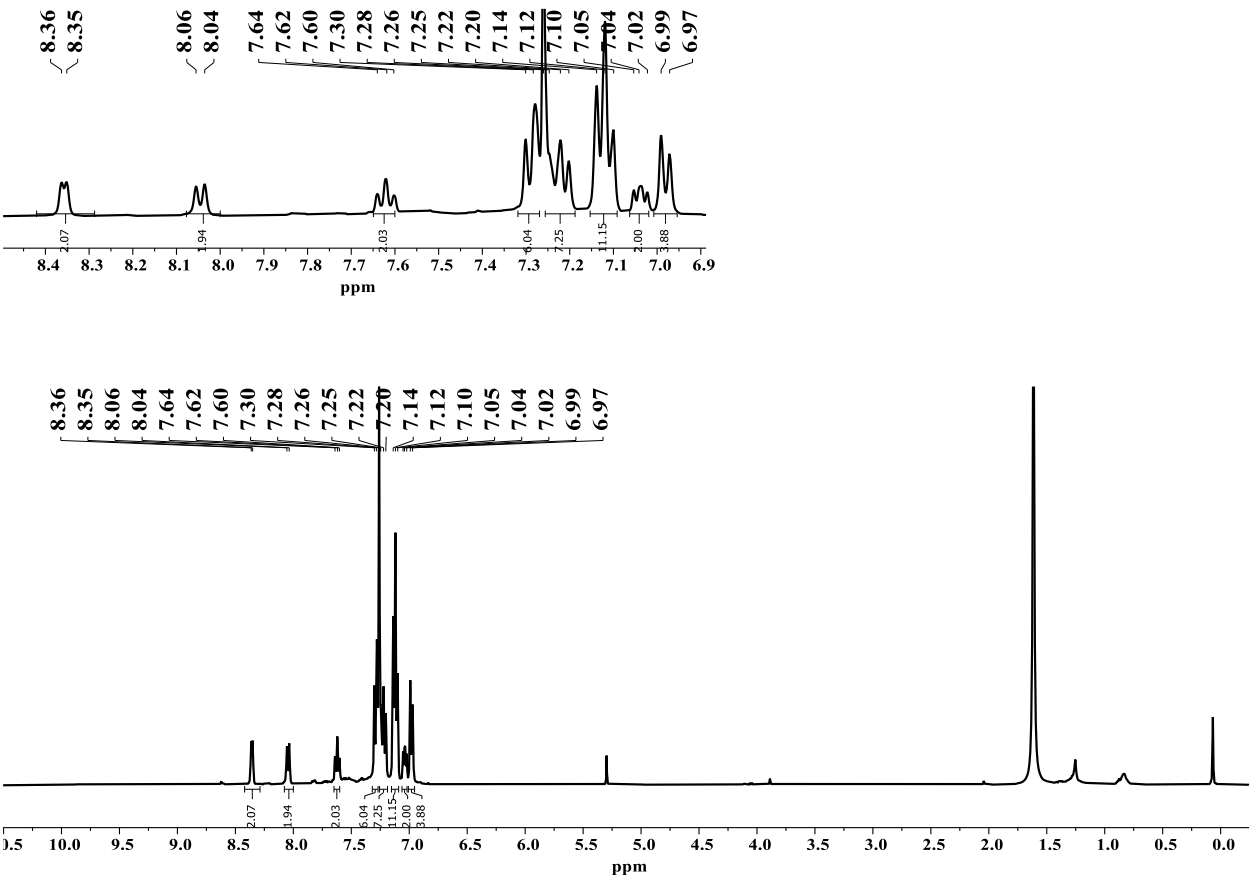

Fig. S25. ^{1}H NMR spectrum of **6** in $CDCl_3$ (400 MHz).

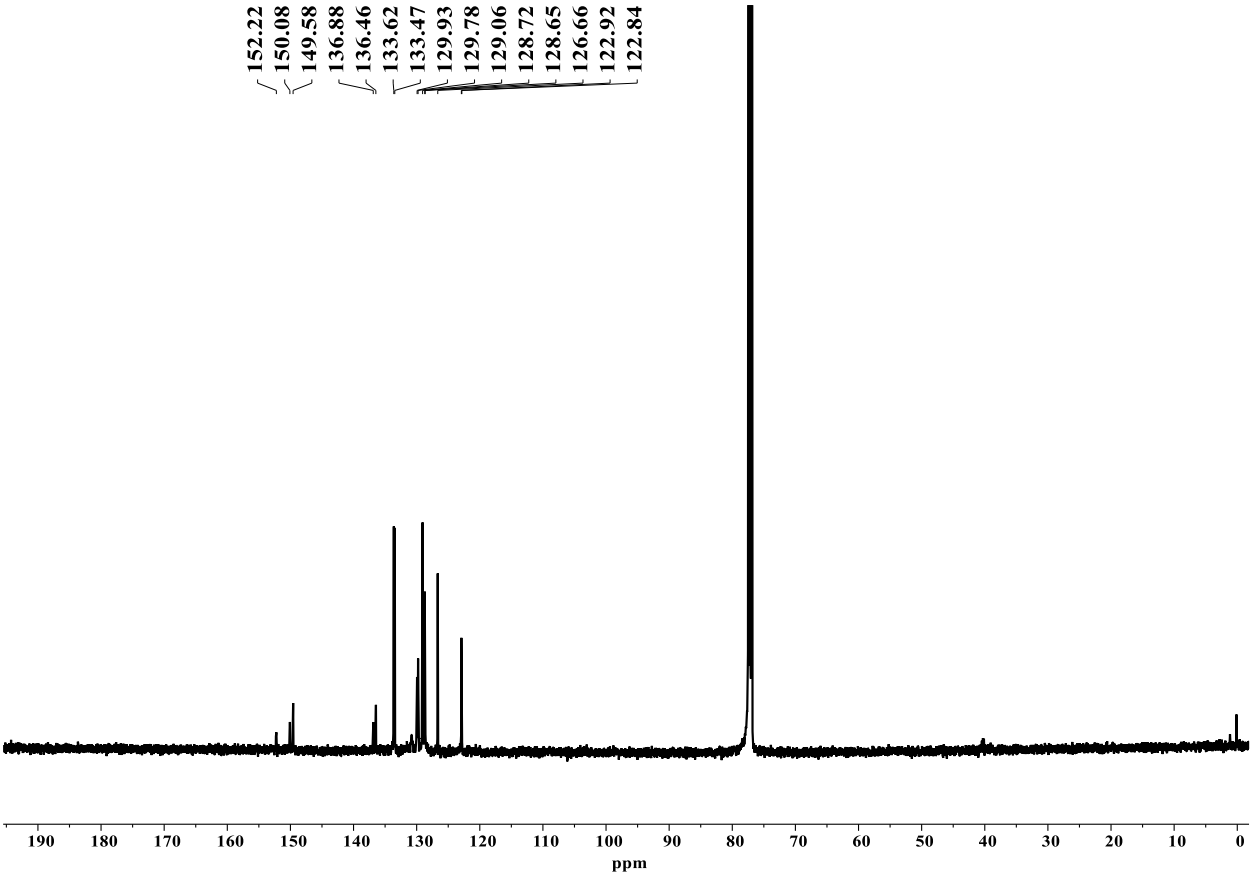

Fig. S26. $^{13}C\{^{1}H\}$ NMR spectrum of **6** in $CDCl_3$ (100 MHz).

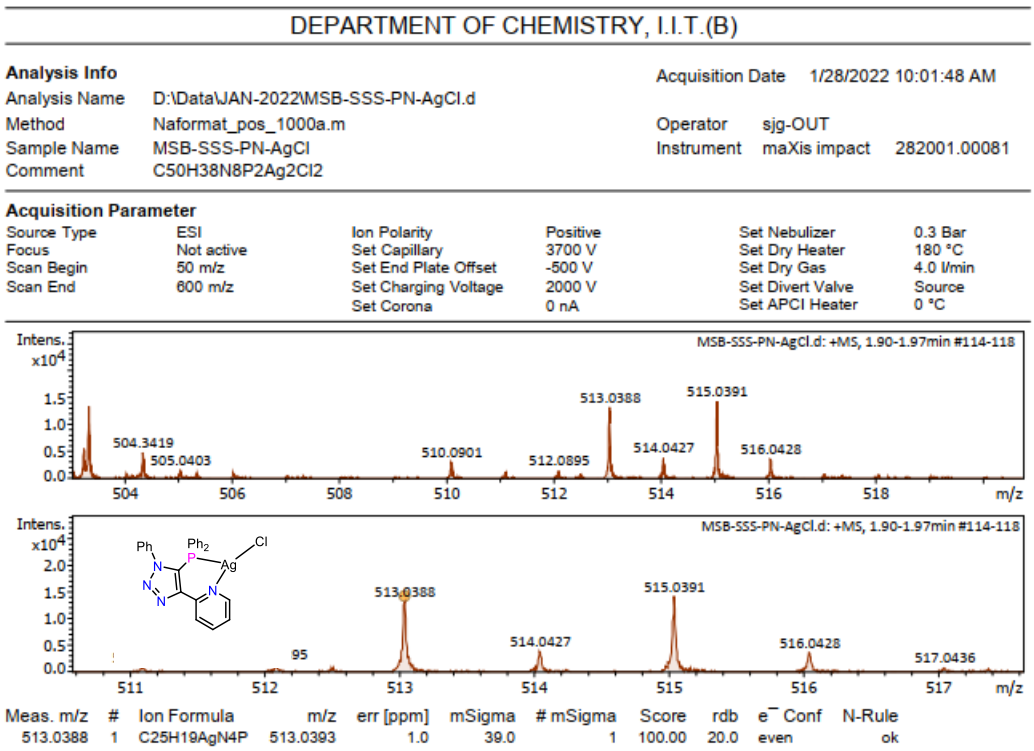

Fig. S27a. HRMS spectrum of **6**.

DEPARTMENT OF CHEMISTRY, I.I.T.(B)

Analysis Info

Analysis Name	D:\Data\DEC-2022\MSB-SSS-AGCl-B.d	Acquisition Date	12/19/2022 2:46:32 PM
Method	Naformat_pos_1500A.m	Operator	SRK-IN
Sample Name	MSB-SSS-AGCl-B	Instrument	maXis impact 282001.00081
Comment	C50H38N8P2Ag2Cl2		

Acquisition Parameter

Source Type	ESI	Ion Polarity	Positive	Set Nebulizer	0.3 Bar
Focus	Not active	Set Capillary	3700 V	Set Dry Heater	180 °C
Scan Begin	50 m/z	Set End Plate Offset	-500 V	Set Dry Gas	4.0 l/min
Scan End	1500 m/z	Set Charging Voltage	2000 V	Set Divert Valve	Source
		Set Corona	0 nA	Set APCI Heater	0 °C

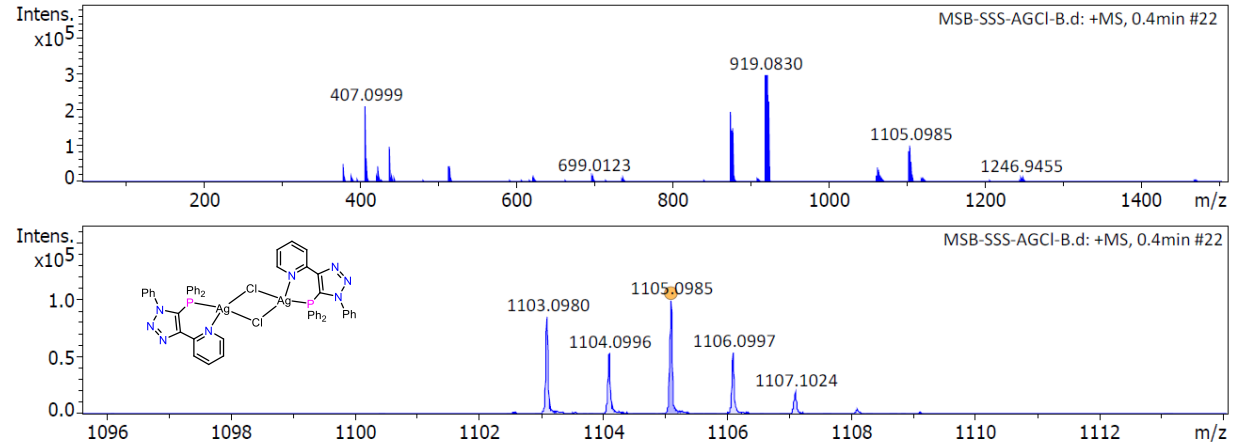

Meas. m/z	#	Ion Formula	m/z	err [ppm]	mSigma	# mSigma	Score	rdb	e¯ Conf	N-Rule
1105.0985	1	C50H38Ag2Cl2LiN8P2	1103.0328	-60.0	344.5	3	100.00	43.0	even	ok

Fig. S27b. LRMS spectrum of **6**.

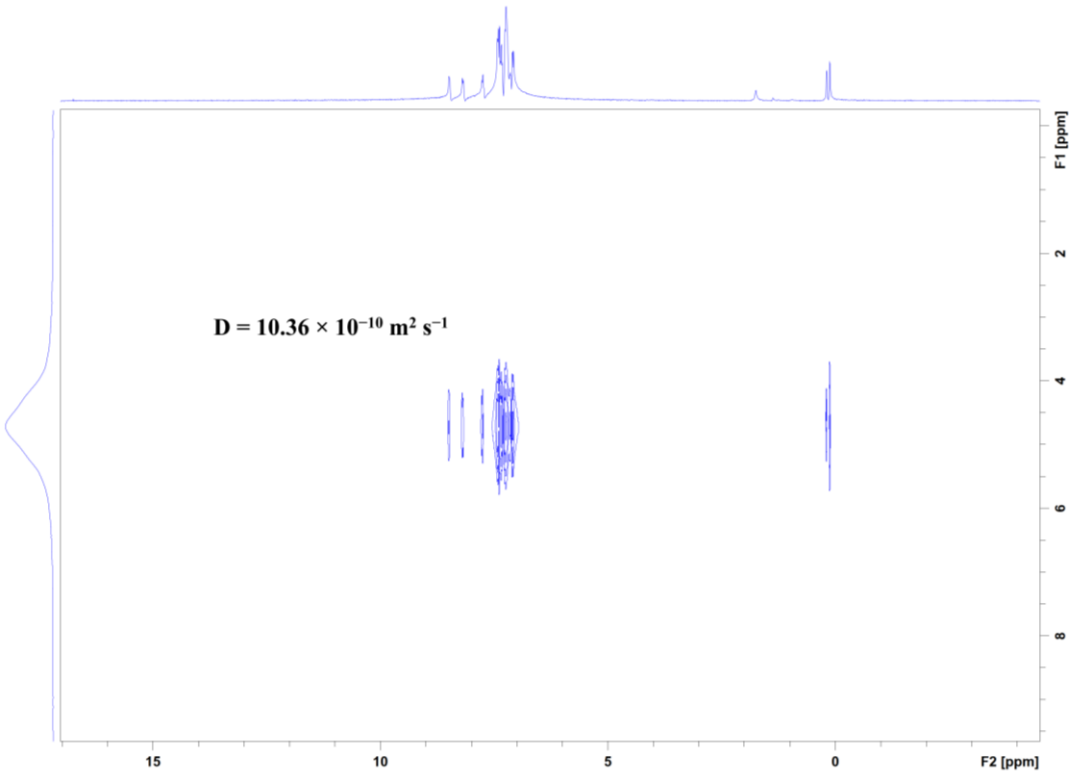

Fig. S28. DOSY ^{1}H NMR spectrum of complex **6** in $CDCl_3$ at 25 °C with the calculated diffusion coefficient.

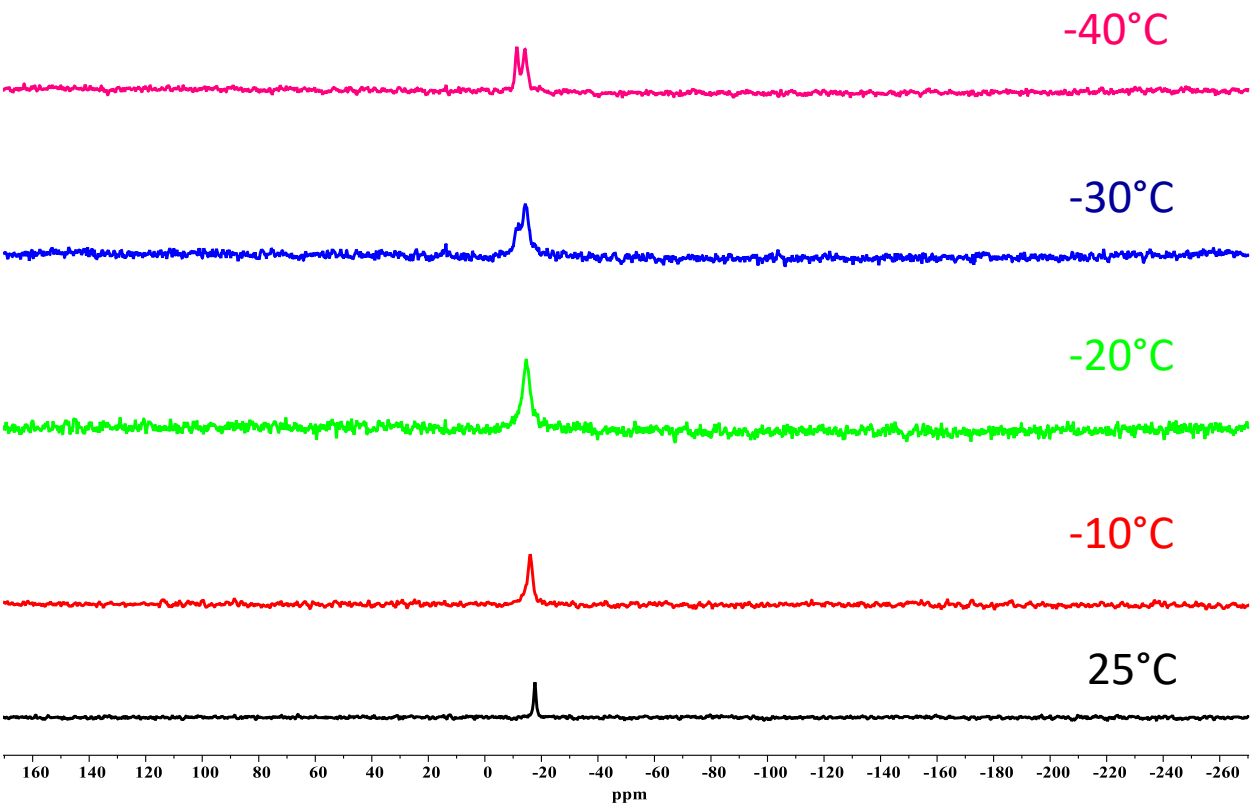

Fig. S29. $^{31}P\{^{1}H\}$ VT NMR spectrum of **6** in $CDCl_3$ (162 MHz).

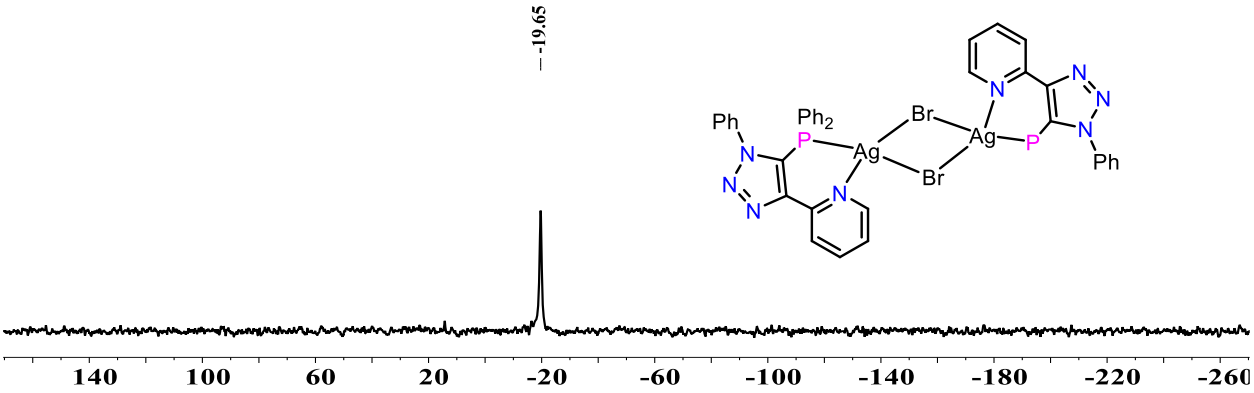

Fig. S30. $^{31}P\{^{1}H\}$ NMR spectrum of **7** in $CDCl_3$ (162 MHz).

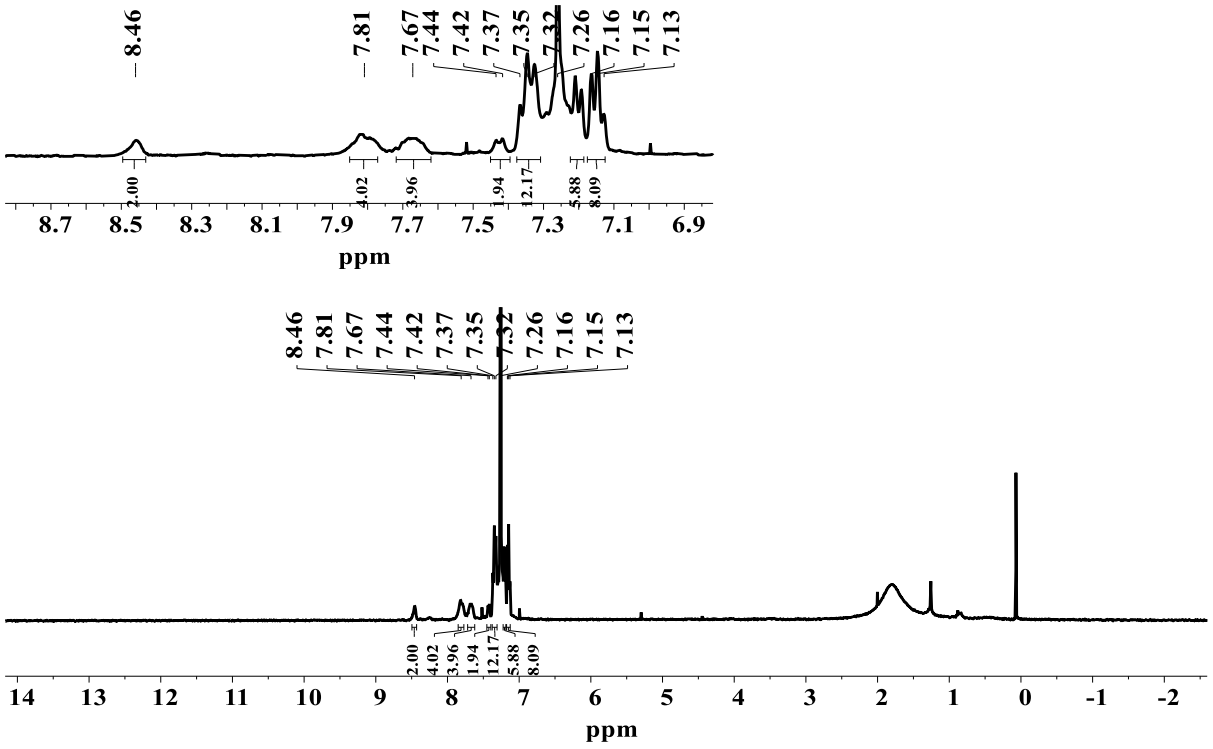

Fig. S31. ^{1}H NMR spectrum of **7** in $CDCl_3$ (400 MHz).

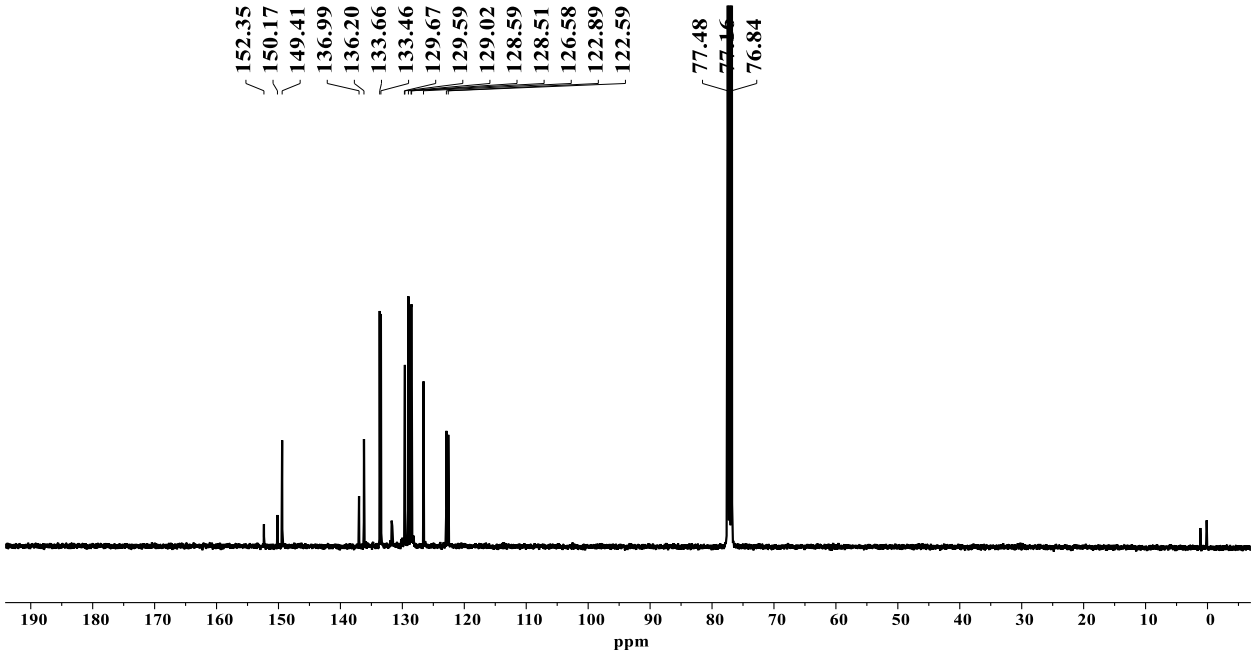

Fig. S32. $^{13}C\{^{1}H\}$ NMR spectrum of **7** in $CDCl_3$ (101 MHz).

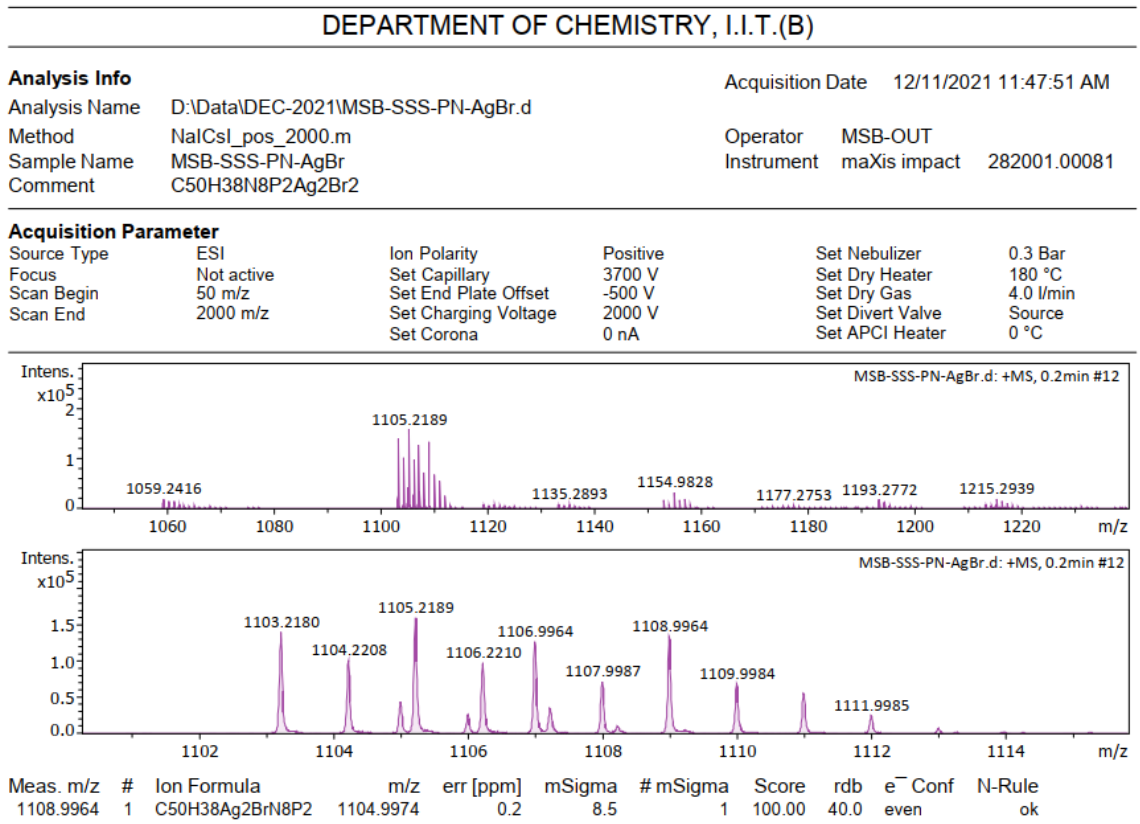

Fig. S33. HRMS spectrum of **7**.

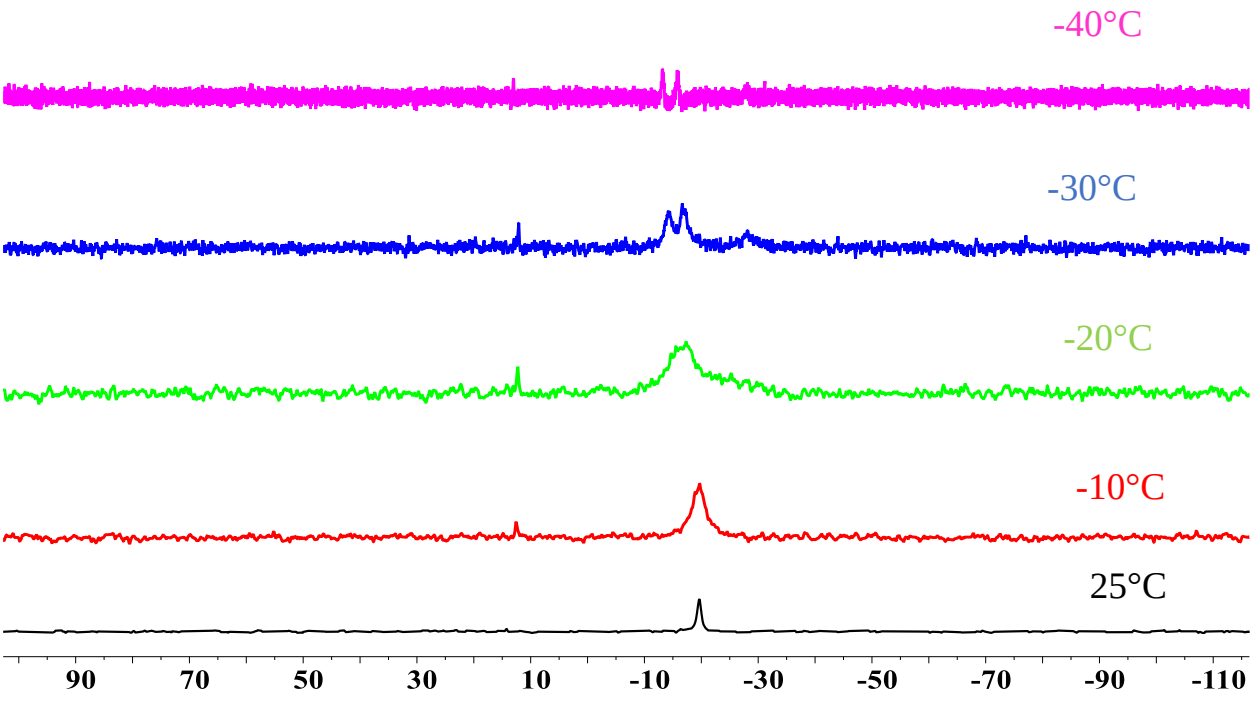

Fig. S34. $^{31}P\{^{1}H\}$ VT NMR spectrum of **7** in $CDCl_3$ (162 MHz).

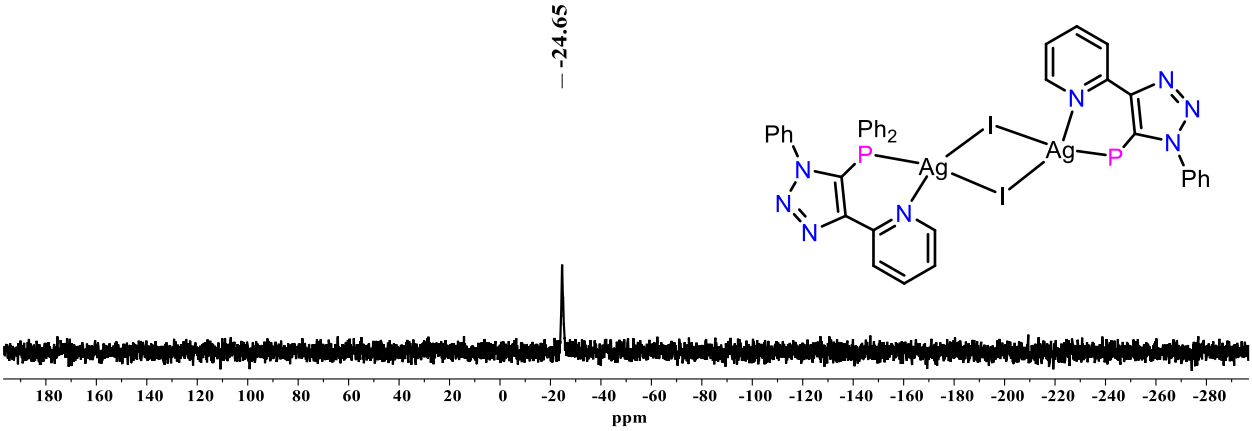

Fig. S35. $^{31}P\{^{1}H\}$ NMR spectrum of **8** in $CDCl_3$ (162 MHz).

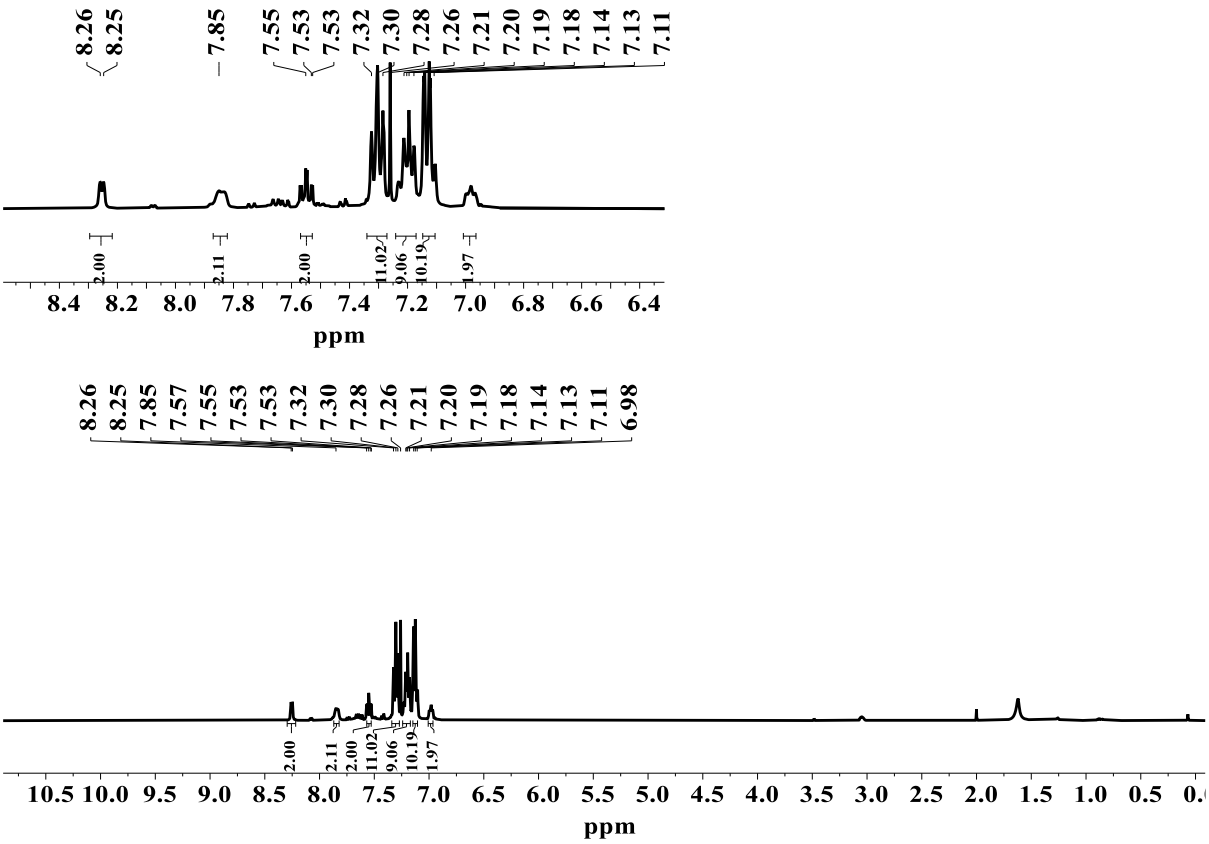

Fig. S36. ^{1}H NMR spectrum of **8** in $CDCl_3$ (400 MHz).

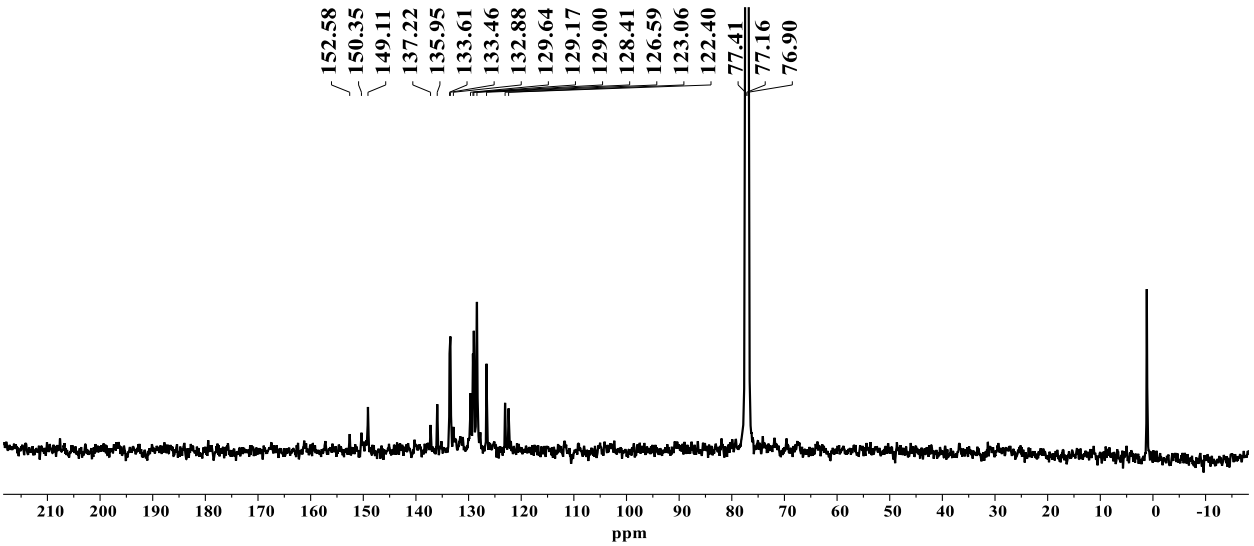

Fig. S37. $^{13}C\{^{1}H\}$ NMR spectrum of **8** in $CDCl_3$ (101 MHz).

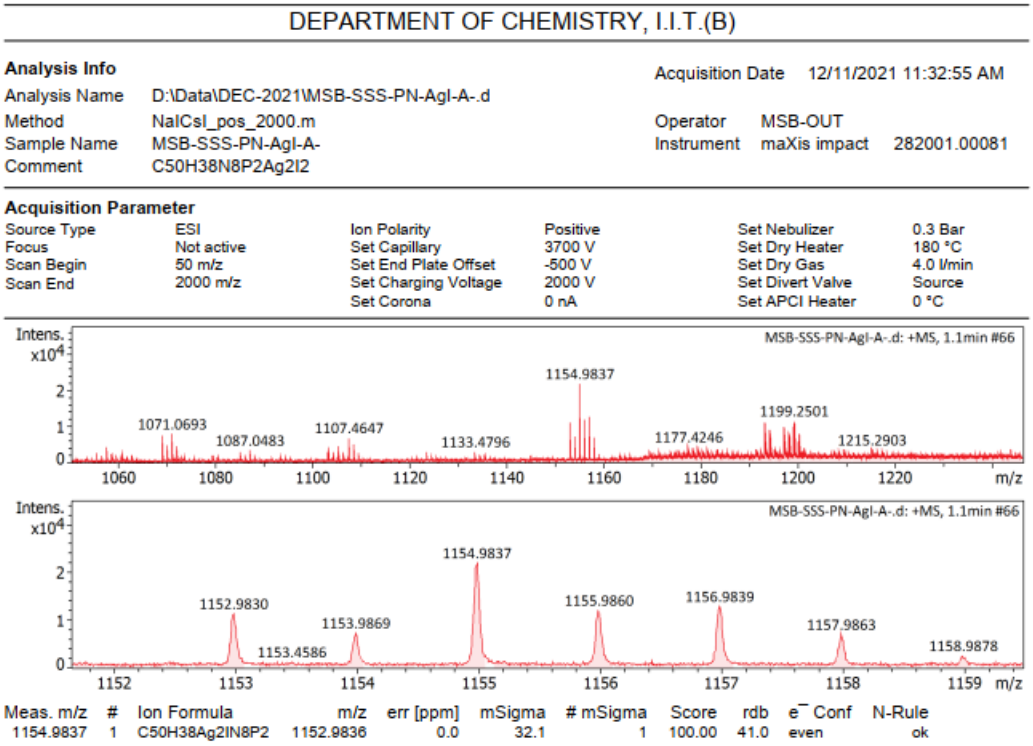

Fig. S38. HRMS spectrum of **8**.

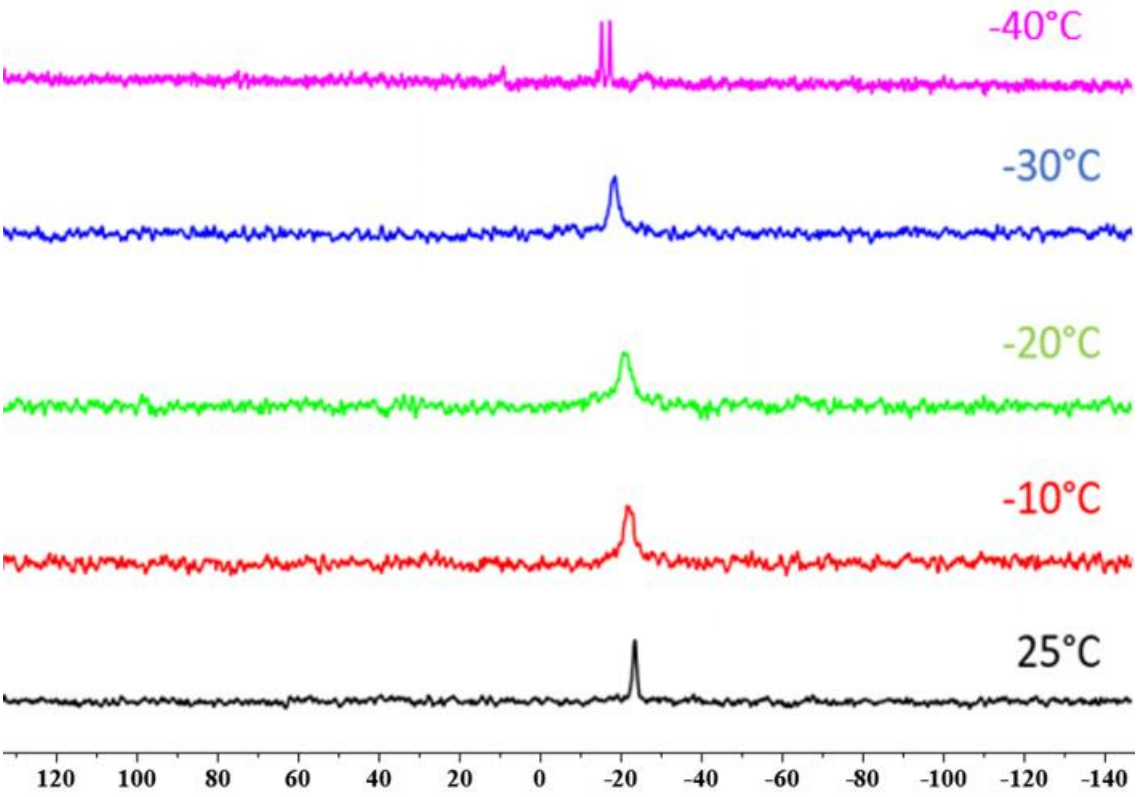

Fig. S39. $^{31}P\{^{1}H\}$ VT NMR spectrum of **8** in $CDCl_3$ (162 MHz).

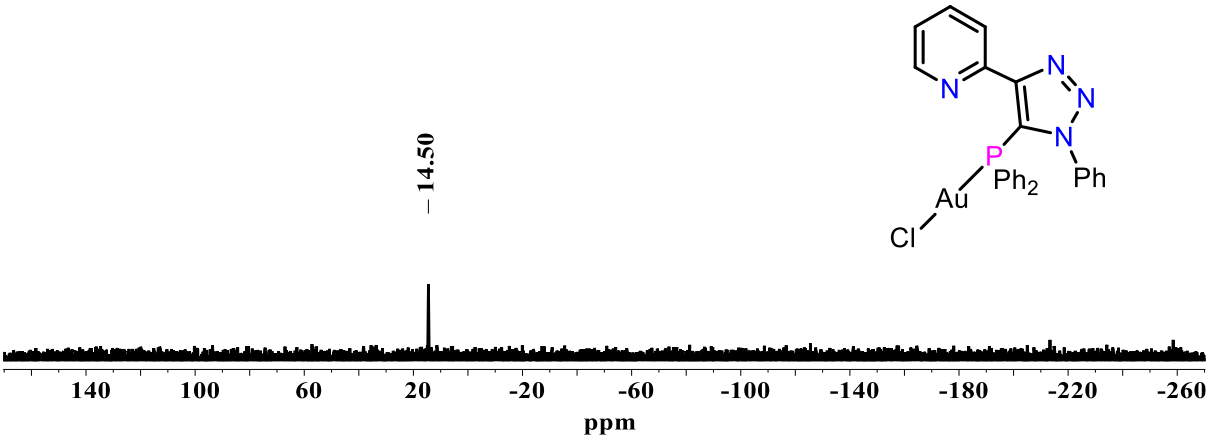

Fig. S40. $^{31}P\{^{1}H\}$ NMR spectrum of **9** in $CDCl_3$ (162 MHz).

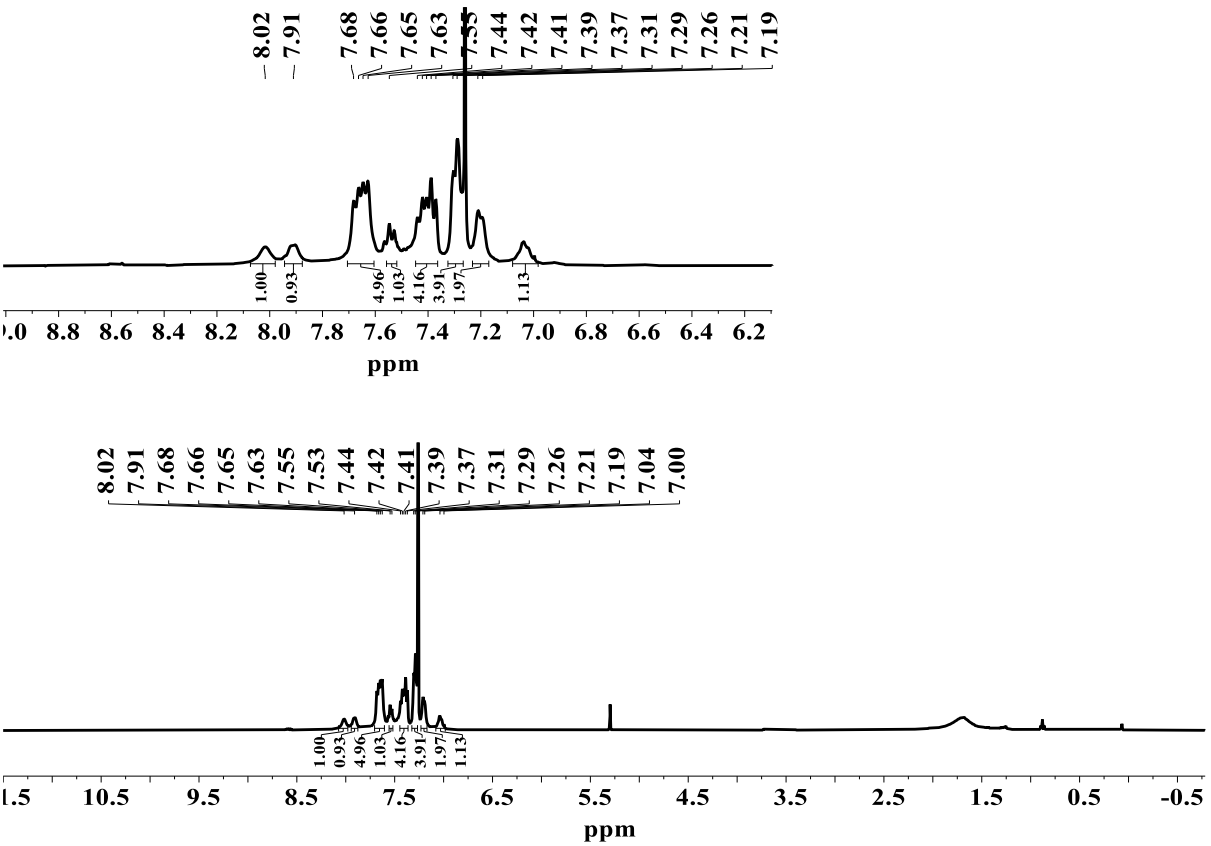

Fig. S41. ^{1}H NMR spectrum of **9** in $CDCl_3$ (400 MHz).

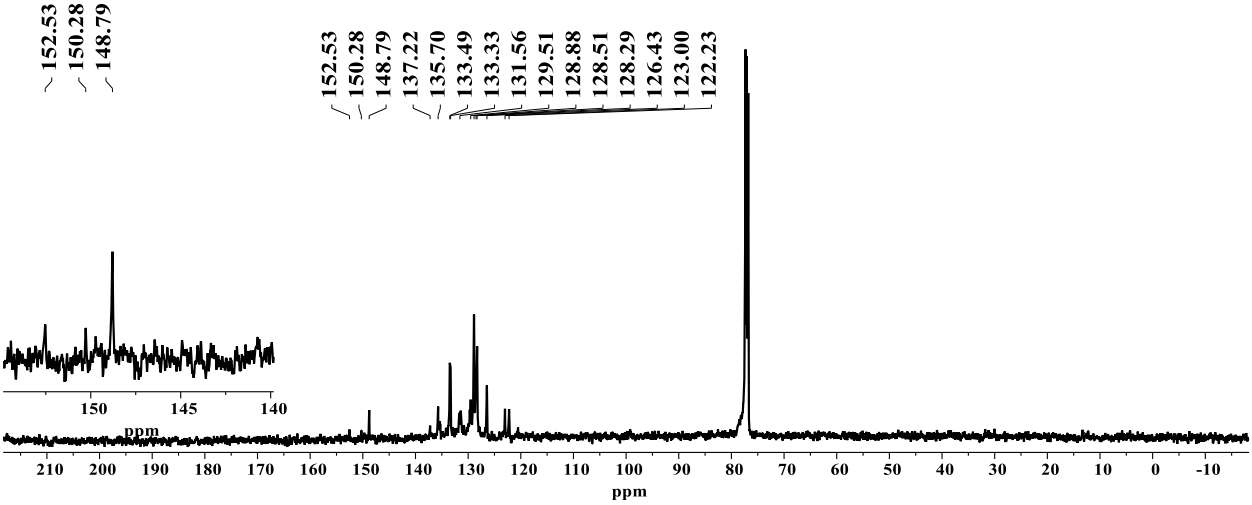

Fig. S42. $^{13}C\{^{1}H\}$ NMR spectrum of **9** in $CDCl_3$ (126 MHz).

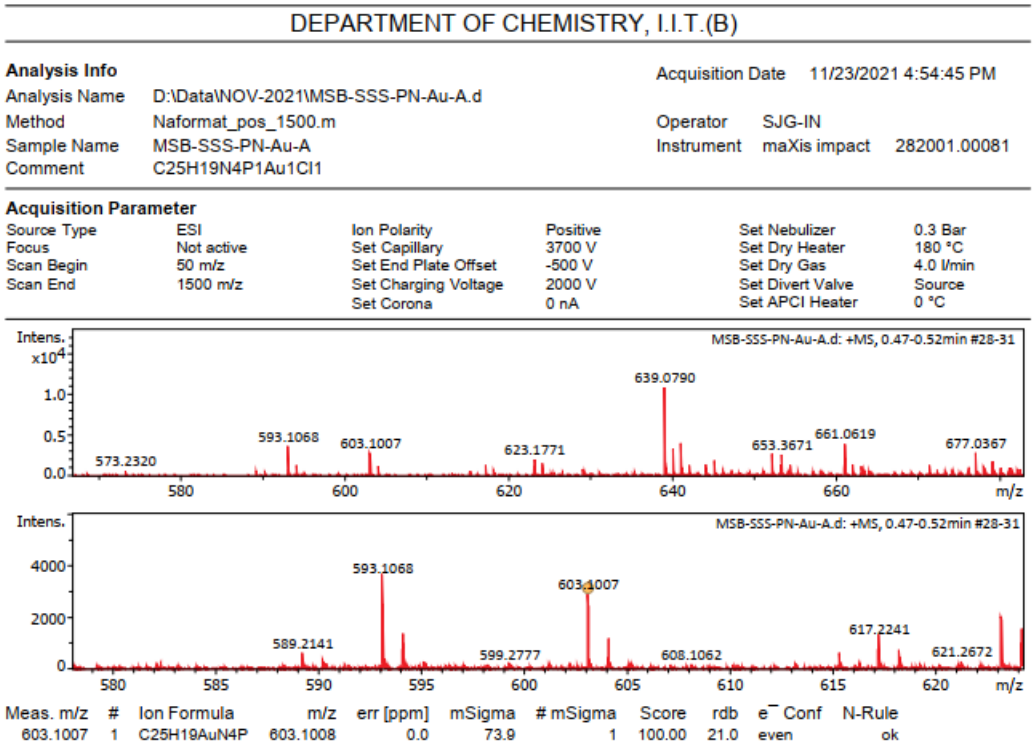

Fig. S43. HRMS spectrum of **9**.

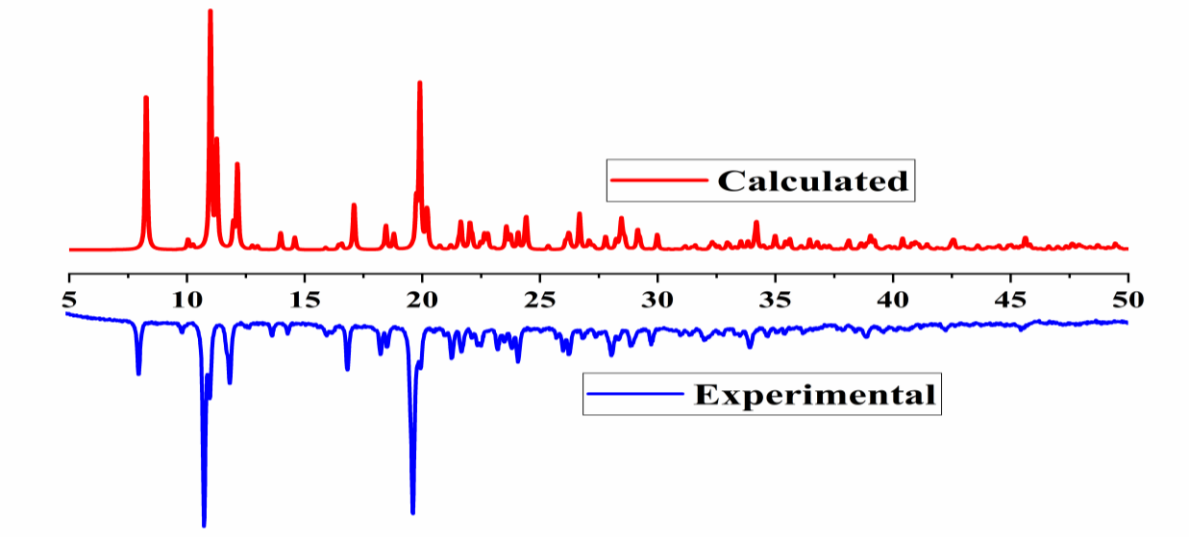

Fig. S44. PXRD profiles of PN-CuCl (**2**) at 298 K.

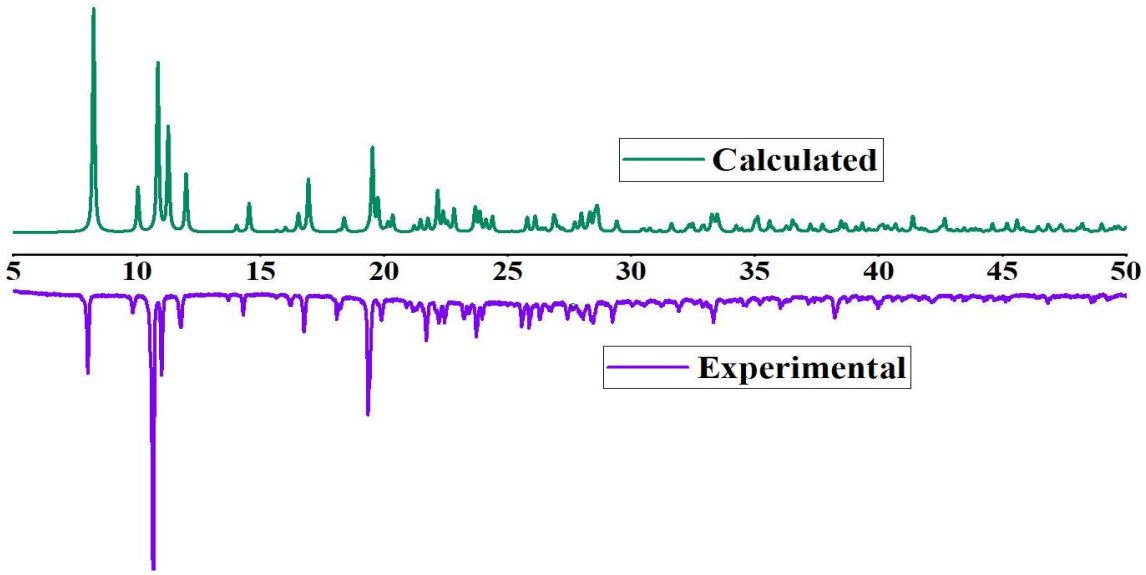

Fig. S45. PXRD profiles of PN-CuBr (**3**) at 298 K.

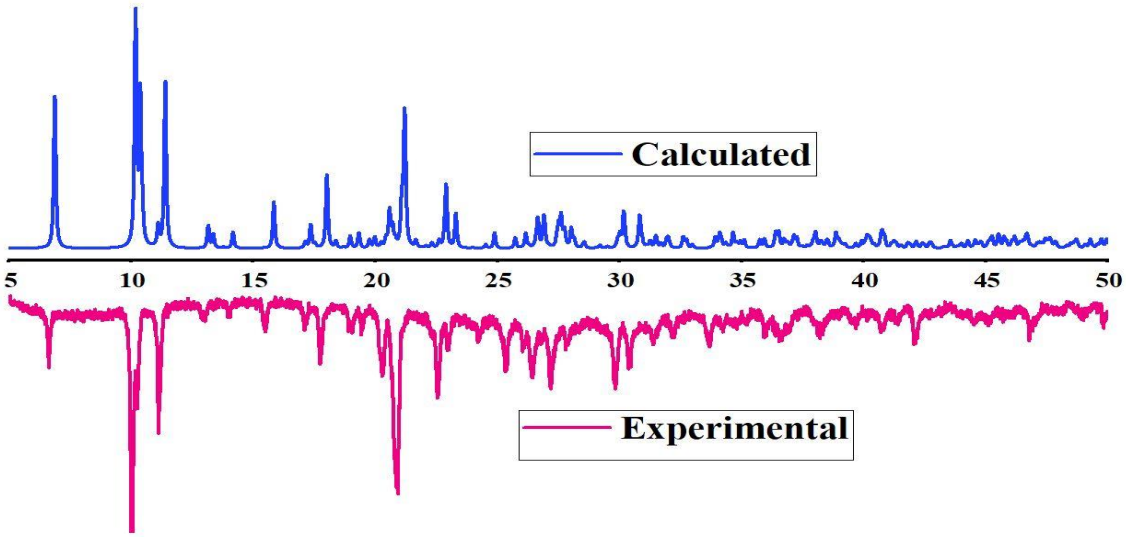

Fig. S46. PXRD profiles of PN-CuI (**4**) at 298 K.

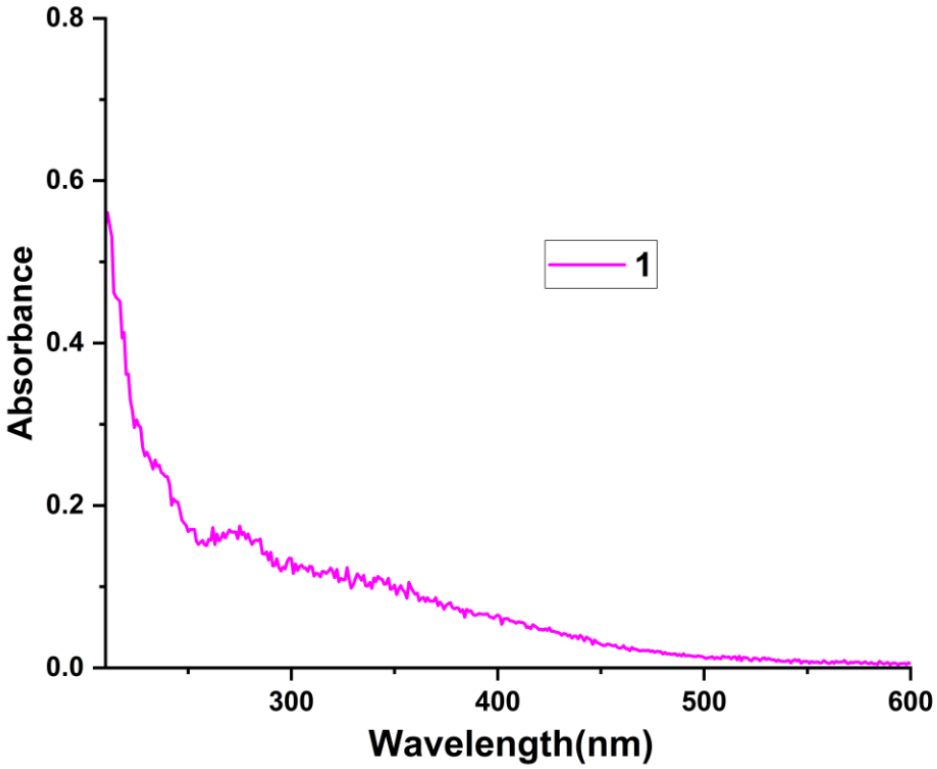

Fig. S47. Solid state UV absorption spectra for **1**.

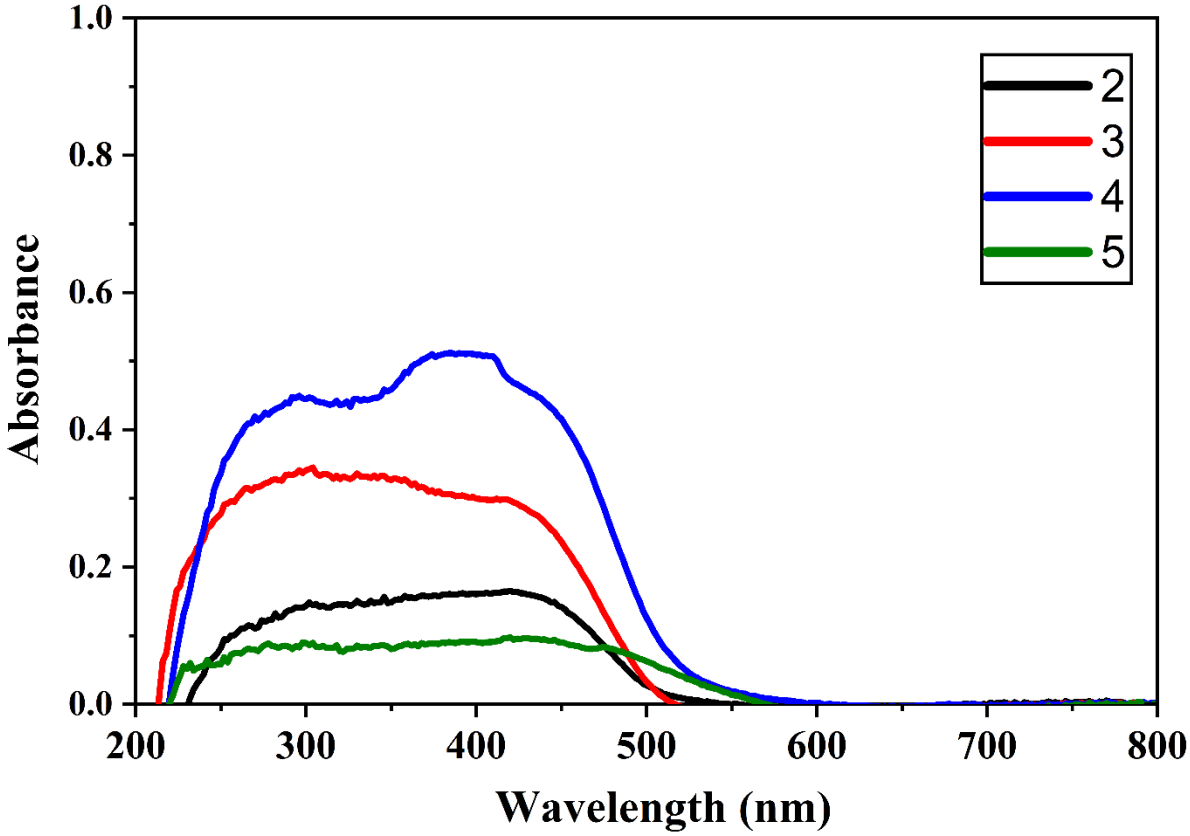

Fig. S48. Solid state UV-Vis spectra for **2-5**.

General procedure for cross-coupling

Phenol (1 eq) and bromobenzene (1 eq) derivatives were taken in a 10 ml catalytic tube: catalyst (0.5 mol%) with K_3PO_4 (1 eq) loaded in DMSO (2 mL) as a solvent. The reaction mixture was stirred at 120 °C for 15 h, the corresponding product was isolated through the column chromatography technique.

NMR spectral data of catalytic products

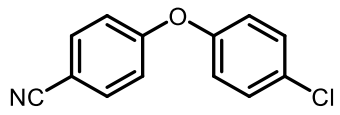

4-(4-chlorophenoxy)benzonitrile (**I**).[7] Purified by column chromatography on silica gel using petroleum ether and ethyl acetate as eluents, 92 % (106 mg) yielded a white solid. ^{1}H NMR (400 MHz, $CDCl_3$) δ 7.62 (s, 1H), 7.60 (s, 1H), 7.38 (s, 1H), 7.36 (s, 1H), 7.02 (d, *J* = 1.7 Hz, 2H), 7.00 (d, *J* = 3.9 Hz, 2H). ^{13}C{^{1}H} NMR (101 MHz, $CDCl_3$) δ 161.35, 154.25, 134.34, 130.52, 130.43, 121.80, 119.14, 118.13, 105.24.

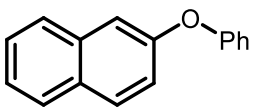

2-phenoxynaphthalene (**II**).[8] Purified by column chromatography on silica gel using petroleum ether and ethyl acetate as eluents, 90 % (99 mg) yielded a white solid. ^{1}H NMR (400 MHz, $CDCl_3$) δ 8.21 (d, *J* = 8.4 Hz, 1H), 7.88 (d, *J* = 8.7 Hz, 1H), 7.63 (d, *J* = 8.3 Hz, 1H), 7.55 – 7.46 (m, 2H), 7.41 – 7.31 (m, 3H), 7.14 – 7.08 (m, 1H), 7.05 (d, *J* = 8.7 Hz, 2H), 6.95 (d, *J* = 7.6 Hz, 1H). ^{13}C{^{1}H} NMR (101 MHz, $CDCl_3$) δ 158.02, 153.17, 135.09, 129.93, 127.90, 127.02, 126.62, 126.07, 125.94, 123.49, 123.28, 122.25, 118.73, 113.64.

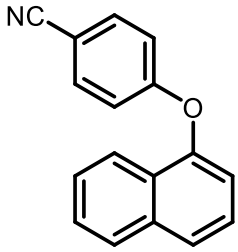

4-(naphthalen-1-yloxy)benzonitrile (**III**).[9] Purified by column chromatography on silica gel using petroleum ether and ethyl acetate as eluents, 79 % (97 mg) yielded a white solid. ^{1}H NMR (500 MHz, $CDCl_3$) δ 7.93 (dd, *J* = 14.4, 8.3 Hz, 2H), 7.76 (d, *J* = 8.2 Hz, 1H), 7.59 (d, *J* = 8.8 Hz, 2H), 7.55 (d, *J* = 8.2 Hz, 1H), 7.48 (dd, *J* = 16.3, 5.6 Hz, 2H), 7.14 (d, *J* = 7.5 Hz, 1H), 7.01 (d, *J* = 8.8 Hz, 2H). ^{13}C{^{1}H} NMR (126 MHz, $CDCl_3$) δ 162.41, 150.58, 135.29, 134.37, 128.26, 127.05, 126.74, 125.96, 125.65, 121.76, 118.99, 117.64, 116.48, 105.91.

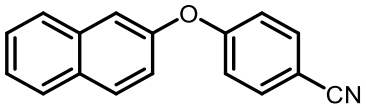

4-(naphthalen-2-yloxy)benzonitrile (**IV**).[10] Purified by column chromatography on silica gel using petroleum ether and ethyl acetate as eluents, 85 % (104 mg) yielded a white solid. ^{1}H NMR (500 MHz, $CDCl_3$) δ 7.52 (dd, *J*

= 16.0, 8.2 Hz, 2H), 7.41 (d, *J* = 9.5 Hz, 1H), 7.26 (d, *J* = 8.9 Hz, 2H), 7.17 – 7.10 (m, 3H), 6.89 (d, *J* = 10.5 Hz, 1H), 6.70 (d, *J* = 4.7 Hz, 2H). $^{13}C\{^{1}H\}$ NMR (126 MHz, $CDCl_3$) δ 161.79, 152.59, 134.32, 131.15, 130.64, 128.01, 127.50, 127.08, 125.79, 120.40, 118.96, 118.26, 116.89, 106.15.

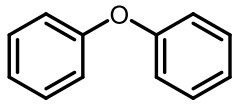

oxydibenzene (**V**).[8] Purified by column chromatography on silica gel using petroleum ether and ethyl acetate as eluents, 97 % (82 mg) colorless liquid. ^{1}H NMR (500 MHz, $CDCl_3$) δ 7.49 (t, *J* = 8.0 Hz, 2H), 7.39 (t, *J* = 8.0 Hz, 2H), 7.26 (t, *J* = 6.9 Hz, 1H), 7.17 (d, *J* = 8.9 Hz, 3H), 7.08 (d, *J* = 10.5 Hz, 2H). ^{13}C NMR (126 MHz, $CDCl_3$) δ 157.38, 129.87, 123.35, 119.02.

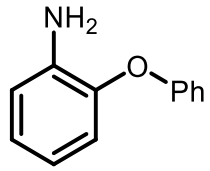

2-phenoxyaniline (**VI**).[11] Purified by column chromatography on silica gel using petroleum ether and ethyl acetate as eluents, 75 % (70 mg) yielded a white solid. ^{1}H NMR (400 MHz, $CDCl_3$) δ 7.28 (dd, *J* = 8.7, 7.4 Hz, 2H), 7.03 (t, *J* = 7.4 Hz, 1H), 6.99 – 6.92 (m, 3H), 6.86 (d, *J* = 1.6 Hz, 1H), 6.84 (d, *J* = 2.4 Hz, 1H), 6.75 – 6.69 (m, 1H), 3.63 (br, 2H) $^{13}C\{^{1}H\}$ NMR (101 MHz, $CDCl_3$) δ 157.47, 143.71, 137.79, 129.86, 124.92, 122.91, 120.18, 119.58, 117.46, 117.13.

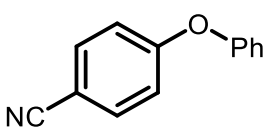

4-phenoxybenzonitrile (**VII**).[12] Purified by column chromatography on silica gel using petroleum ether and ethyl acetate as eluents, 82 % (80 mg) yielded a colorless liquid. ^{1}H NMR (400 MHz, $CDCl_3$) δ 7.60 (d, *J* = 9.1 Hz, 2H), 7.41 (t, *J* = 7.6 Hz, 2H), 7.22 (d, *J* = 7.5 Hz, 1H), 7.07 (d, *J* = 8.8 Hz, 2H), 7.00 (d, *J* = 8.9 Hz, 2H). $^{13}C\{^{1}H\}$ NMR (101 MHz, $CDCl_3$) δ 161.78, 154.92, 134.24, 130.35, 125.26, 120.52, 118.96, 118.03, 105.93.

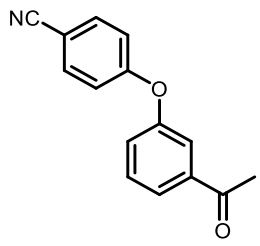

4-(3-acetylphenoxy)benzonitrile (**VIII**). Purified by column chromatography on silica gel using petroleum ether and ethyl acetate as eluents, 83 % (98 mg) yielded a colorless liquid. ^{1}H NMR (500 MHz, $CDCl_3$) δ 7.81 (d, *J* = 7.8 Hz, 1H), 7.66 – 7.60 (m, 3H), 7.54 – 7.49 (m, 1H), 7.27 (d, *J* = 8.1 Hz, 1H), 7.02 (d, *J* = 7.5 Hz, 2H), 2.60 (s, 3H). ^{13}C{^{1}H} NMR (126 MHz, $CDCl_3$) δ 197.02, 161.06, 155.41, 139.34, 134.36, 130.60, 125.08, 124.95, 119.68, 118.70, 118.30, 106.56, 26.81.

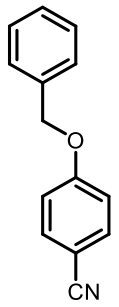

4-(benzyloxy)benzonitrile (**IX**).[13] Purified by column chromatography on silica gel using petroleum ether and ethyl acetate as eluents, 65 % (68 mg) yielded a yellow oil. ^{1}H NMR (400 MHz, $CDCl_3$) δ 7.60 (s, 1H), 7.58 (s, 1H), 7.41 (d, *J* = 5.1 Hz, 4H), 7.03 (s, 1H), 7.01 (s, 1H), 5.12 (s, 2H). ^{13}C{^{1}H} NMR (101 MHz, $CDCl_3$) δ 161.98, 135.70, 134.04, 128.79, 128.44, 127.49, 119.19, 115.61, 104.26, 70.30.

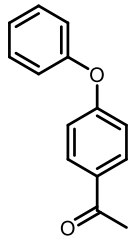

1-(4-phenoxyphenyl)ethan-1-one (**X**).[14] Purified by column chromatography on silica gel using petroleum ether and ethyl acetate as eluents, 78 % (83 mg) yielded as a yellowish liquid. ^{1}H NMR (400 MHz, $CDCl_3$) δ 7.98 (d, *J* = 6.8 Hz, 2H), 7.44 (d, *J* = 9.5 Hz, 2H), 7.26 – 7.21 (m, 1H), 7.11 (d, *J* = 6.7 Hz, 2H), 7.04 (d, *J* = 8.9 Hz, 2H), 2.61 (s, 3H). ^{13}C{^{1}H} NMR (101 MHz, $CDCl_3$) δ 196.91, 162.13, 155.62, 132.02, 130.73, 130.19, 124.75, 120.31, 117.42, 26.59.

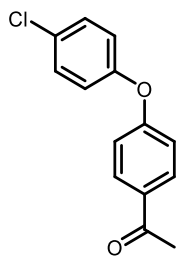

1-(4-(4-chlorophenoxy)phenyl)ethan-1-one (**XI**).[15] Purified by column chromatography on silica gel using petroleum ether and ethyl acetate as eluents, 81 % (100 mg) yield as yellowish liquid. ^{1}H NMR (500 MHz, $CDCl_3$) δ 7.94 (d, *J* = 8.9 Hz, 2H), 7.35 (d, *J* = 9.0 Hz, 2H), 7.00 (d, *J* = 5.3 Hz, 2H), 6.99 (d, *J* = 5.3 Hz,

2H), 2.57 (s, 3H). $^{13}C\{^{1}H\}$ NMR (126 MHz, $CDCl_3$) δ 196.80, 161.63, 154.29, 132.39, 130.79, 130.22, 129.87, 121.50, 117.52, 26.60.

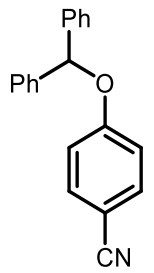

4-(benzhydryloxy)benzonitrile (**XII**).[16] Purified by column chromatography on silica gel using petroleum ether and ethyl acetate as eluents, 60 % (85 mg) yield as colorless liquid. ^{1}H NMR (500 MHz, $CDCl_3$) δ 7.51 (d, *J* = 8.2 Hz, 2H), 7.41 – 7.33 (m, 8H), 7.30 (t, *J* = 7.0 Hz, 2H), 7.00 (d, *J* = 8.4 Hz, 2H), 6.25 (s, 1H). $^{13}C\{^{1}H\}$ NMR (126 MHz, $CDCl_3$) δ 161.41, 140.15, 134.06, 128.97, 128.35, 126.91, 119.26, 116.82, 104.40, 82.27.

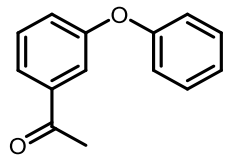

1-(3-phenoxyphenyl)ethan-1-one (**XIII**). Purified by column chromatography on silica gel using petroleum ether and ethyl acetate as eluents, 83 % (88 mg) yield as yellowish liquid. ^{1}H NMR (500 MHz, $CDCl_3$) δ 7.70 – 7.66 (m, 1H), 7.58 (s, 1H), 7.42 (t, *J* = 7.9 Hz, 1H), 7.38 – 7.34 (m, 2H), 7.21 (d, *J* = 10.7 Hz, 1H), 7.15 (d, *J* = 7.5 Hz, 1H), 7.02 (d, *J* = 9.8 Hz, 2H), 2.57 (s, 3H).$^{13}C\{^{1}H\}$ NMR (126 MHz, $CDCl_3$) δ 197.63, 157.90, 156.74, 139.03, 130.10, 123.98, 123.48, 123.24, 119.26, 118.25, 26.89.

NMR spectra of catalytic products

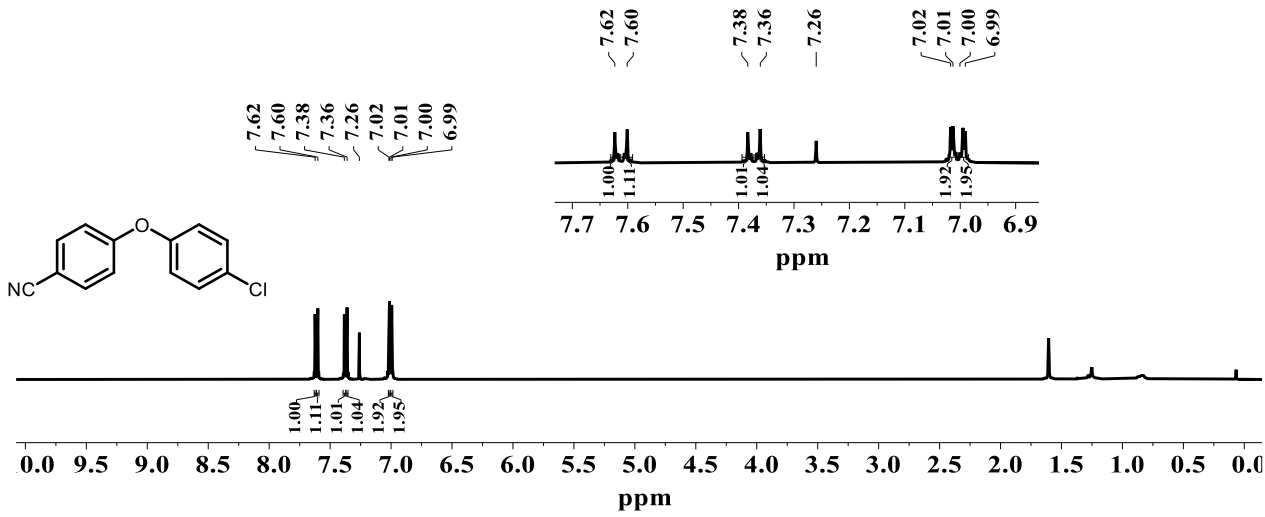

Fig. S49. ^{1}H NMR spectrum of **I** in $CDCl_3$ (400 MHz).

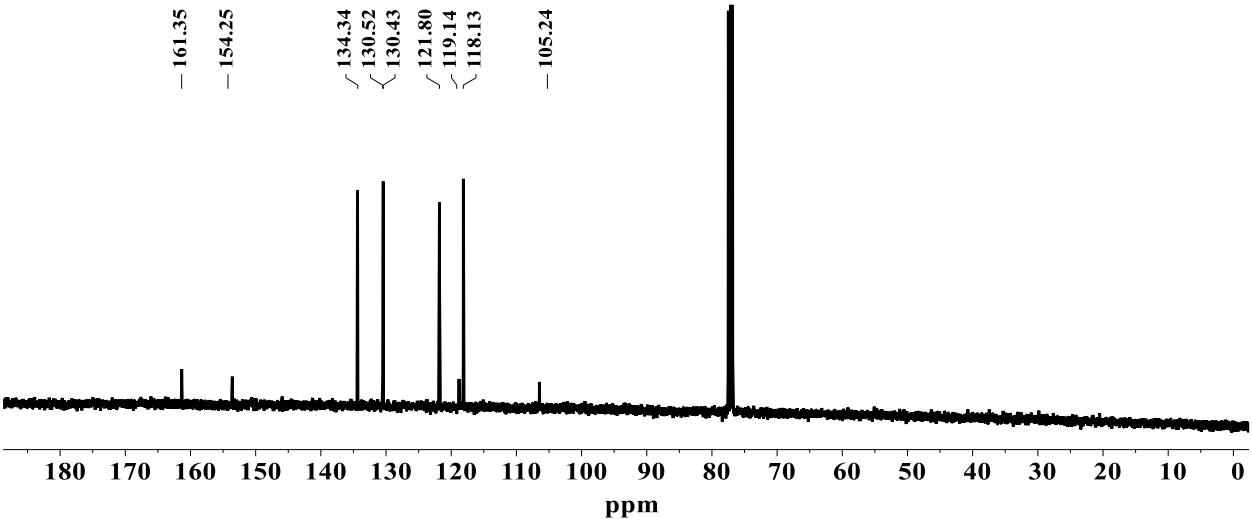

Fig. S50. $^{13}C\{^{1}H\}$ NMR spectrum of **I** in $CDCl_3$ (101 MHz).

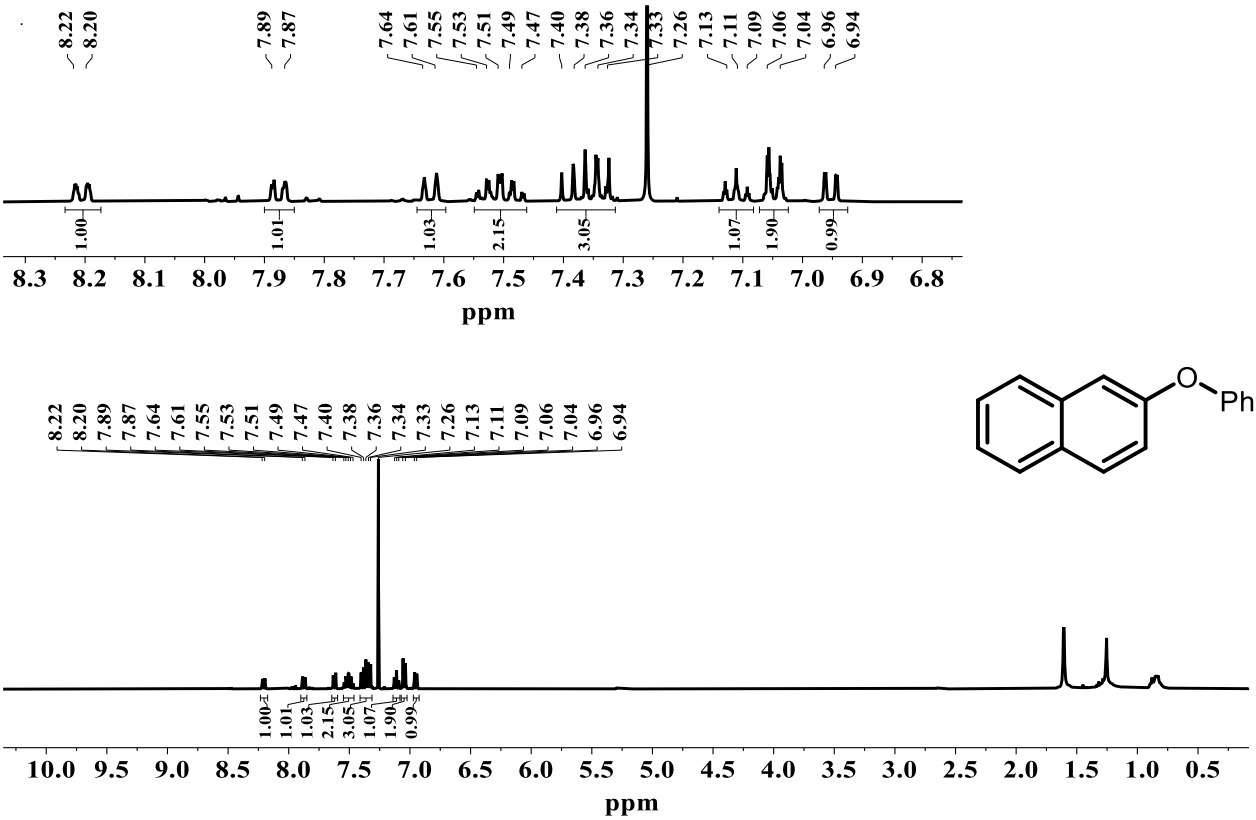

Fig. S51. ^{1}H NMR spectrum of **II** in $CDCl_3$ ((400 MHz).

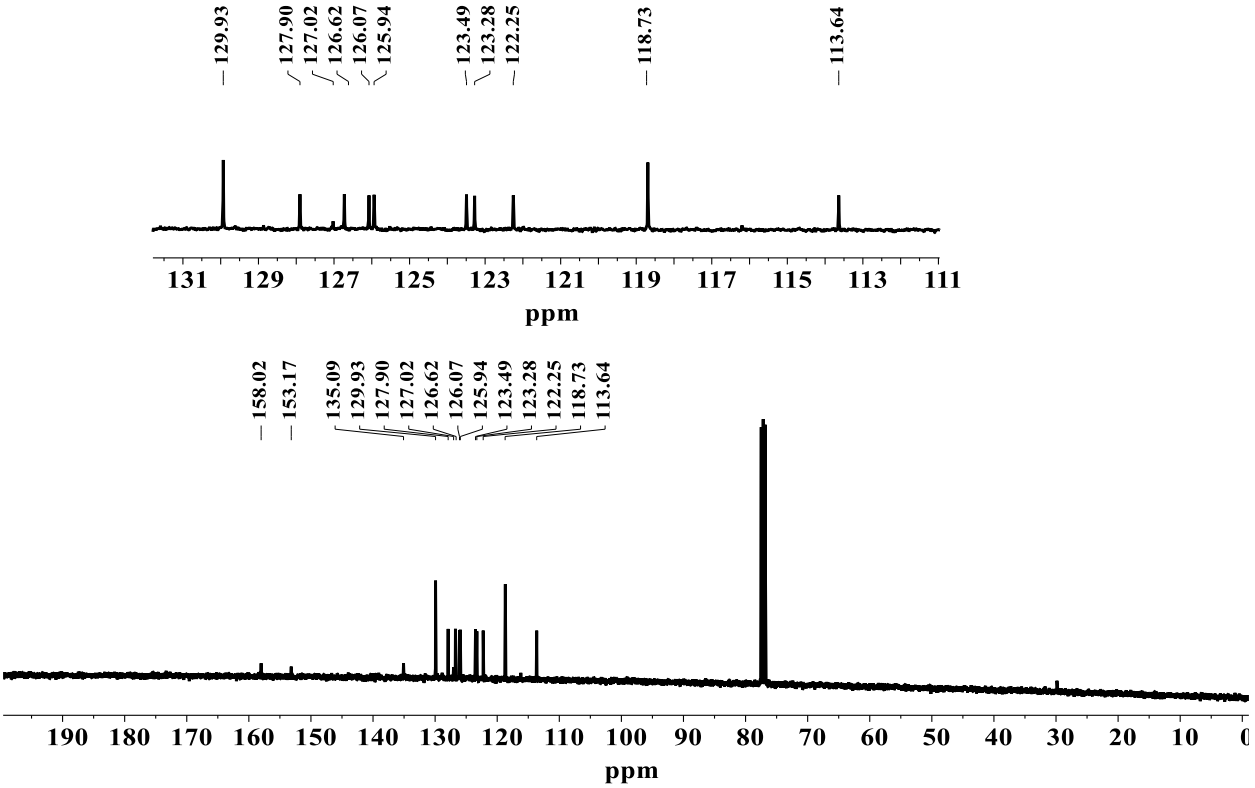

Fig. S52. $^{13}C\{^{1}H\}$ NMR spectrum of **II** in $CDCl_3$ ((101 MHz).

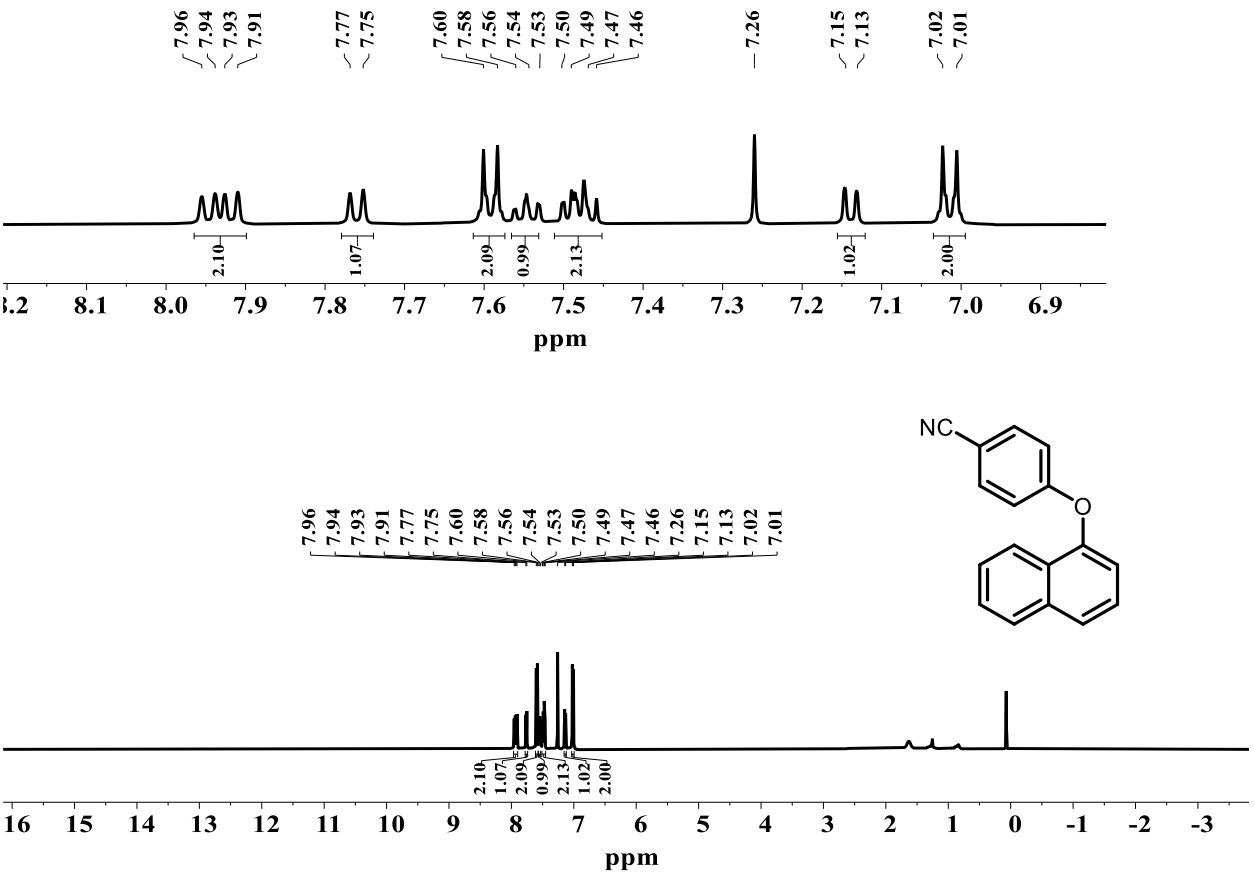

Fig. S53. ^{1}H NMR spectrum of **III** in $CDCl_3$ (500 MHz).

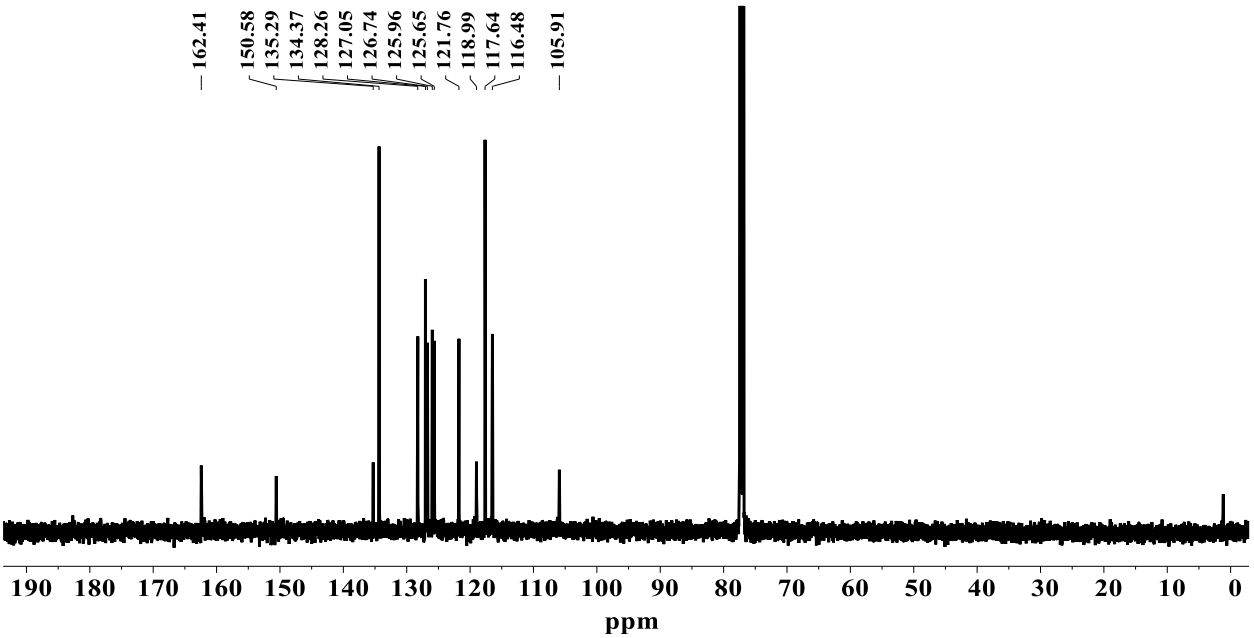

Fig. S54. ^{13}C{^{1}H} NMR spectrum of **III** in $CDCl_3$ (126 MHz).

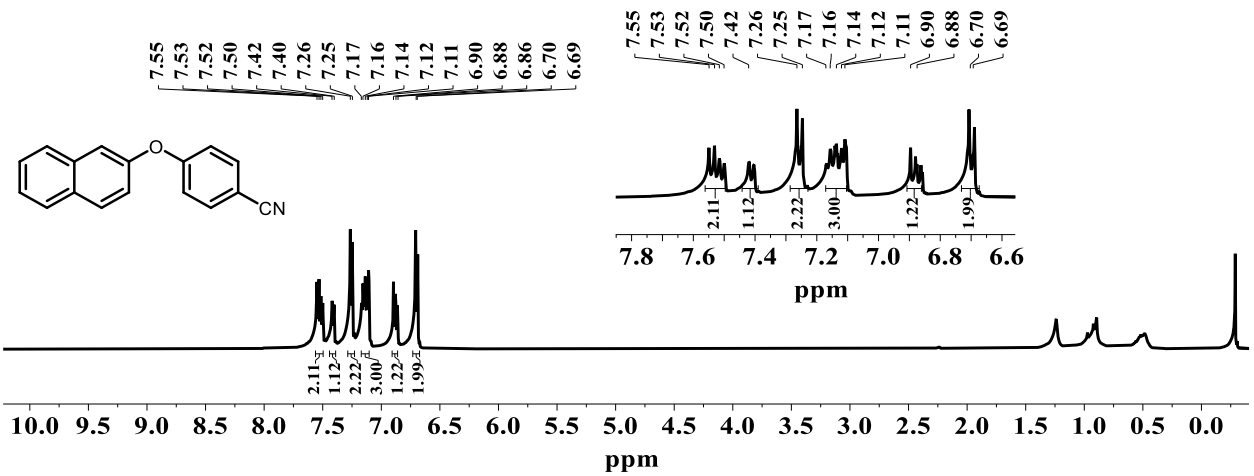

Fig. S55. ^{1}H NMR spectrum of **IV** in $CDCl_3$ (500 MHz).

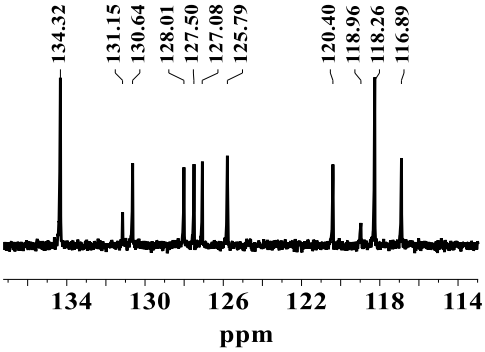

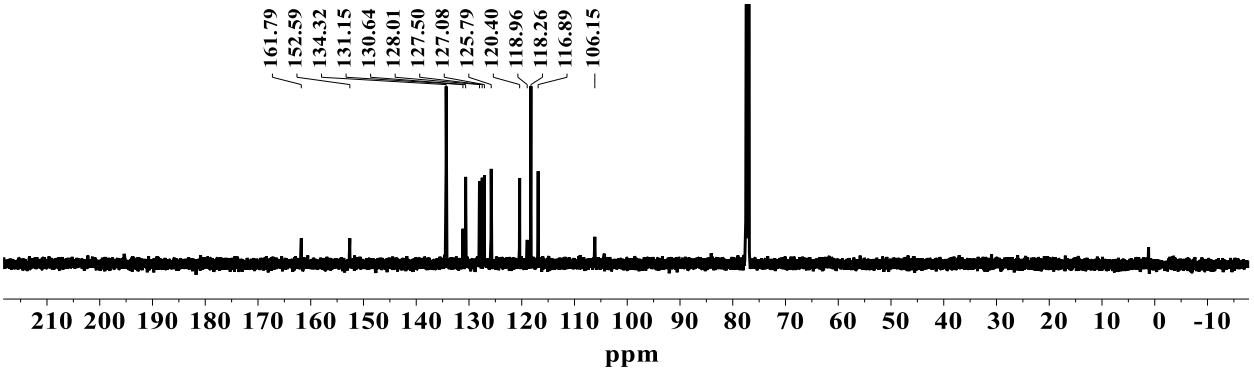

Fig. S56. $^{13}C\{^{1}H\}$ NMR spectrum of **IV** in $CDCl_3$ (126 MHz).

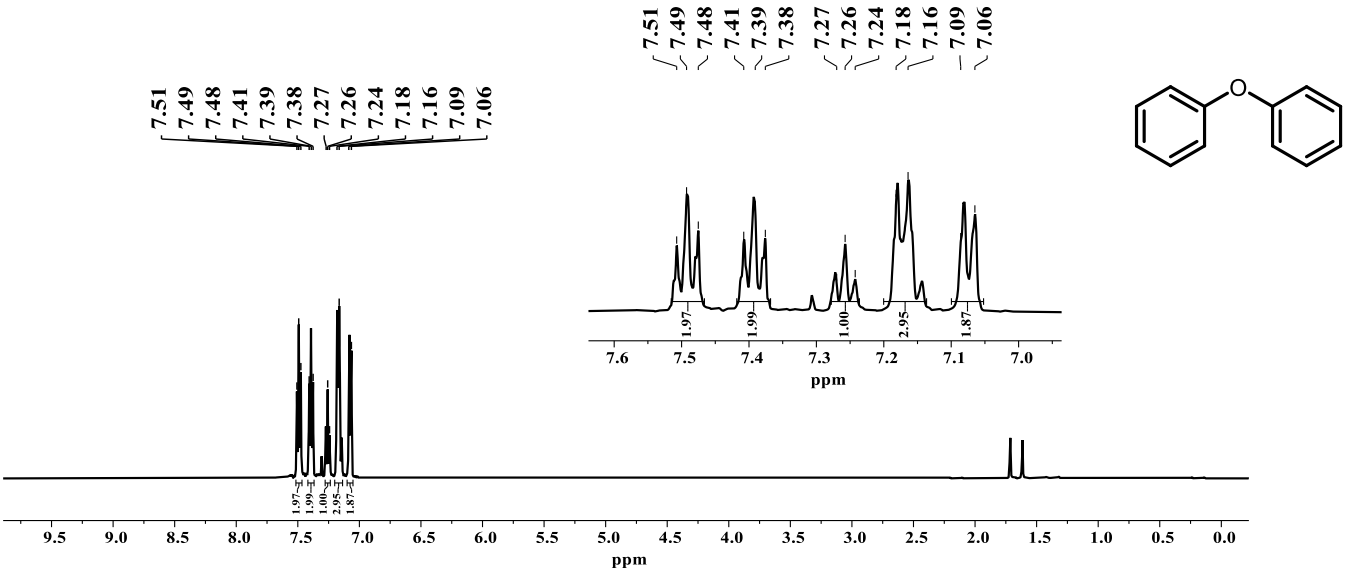

Fig. S57. ^{1}H NMR spectrum of **V** in $CDCl_3$ (500 MHz).

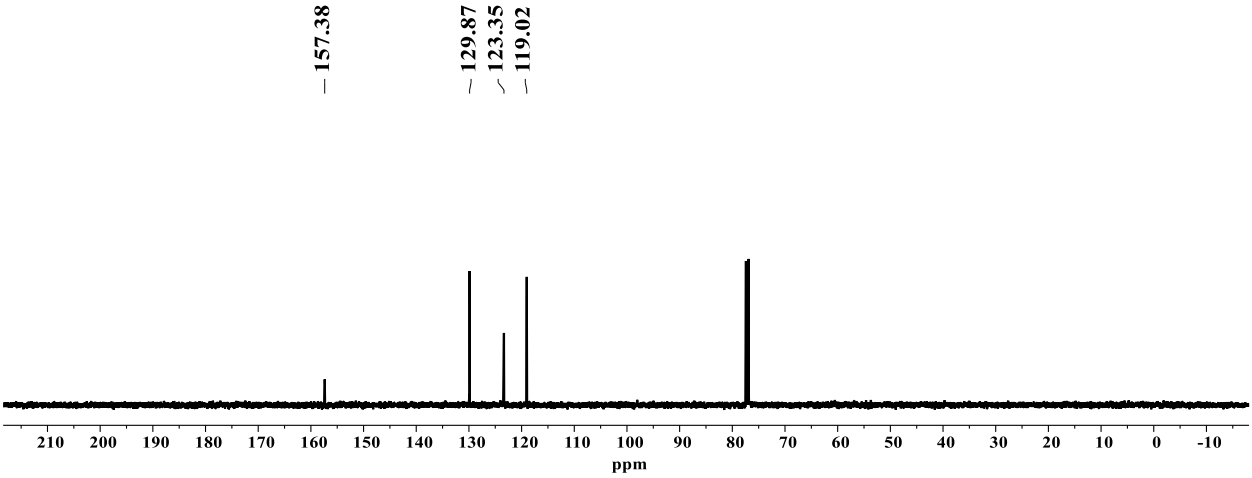

Fig. S58. ^{13}C{^{1}H} NMR spectrum of **V** in $CDCl_3$ (126 MHz).

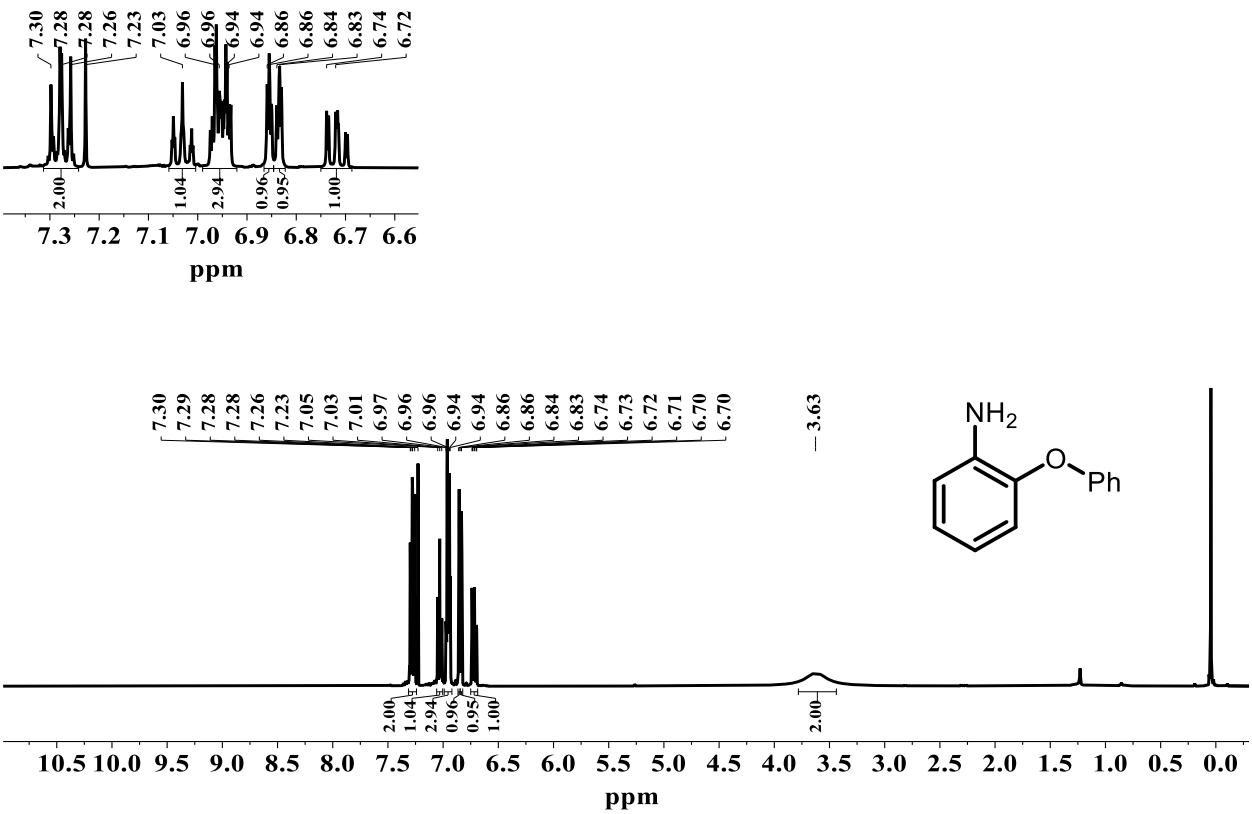

Fig. S59. ^{1}H NMR spectrum of **VI** in $CDCl_3$ (400 MHz).

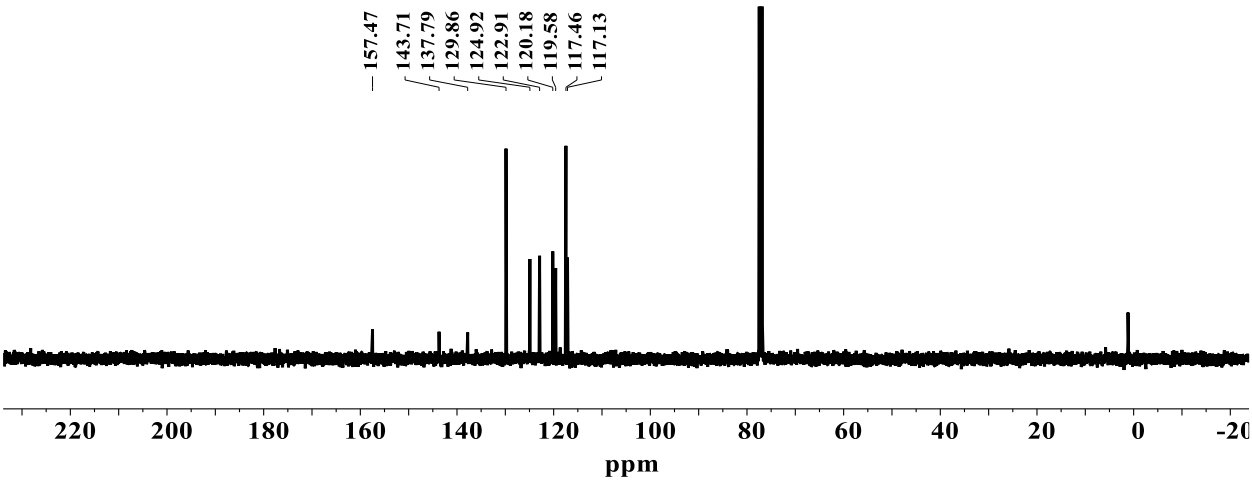

Fig. S60. ^{13}C{^{1}H} NMR spectrum of **VI** in $CDCl_3$ (126 MHz).

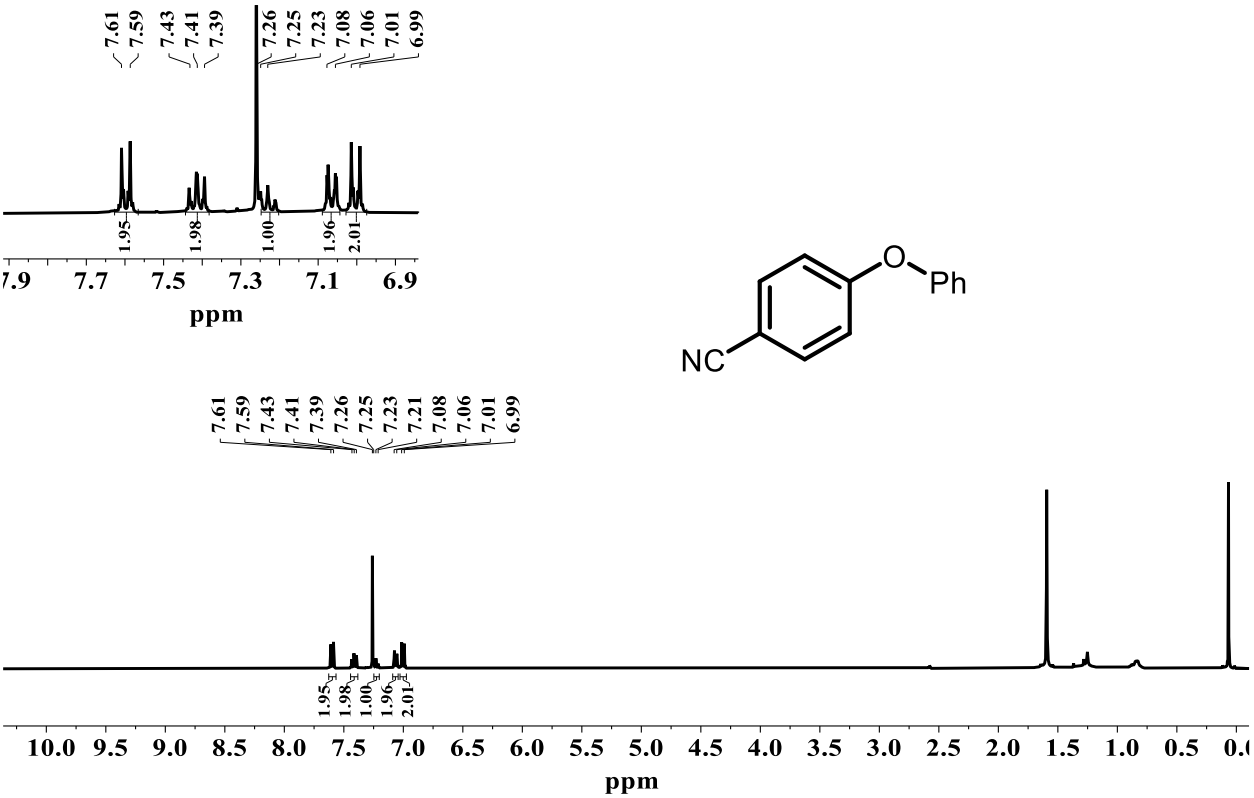

Fig. S61. ^{1}H NMR spectrum of **VII** in $CDCl_3$ (400 MHz).

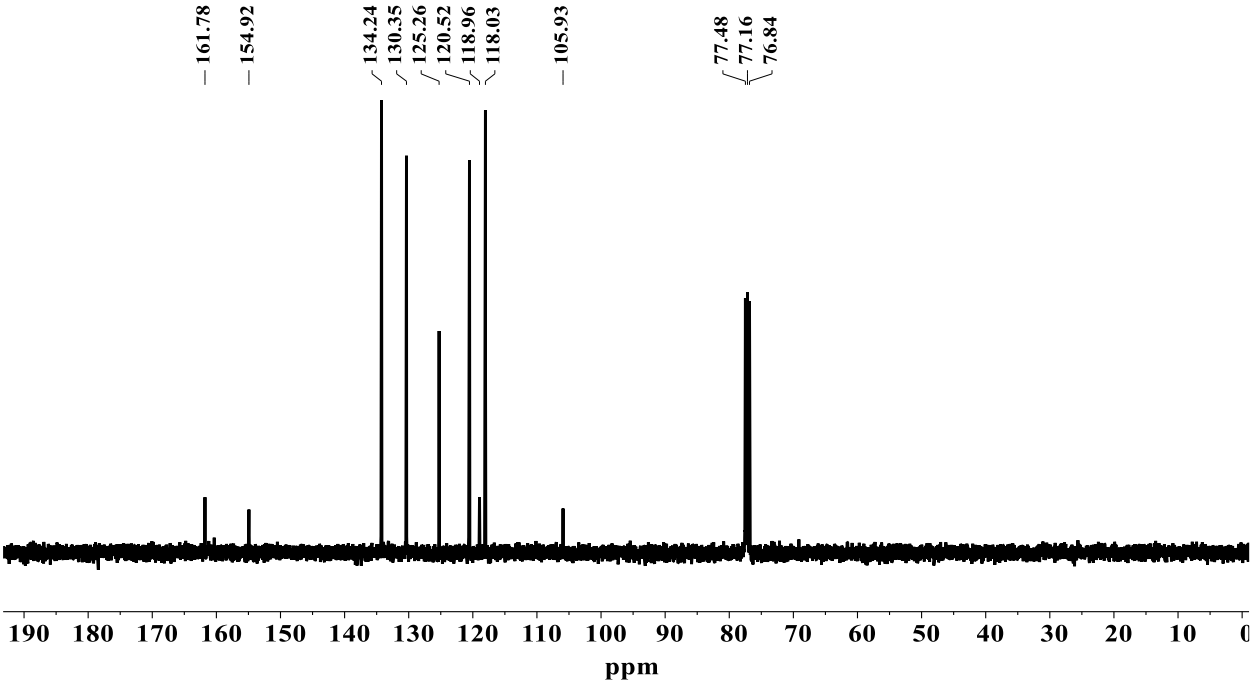

Fig. S62. $^{13}C\{^{1}H\}$ NMR spectrum of **VII** in $CDCl_3$ (126 MHz).

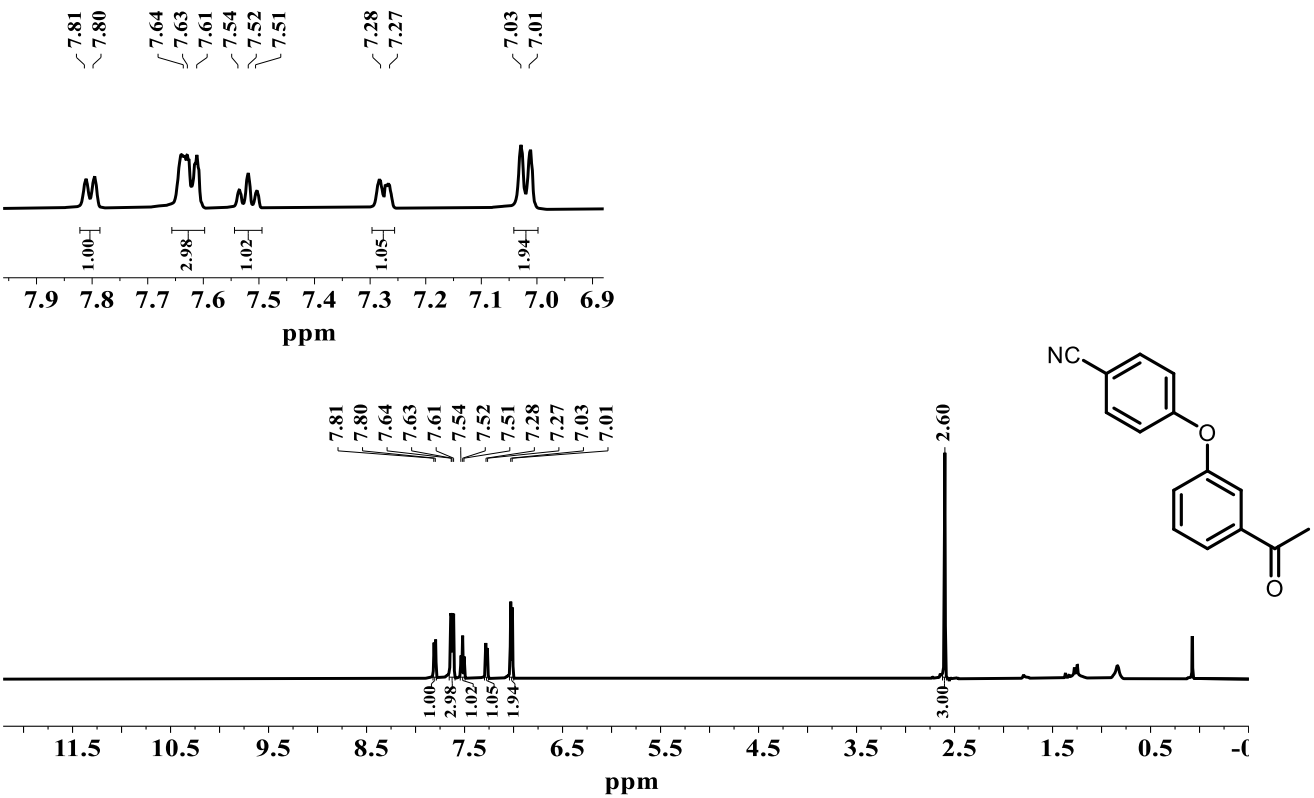

Fig. S63. ^{1}H NMR spectrum of **VIII** in $CDCl_3$ (500 MHz).

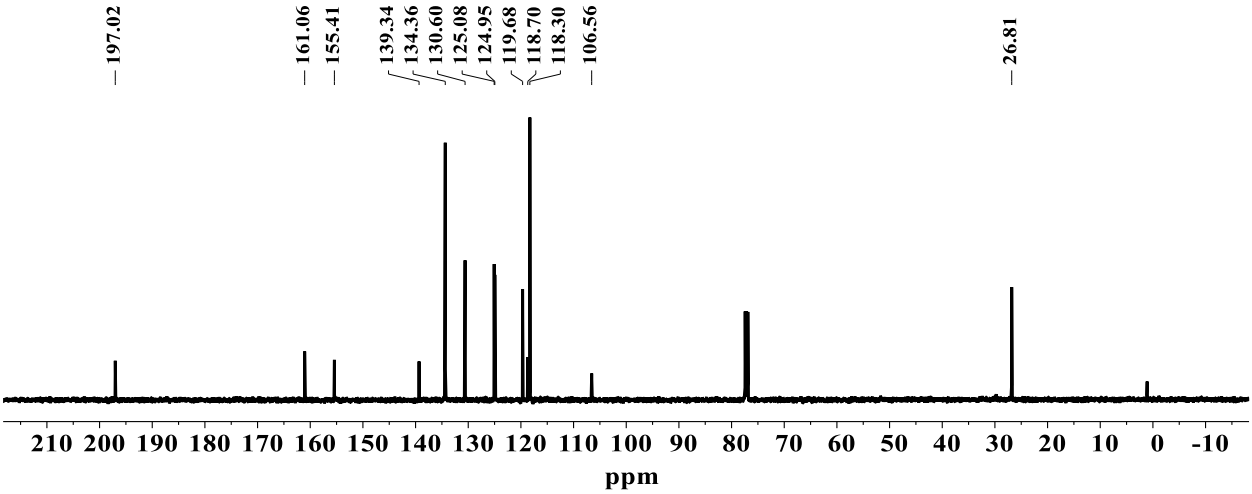

Fig. S64. $^{13}C\{^{1}H\}$ NMR spectrum of **VI**II in $CDCl_3$ (126 MHz).

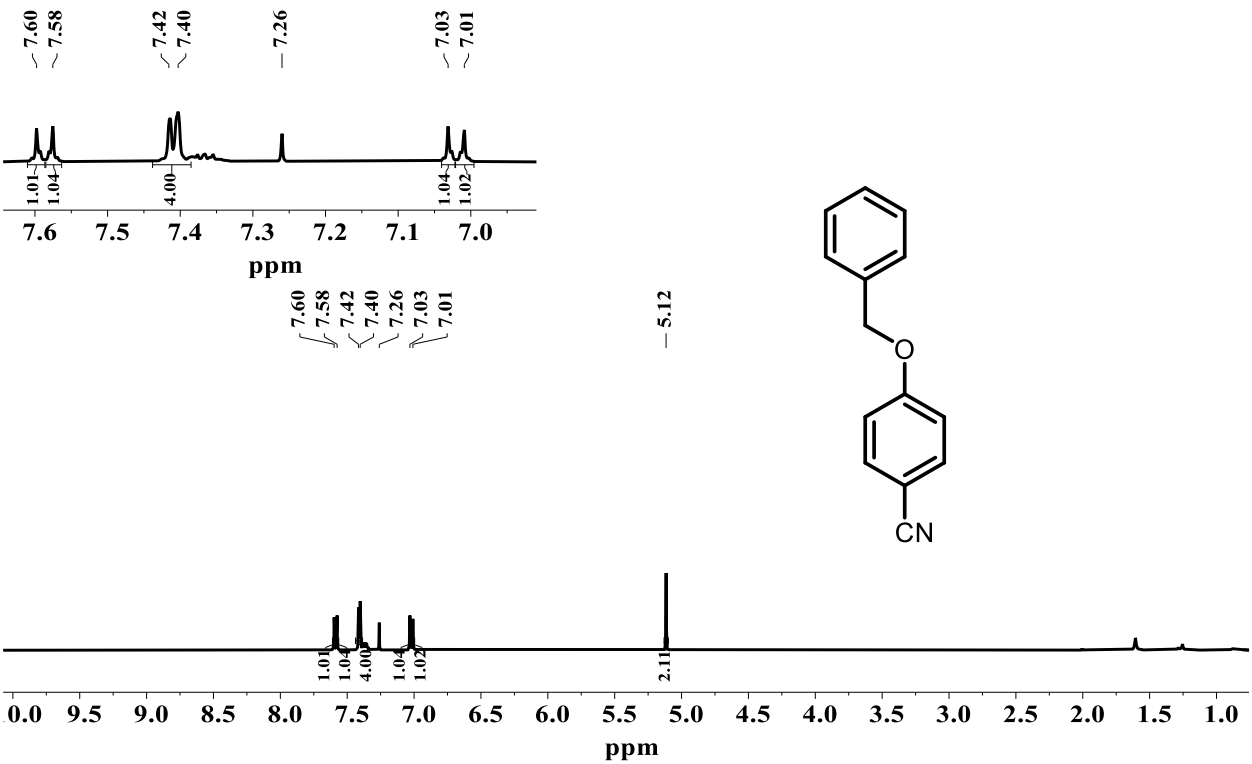

Fig. S65. ^{1}H NMR spectrum of **IX** in $CDCl_3$ (400 MHz).

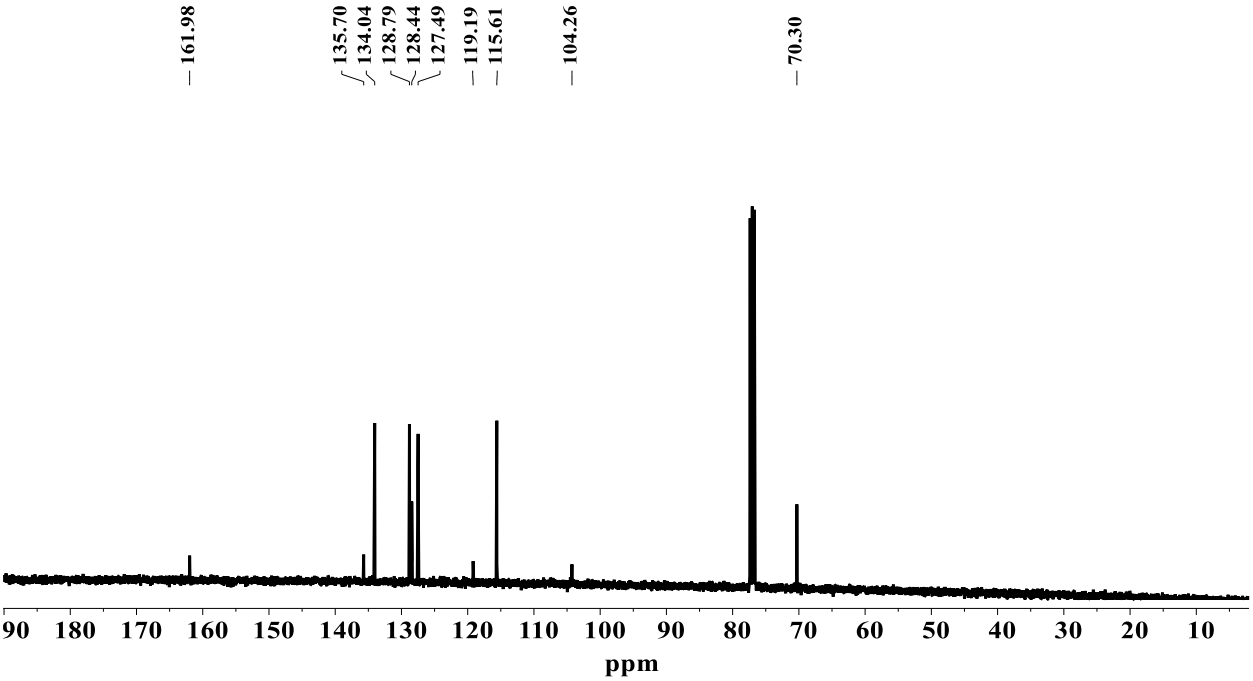

Fig. S66. $^{13}C\{^{1}H\}$ NMR spectrum of **IX** in $CDCl_3$ (101 MHz).

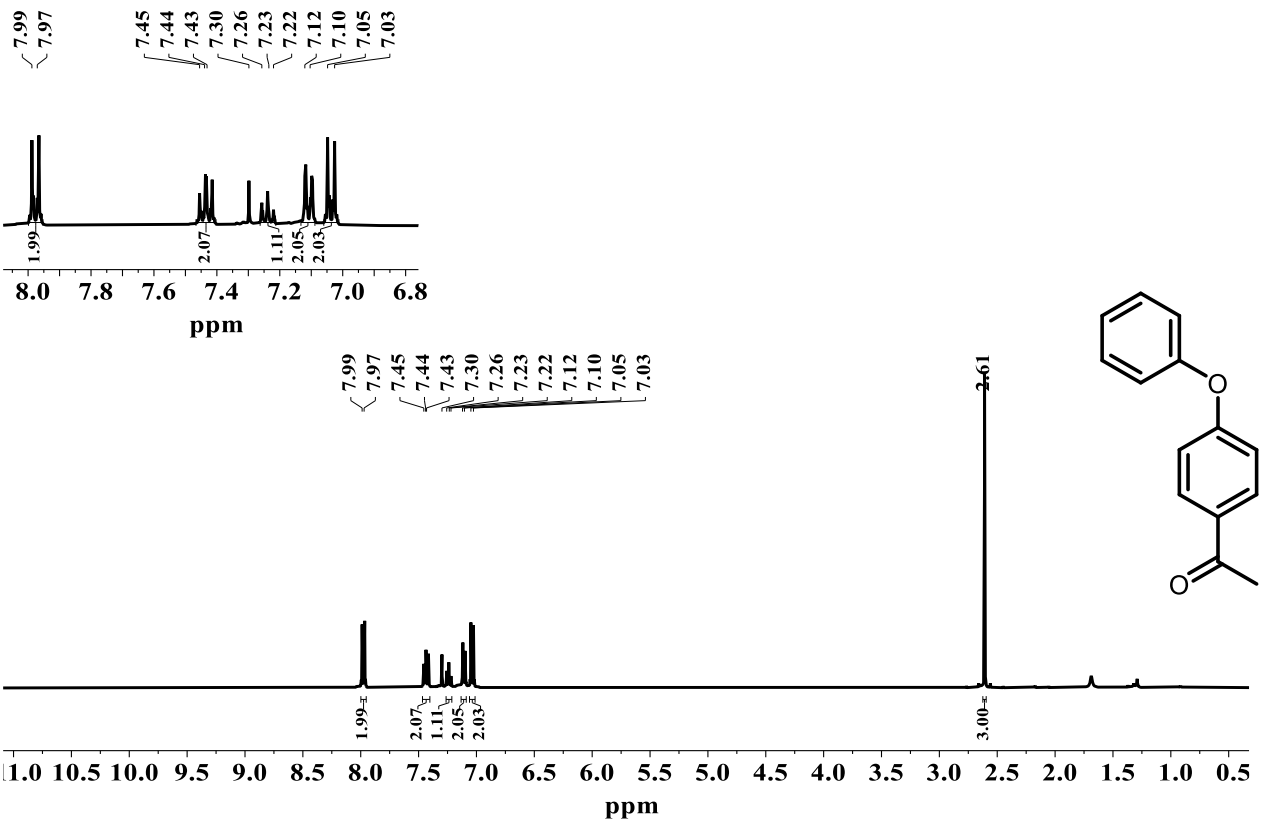

Fig. S67. $^{13}C\{^{1}H\}$ NMR spectrum of **X** in $CDCl_3$ (400 MHz).

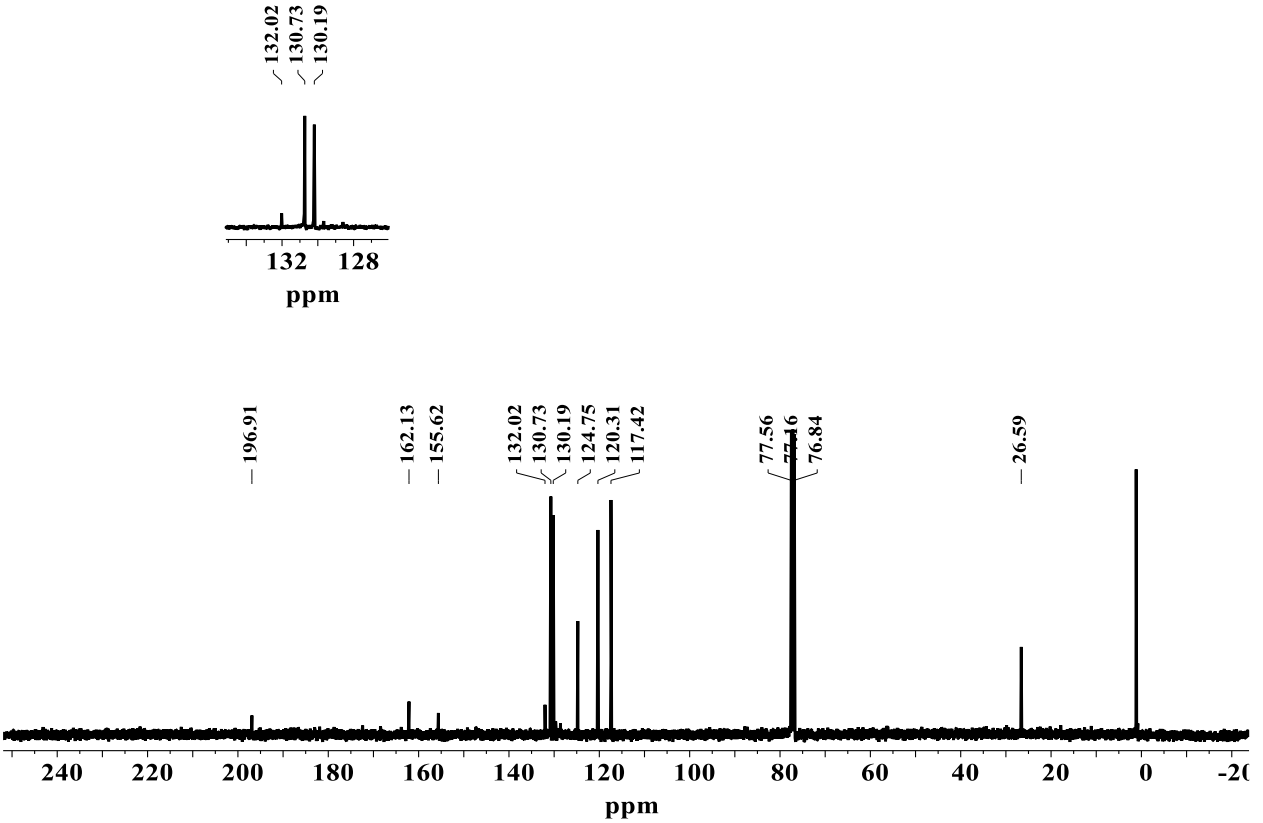

Fig. S68. $^{13}C\{^{1}H\}$ NMR spectrum of **X** in $CDCl_3$ (101 MHz).

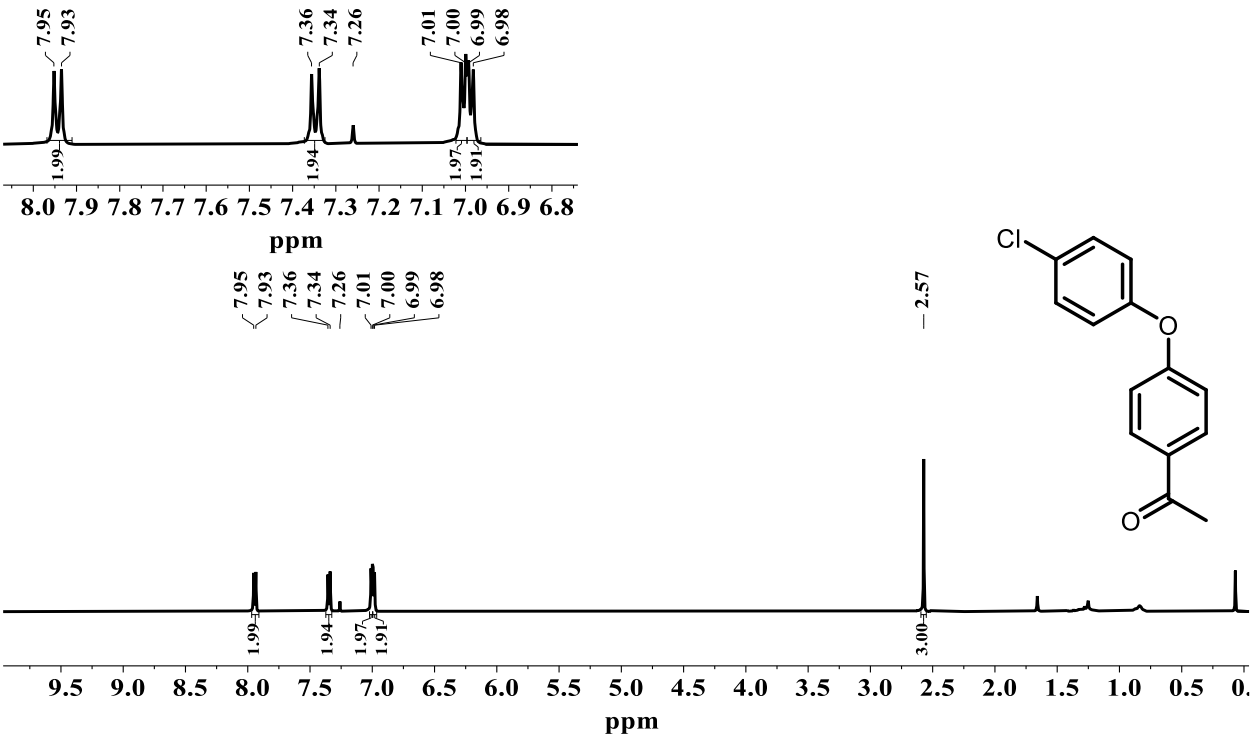

Fig. S69. ^{1}H NMR spectrum of **XI** in $CDCl_3$ (500 MHz).

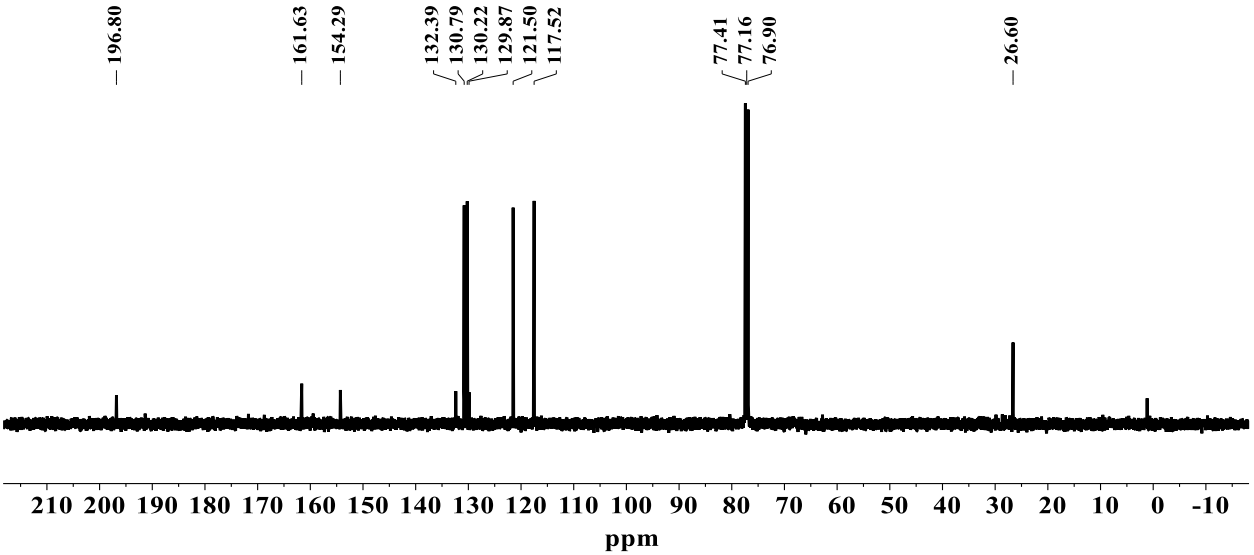

Fig. S70. $^{13}C\{^{1}H\}$ NMR spectrum of **XI** in $CDCl_3$ (126 MHz).

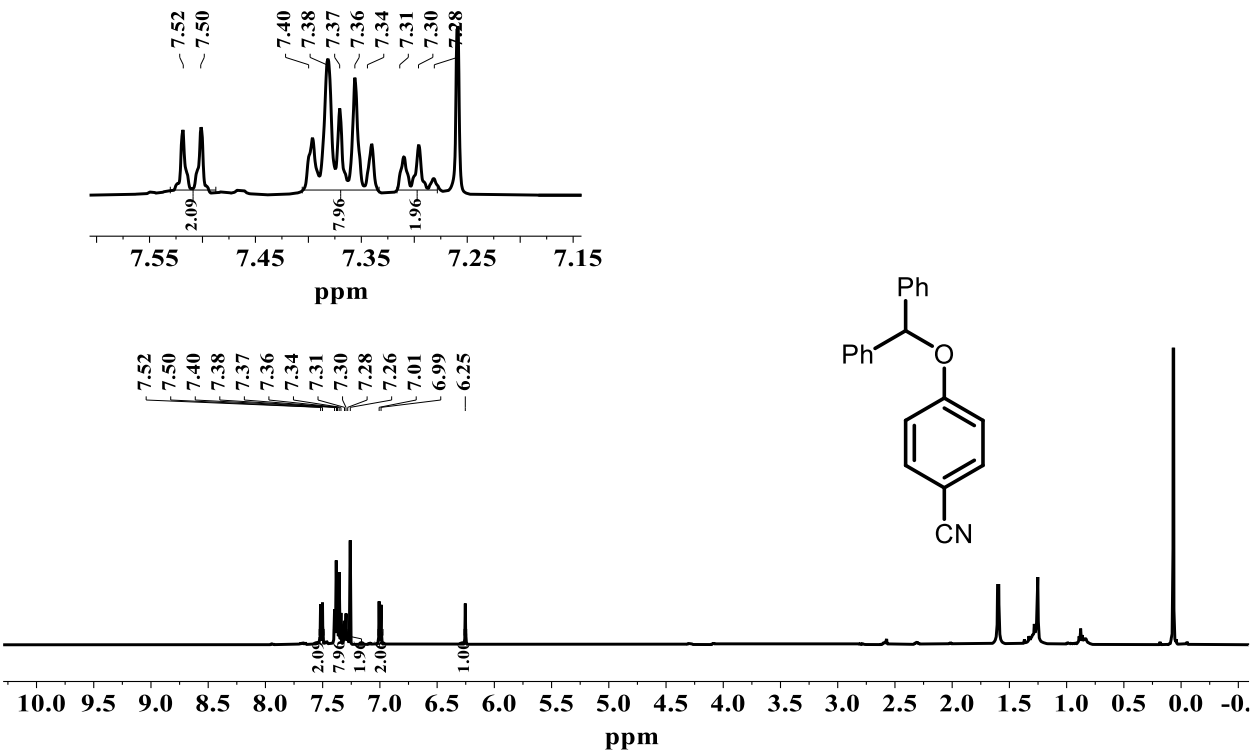

Fig. S71. ^{1}H NMR spectrum of **XII** in $CDCl_3$ (500 MHz).

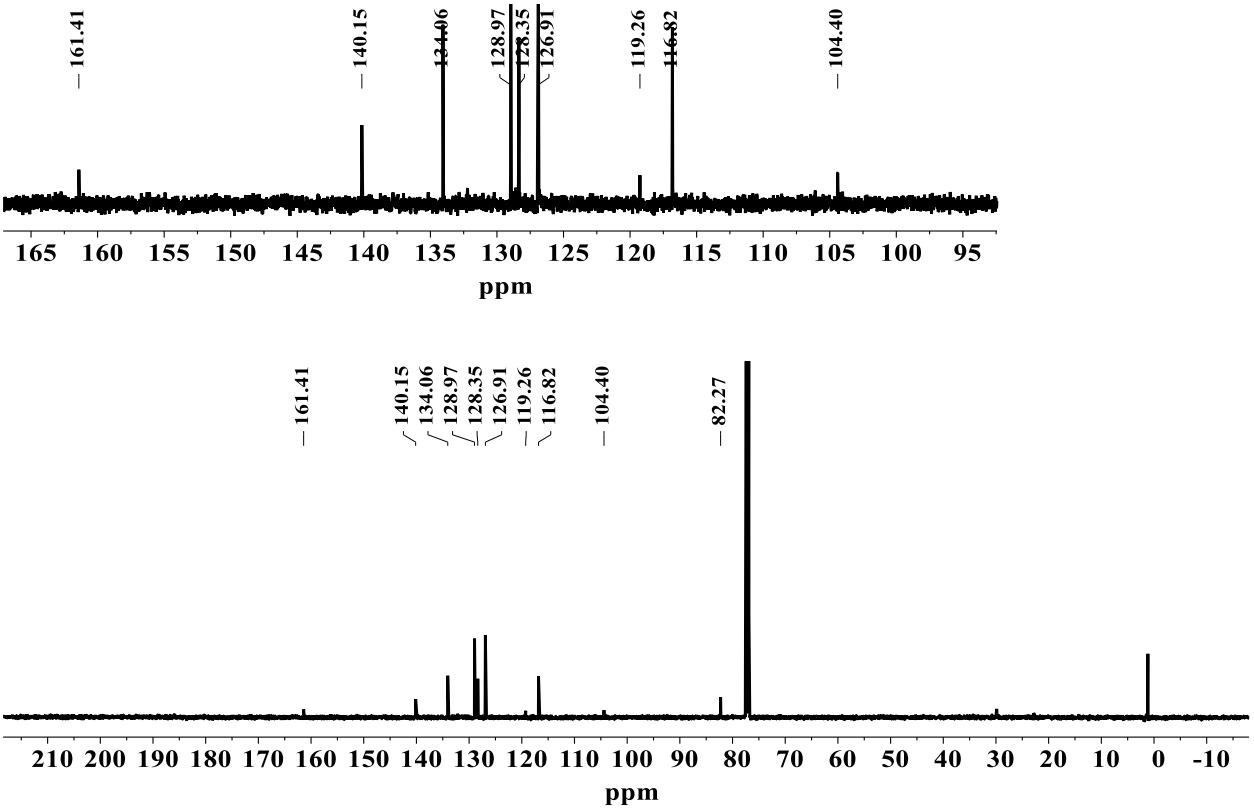

Fig. S72. $^{13}C\{^{1}H\}$ NMR spectrum of **XII** in $CDCl_3$ (126 MHz).

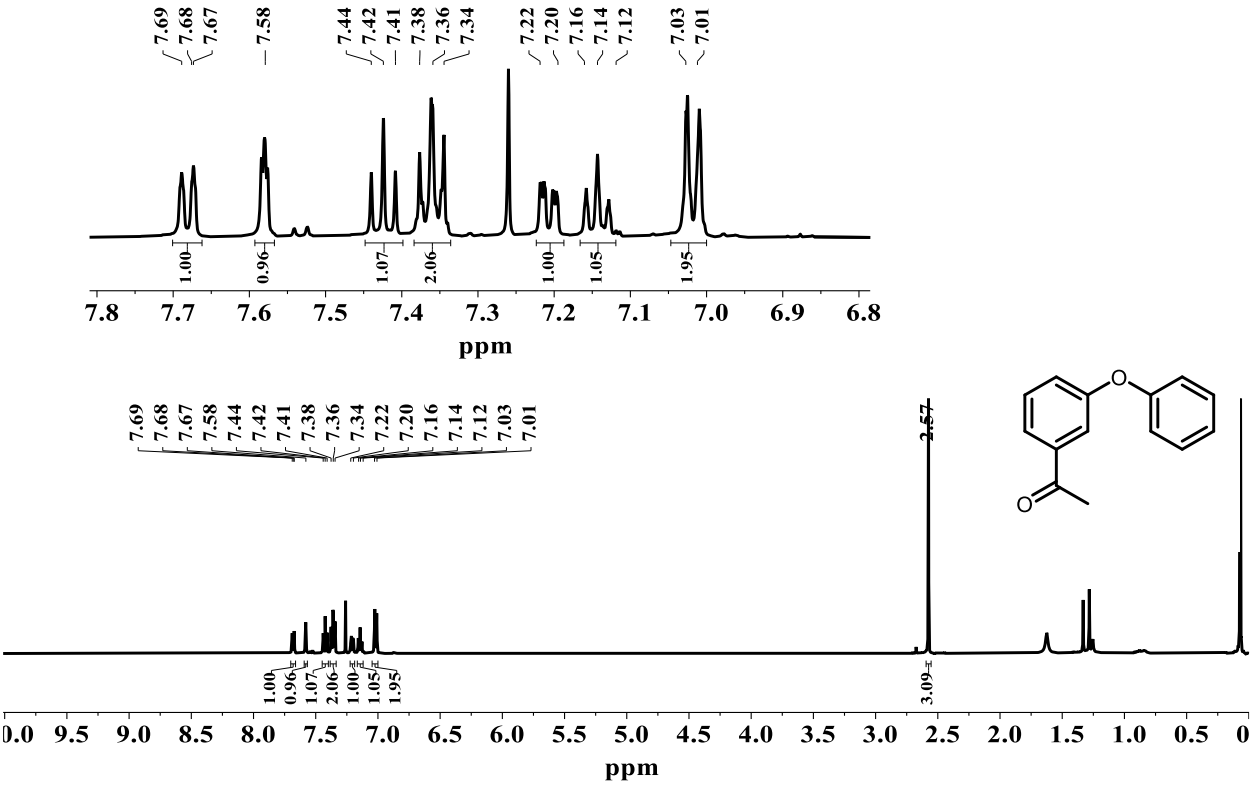

Fig. S73. ^{1}H NMR spectrum of **XIII** in $CDCl_3$ (500 MHz).

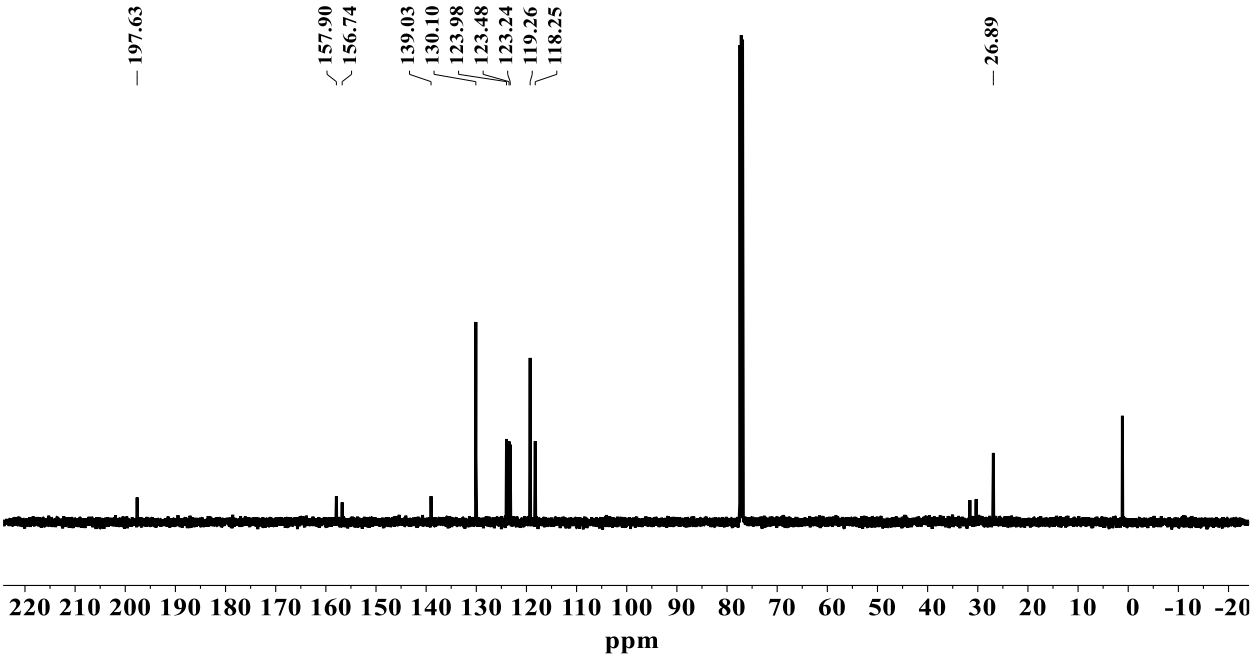

Fig. S74. $^{13}C\{^{1}H\}$ NMR spectrum of **XIII** in $CDCl_3$ (126 MHz).

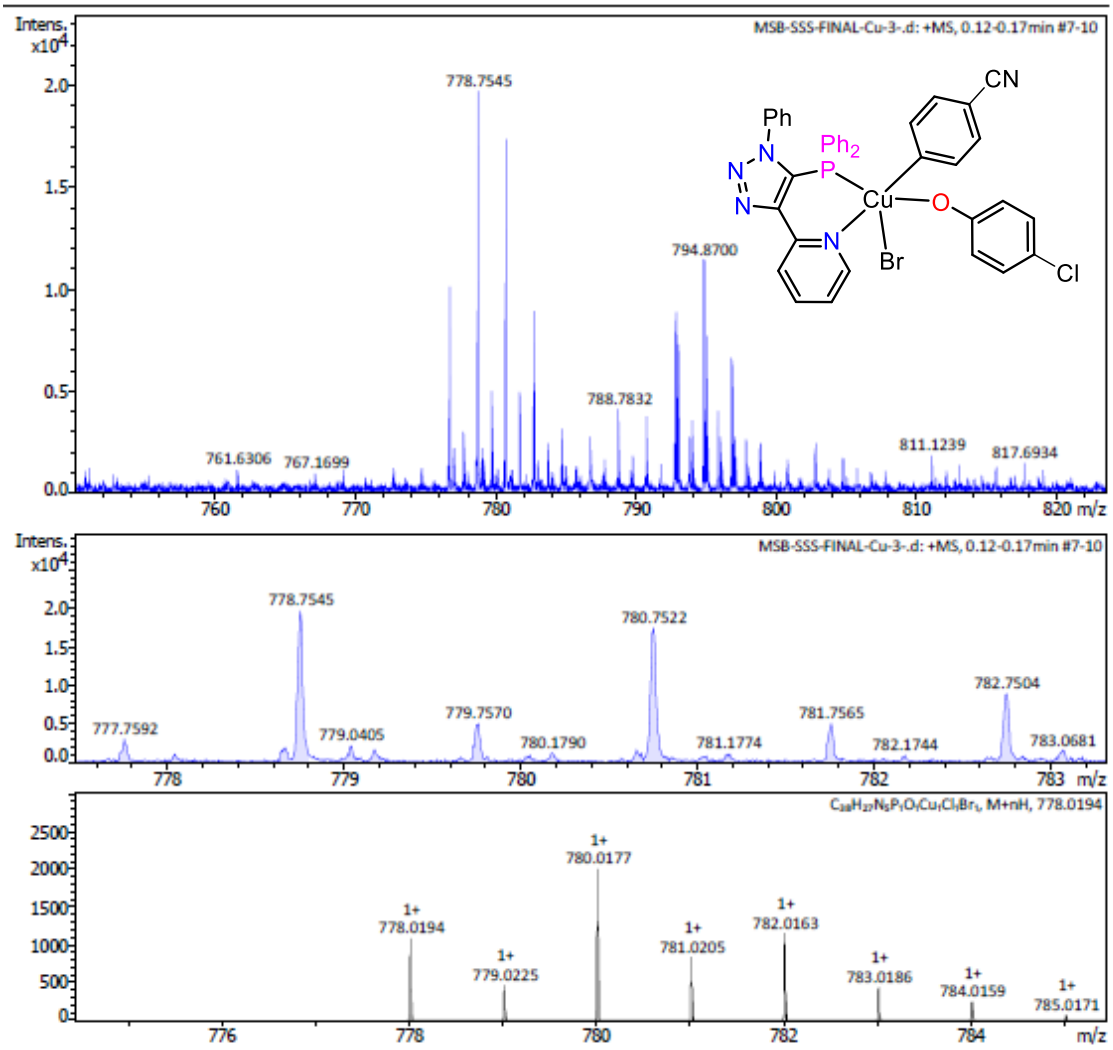

Fig. S75. LRMS corresponding to Cu(III)-intermediate.

References:

1. Z. Li, C. Brouwer and C. He, *Chem. Rev.*, 2008, **108**, 3239-3265.
2. O. V. Dolomanov, L. J. Bourhis, R. J. Gildea, J. A. K. Howard and H. Puschmann, *J. Appl. Cryst.*, 2009, **42**, 339-341.
3. G. Sheldrick, *Acta Crystallogr., Sect. A: Found. Crystallogr.*, 2015, **71**, 3-8.
4. G. Sheldrick, *Acta Crystallogr., Sect. C: Struct. Chem.*, 2015, **71**, 3-8.
5. M. J. Frisch, G. W. Trucks, H. B. Schlegel, G. E. Scuseria, M. A. Robb, J. R. Cheeseman, G. Scalmani, V. Barone, B. Mennucci, G. A. Petersson, H. Nakatsuji, M. Caricato, X. Li, H. P. Hratchian, A. F. Izmaylov, J. Bloino, G. Zheng, J. L. Sonnenberg, M. Hada, M. Ehara, K. Toyota, R. Fukuda, J. Hasegawa, M. Ishida, T. Nakajima, Y. Honda, O. Kitao, H. Nakai,

T. Vreven, J. A. Montgomery Jr., J. E. Peralta, F. Ogliaro, M. Bearpark, J. J. Heyd, E. Brothers, K. N. Kudin, V. N. Staroverov, T. Keith, R. Kobayashi, J. Normand, K. Raghavachari, A. Rendell, J. C. Burant, S. S. Iyengar, J. Tomasi, M. Cossi, N. Rega, J. M. Millam, M. Klene, J. E. Knox, J. B. Cross, V. Bakken, C. Adamo, J. Jaramillo, R. Gomperts, R. E. Stratmann, O. Yazyev, A. J. Austin, R. Cammi, C. Pomelli, J. W. Ochterski, R. L. Martin, K. Morokuma, V. G. Zakrzewski, G. A. Voth, P. Salvador, J. J. Dannenberg, S. Dapprich, A. D. Daniels, O. Farkas, J. B. Foresman, J. V. Ortiz, J. Cioslowski and D. J. Fox, *Gaussian 09*, revision D.01, Gaussian, Inc., Wallingford, CT, 2013. .

6. A. E. Reed, L. A. Curtiss and F. Weinhold, *Chem. Rev.*, 1988, **88**, 899-926.
7. R. Ray and J. F. Hartwig, *Angew. Chem. Int. Ed.*, 2021, **60**, 8203-8211.
8. C. Sambiagio, R. H. Munday, S. P. Marsden, A. J. Blacker and P. C. McGowan, *Chem. Eur. J.*, 2014, **20**, 17606-17615.
9. S. D. Ghodke, A. B. Tamboli, A. V. Diwate, M. B. Gurame, V. P. Ubale, M. D. Joshi and N. N. Maldar, *Journal of Polymer Research*, 2021, **28**, 342.
10. J. M. Bryan and W. K. George, *Heterocycles* 2015, **90**, 271-297.
11. C. Zhang, C. Li, J. Bai and H. Li, *Catal Lett*, 2015, **145**, 1764-1770.
12. P. I. O'Daniel, Z. Peng, H. Pi, S. A. Testero, D. Ding, E. Spink, E. Leemans, M. A. Boudreau, T. Yamaguchi, V. A. Schroeder, W. R. Wolter, L. I. Llarrull, W. Song, E. Lastochkin, M. Kumarasiri, N. T. Antunes, M. Espahbodi, K. Lichtenwalter, M. A. Suckow, S. Vakulenko, S. Mobashery and M. Chang, *J. Am. Chem. Soc.*, 2014, **136**, 3664-3672.
13. D.-Y. Wang, Z.-K. Yang, C. Wang, A. Zhang and M. Uchiyama, *Angew. Chem. Int. Ed.*, 2018, **57**, 3641-3645.
14. N. T. S. Phan, T. T. Nguyen, V. T. Nguyen and K. D. Nguyen, *ChemCatChem*, 2013, **5**, 2374-2381.
15. Y. T. Han, K. Kim, G.-I. Choi, H. An, D. Son, H. Kim, H.-J. Ha, J.-H. Son, S.-J. Chung, H.-J. Park, J. Lee and Y.-G. Suh, *Eur. J. Med. Chem.*, 2014, **79**, 128-142.
16. R. A. McClelland, V. M. Kanagasabapathy, N. S. Banait and S. Steenken, *J. Am. Chem. Soc.*, 1989, **111**, 3966-3972.